Inquiry: The University of Arkansas Undergraduate Research Journal

Volume 12 Article 1

Fall 2011

Inquiry: The University of Arkansas Undergraduate Research Journal - Volume 12 - Fall 2011

Inquiry Editors

THE UNIVERSITY OF ARKANSAS
UNDERGRADUATE RESEARCH JOURNAL

INQUIRY

Volume 12 Fall 2011

CONTENTS

INQUIRY

The Undergraduate Research Journal of the University of Arkansas

Volume 12 **Fall 2011**

Winners of the 2011 Undergraduate Research Award

Remaining Table of Contents in Alphabetical Order by Last Name

Cover image courtesy of Stanislav Bobovych

FOREWORD

The *Inquiry* journal was developed by the Teaching Academy of the University of Arkansas. The journal is supported financially and conceptually by the offices of the Provost and the Vice Provost for Research. Through print and on-line publication, *Inquiry* provides a forum for sharing the research and creative endeavors of undergraduate students at the U of A.

This issue of *Inquiry* records the scholarly contributions of 8 U of A student/faculty mentor pairs during the 2010/2011 academic year. The first three manuscripts by Fulton, Teague, and Walchuk are also the recipients of the 2011 Undergraduate Research Award. The work of Fulton and Teague shows the tenacity and commitment of undergraduate researchers as they took on projects that extended over several years and involved multiple stakeholders. Walchuk addressed an issue of vital importance at home and abroad – the link between immigration and far right sentiment and voting trends. The remaining articles display the remarkable diversity of research endeavors on this campus. It is particularly encouraging to see these leaders of the future engaged in studies that will ultimately make the world a better place – in business, computer technology, biomedical nanotechnology, inexpensive clean water, and cardiac health. The faculty mentors uniformly demonstrated belief in their students' abilities and a commitment to enhancing their students' growth in the research domain.

As always, many more high quality manuscripts were received than could be accepted for publication. Despite that fact, it was satisfying to note that the work in this issue reflects initiatives in five different colleges. Articles are selected for publication after review by faculty members with relevant content expertise. Manuscript reviews are needed at the end of the spring semester and into the summer (the worst possible time), yet faculty graciously agree to help in this process year after year. Space does not permit recognition of all of these individuals, but I am deeply appreciative. As Editor, I must also thank the members of the Publication and Undergraduate Research Award Review Board who gave so generously of their time.

While the papers chosen for publication vary in subject, method, writing style, and manuscript format, they are uniformly excellent in content. As much as possible, we have endeavored to maintain discipline-specific styles to provide students with a publication experience comparable to one they might find in their individual disciplines. I hope you enjoy reading this issue of *Inquiry.* On a personal note, this is my last year serving as Editor. It has been a wonderful opportunity to meet faculty and students and develop a greater appreciation for the research work that goes on at the University of Arkansas.

Barbara B. Shadden, Editor

INQUIRY PUBLICATION AND UG RESEARCH AWARD REVIEW BOARD FOR 2010-2011 ACADEMIC YEAR

The following individuals made the selection of UG Research Award Winners and publication of Inquiry possible through their guidance and their willingness to take on reviewing responsibilities at the most hectic time of the academic year: David E. Gay, Amy Herzberg, Marcia Imbeau, Pat Koski, John Norwood, Janine Parry, Molly Rapert, Mary Jo Schneider, Mike Wavering.

INDUSTRIAL EVOLUTION: A COMPARATIVE CASE STUDY OF THE TRANSFORMATION FROM INDUSTRY TO LEISURE IN THE PORTS OF SAN FRANCISCO AND OAKLAND, CALIFORNIA

By Annie Fulton
Department of Architecture

Faculty Mentor: Kim Sexton
Department of Architecture

Abstract

This case study examined two waterfront sites on the San Francisco Bay – The Piers in San Francisco and Jack London Square in Oakland. The Piers, actually consisting of Piers 1 ½, 3 and 5, was formerly the point of entry for immigrants to the city and today is home to offices and restaurant space. Jack London Square, which covers four city blocks, is a project whose aim is to revitalize an industrial shipping port and warehousing district. Today, it is about halfway through its phased development schedule. Multiple techniques were used to investigate the process by which these two cities have transformed their waterfronts to improve their economic and environmental possibilities and the problems they have encountered in doing so. Documentation review, interviews with those involved with the two redevelopment projects, and visual observation on site were the means of collecting data which was then triangulated in order to identify patterns and principles of urban waterfront redevelopment. This process also identified three potential points of action for Oakland in its continued development of Jack London Square: 1) a more explicit integration of the Green Movement into the city's planning strategies, 2) the fostering of a more authentic sense of place on Oakland's waterfront, and 3) the improvement of Broadway as a connective corridor between Jack London Square and downtown Oakland.

Introduction

All cities possess possibilities. The potential for each city is inherent in its design and the various assets of its environment: climate, waterways, and natural resources. While cities in the past have often used natural resources for industrial production, an increasingly post-manufacturing America has been witnessing a shift in urban priorities. Industrial economies are transforming into leisure marketplaces. Streets once filled with blue-collar workers are giving way to tourists and consumers of recreational activity. A close analysis of this shift in San Francisco and Oakland, California yields valuable knowledge about how cities might appropriately utilize their economic resources, while simultaneously reclaiming their environmental and cultural heritage. In doing so, each city would not only create possibilities for enjoyment but also restore a sense of place for its citizens.

Seaports are optimal sites in which to study the changing relationship of cities to their natural environment. Comparisons of two distinct but closely related harbor locations which have redeveloped previously industrial sites into new uses reveal just how important an environment-based sense of place is in the successful conversion of an industrial port into a recreational urban waterfront. Two optimal cases for study are found in the San Francisco Bay Area: Piers 1 ½, 3, and 5 (constructed in 1931) in San Francisco and Jack London Square (founded in the late 19th century) in the former cargo port of Oakland. While some industry still exists in both cities out of necessity, the waterfront has become the public's again. These cities exhibit a phenomenon that is consistent throughout the United States regardless of a community's size, scope, or saga. Cities are reworking their environmental possibilities. The presence of water – be it in the form of a river, lake, ocean or bay—has become an opportunity to showcase and develop a city's culture, even though it may previously have served primarily as an industrial or trade resource.

While historically Oakland and San Francisco have relied heavily on the Bay for their livelihoods, their relationships with the water have been strictly utilitarian with little regard for environmental or social consequences. Today, however, San Francisco's relationship with water is primarily aesthetic, recreational, and tourist-driven, while Oakland's port strives to keep up with industrial demand while it develops its high-valued waterfront property. The question is, how does the history of the redevelopment of former industrial ports on San Francisco Bay help Oakland succeed in creating a distinct sense of place in Jack London Square?

Understanding how Americans perceive their relationship to surrounding space is paramount to understanding how they utilize the natural environment. As wilderness gives way to parking lots, landscaped parks, and city blocks, American towns and cities are losing an essential component of place-based character. An identity crisis results, one rooted in the loss of connections to natural processes. A space with strong identity should be almost unique to its cultural location and genuinely representative of its natural setting. A strange disconnection with nature in much of American life exists side by side with an intense yearning to inhabit it in the form of suburban lawns, trails and parks, or vacations in relaxing, idyllic landscapes.

When American cities were forming in the 15th and 16th centuries on the east coast, and the 17th and 18th centuries on the west coast, the presence of water was imperative to the establishment of a city. Rivers, lakes, and oceans provided a source of transportation, defense, food, and other resources. The settling of the San Francisco Bay, or the Golden Gate, is evidence of achieving the 19th century American belief in Manifest Destiny as well as opening a portal to future contacts with the Far East. The

cities of San Francisco and Oakland as well as other cities lining the bay were established because of the deep, naturally protected harbor the bay provided. By the 1960's, shipping traffic moved from the Port of San Francisco to Oakland on the eastern side of the bay. Since then, both cities have been attempting to shape their new waterfront identities.

This study examined how one public space in the port of San Francisco represents a variety of urban parameters and waterfront possibilities, all of which can guide the development of a public space on Oakland's port, Jack London Square, which is currently undergoing renovation. The site in San Francisco is constituted by Piers 1 ½, 3, and 5, commonly known today as "The Piers". Historically, the Piers was a point of arrival for numerous migrants and visitors who arrived at the nearby Ferry Building. For many years in the late 20th century, it remained relatively unused, but a 2003 restoration project reintroduced the area as vitally relevant to the city. It now consists of restaurants, high-end office space, and a public waterfront walkway. Jack London Square, on the other hand, was formerly a fishing dock and warehousing district. Currently it is being developed, in phases, into a multi-use district, filled with a hotel, recreational retail, restaurants and office spaces, along with significant exterior public space.

While there are several standardized ways of approaching waterfront development, professionals know that nothing can really be done by the book.[1] Experts recognize that context is important, but they often disregard it, claiming that local context and "character" is fine as long as it does not get in the way of profitability. At the level of public image, Oakland and San Francisco seem to be not only on opposing shores of a bay but on opposite ends of a perception gap. Yet historically, the cities have shared many of the same problems, and, as this study shows, this remains true even at the turn of the 21st century. The common denominators right below the surface are often overlooked.

The research described in this article was a portion of a larger comparative case study of the two Bay Area redevelopment projects. While less than seven miles apart on the same body of water, the case study data showed exactly how place-based contingencies ultimately determine not only the appearance of any one project but its success.

The specific research questions explored in this study were:

- To expose differences in motives for redevelopments of the cities' waterfronts.
- To identify differences in implementation of redevelopments of the cities' waterfronts.
- To define the built features of a leisure-based urban waterfront.
- To investigate how people use the developments for leisure activity on the waterfront.
- To understand the transformation and identify the physical and behavioral qualities of the sites.
- To determine the economic success of the two developments.
- To discover what aspects of the projects regard the natural environment, history, and culture of the area.

The results of this study are especially critical for the still under-construction Jack London Square, where understanding the multifarious contextual factors already at work can help ensure its longevity at a precarious moment in American economic history. This article provides a synopsis of study outcomes in the form of an essay on past, present, and future port development and a recommendation for points of action for the city of Oakland's continued development of Jack London Square. A brief overview of methodology is presented first as context for the discussion.

Methods

An exploratory case study approach was used to determine a pattern for how the San Francisco Bay Area is developing historically industrial areas into leisure-based waterfronts. The two case studies were the Piers in the Port of San Francisco and Jack London Square in Oakland. Robert Yin defined an exploratory case study as an approach in which an already established theory is applied to one or multiple cases, leaving the study questions and hypotheses partially undefined until research has concluded.[2] The characteristics of a case study are: a focus on a set number of real-life cases, attempts to explain causal links, reliance on multiple sources of evidence, importance of theory during the research process, and an ability to create a theory in conclusion. An exploratory case study uses a linear-analytic structure, a narrative sequence, and reliance on theory-building.[3]

Table 1 shows the links between the previously-identified research questions and tactics.[4] The term "tactics" is used to refer to techniques for obtaining information. After the tactics were completed, I triangulated the data to assess validity and discover patterns. Triangulation is a form of cross-examination in qualitative research in which multiple methods are used—in this case, documentation review, interviews, and observation—in order to produce a balanced and detailed picture of the situation.

Documentation Review

Documentation review was the primary tactic for analysis. It was imperative to establish the history, culture, and geography inherent to each site and to explore the histories of the ports as well as the morphologies of the locations. Understanding the culture and demographics of the port location and the larger city helped differentiate the unique qualities of the two sites. By recognizing the backgrounds for each case, a more accurate evaluation of the success of reconnecting people to the port was made possible.

The documentation review also provided written evidence in support of or contradiction to the information gathered during interviews and observations. Public documents, primarily newspaper articles and design plans, were analyzed to identify possible differences in motives and to determine the process of implementation of the waterfront redevelopments. I compared design documents to understand the transformation and physical forms of the sites through zone diagrams. It was also important to obtain historical photographs and descriptions to understand how the waterfront had been altered. I reviewed newspaper articles regarding the businesses within the sites in order to investigate the economic success of and public opinion about the two developments. In order to discover what aspects of the projects

reflected the natural environment, history, and culture, I carefully read newspaper articles and editorials. To understand how the redevelopments affected their surrounding areas, I identified sites mentioned in interviews and newspaper articles on area maps.

Interviews

As a secondary research tactic, I conducted interviews with people with direct knowledge of the sites' development and design. Since many of the other tactics used were secondary sources, interviews provided triangulation and filled in knowledge gaps regarding the development of the waterfronts. The interviews focused on the direct actors involved in the planning, designing, and construction of the sites.[5] The objectives of the interviews corresponded with those identified in Table 1.

Table 1. Research objectives and corresponding tactics.

Research Objective-to find/identify/understand:	**Tactics**
…differences in motives for redevelopments of the cities' waterfronts.	Documentation review Interviews
…differences in implementation of redevelopments of the cities' waterfronts.	Documentation review Interviews
…built features of a leisure-based urban waterfront.	Documentation review On-site observation
…how people use the developments for leisure activity on the waterfront.	Interviews On-site observation
…the transformation and the physical and behavioral qualities of the sites.	Documentation review On-site observation
…the economic success of the two developments.	Documentation review Interview On-site observation
…what aspects of the projects regard the natural environment, history, and culture of the area.	Documentation review Interview On-site observation
…how the redevelopments affect their surrounding areas.	Documentation review Interview On-site observation

Identifying Interviewees. In order to gain comparable data, it was important that each city had an equal number of interviewees with similar roles in the port developments. I identified interviewees based on their role and significance to the sites in Oakland and San Francisco. I attempted to contact three different people from each city: (1) representatives from a design firm for each site, (2) the developer of each project, and (3) the port authority for each site. I identified the designers through internet searches of developers' websites and media sources. The developers of the project were identified through an internet search. I contacted the port authority for each city for information regarding the cities' regulations and preferences for waterfront development.

Interview Format. The interviewees were first contacted through e-mail and phone. I identified myself as an undergraduate researcher, searching for the different elements and patterns of urban waterfront redevelopment. I used the preliminary phone interview to explain briefly the topic of research and establish the relevance and role that the interviewee had in the research process. At that time, an in-person interview time and date were established, when possible. Due to schedule constraints, not all of the identified parties were interviewed for this article.

I traveled to the Bay area to conduct the interviews. All of the in-person interviews were conducted in a semi-structured manner within one week of each other. I asked a series of five essential questions in order to structure the conversation.

- What were the priorities for this project?
- What previous projects did you analyze while working on this project? Why?
- How did you address the waterfront when redeveloping a portion of the city?
- How could this project be considered a success?
- How is this project unique in its surroundings? In the city?

These questions were designed to allow the interviewee to guide the conversation about the developments. I asked supplementary and probing questions as needed.[6]

The interviews were conducted in an office setting and lasted between thirty minutes and one hour. Tape recording and note taking were the primary means of data collection. These raw notes were then interpreted into a research template for comparison. Portions of the interviews were transcribed and added to this document. I used bracketing to include personal notations and thoughts.[7]

Analysis. I derived a common template for data collection summarization from the research documents for each interview.[8] This form helped organize information for each interview. The interview forms were then grouped according to city. I compared the forms among the interviewed and the cities. I used this triangulation method in order to verify sources as well as properly construct the overarching themes for each city and its development.

Observation

To supplement the other two research tactics (documentation review and interviews), I made on-site observations. Observational data was of utmost importance in order to develop a personal analysis of place. I recorded observations primarily through written field notes and photography. The objectives of observing were to identify the physical and behavioral qualities of the sites and then to explore the 3rd through 7th research objectives outlined in Table 1.

Analysis

The scope of this research project extended well beyond what is presented in this article. I began the analysis by analyzing each city's project separately, in order to establish an unobstructed view of each city and its redevelopment, without being influenced by the other project. Each city analysis contained information about the history of the port, the current Port Authority, key related projects, and a section on the specific redevelopment project.

In order to properly triangulate the data, I used a method of cross-examination. I started by extracting key themes within each city's analysis. I then created a table with all of the original research objectives. I placed the themes into this table in accordance with whether the theme contrasted between the two cities or was comparable between the two cities. Some of the themes transcended several of the research objectives, identifying what themes were most important in answering research questions and developing points of action for Oakland.

This article provides an overview of research outcomes. It demonstrates that the relationship of San Francisco's port project to Oakland's is not one of prototype to imitation. Instead, it is a

representation of how two cities can effectively redevelop their waterfronts, deploying different strategies, while acknowledging the existing factors that contribute to their advancement and identity.

Unveiling the Transformation

The Case Studies

San Francisco and Oakland seemingly share only one thing in common—the San Francisco Bay. In reality, however, the two cities' waterfronts share more than simply a body of water. Their motivations for redevelopment are not so different, nor are they different from those of many other cities. Revitalizing waterfront properties to create leisure-based, public spaces is the common goal, yet varying implementation strategies would create outcomes that identify each city as a unique and distinct place. A standardized implementation strategy would diminish each city's individual identity, even when the cities are as closely related historically and geographically.

Since 1850, the two cities have transformed their waterfront in drastically different ways. While the port of San Francisco had deep water, the city lacked terrain level with the water. The hills of San Francisco started to ascend right at the water's edge. Early San Franciscans combated this problem by filling in the Bay with earth to create flat swaths of land along the shore.[9] Oakland, just on the other side of the Bay, had the opposite problem. It had extensive amounts of flat land between the Bay and the Oakland Hills, but its primary location for shipping was along the estuary, where water was too shallow for large ships. Therefore, Oakland dredged its estuary to create deep enough channels for seafaring vessels.[10] This comparative study demonstrates that, through antithetical landscaping interventions in the 19th century, San Francisco and Oakland made their waterfronts alike and for the same purpose: industrial shipping.

Because of the different form and depth of the bay at portside, the cities' docks were built to different specifications. San Francisco has finger piers, which stretch far into deep water to accommodate large vessels with bulk break cargo.[11] However, this form of shipping and pier structure is largely obsolete. Nevertheless, today San Francisco is identifiable by its numerous piers stretching into the Bay (Figure 1). This traditional harbor structure is often what comes to mind when thinking of ports—long, extended slivers for docking ships.

Close observation of Oakland's waterfront, however, reveals a very different character. Small docks supporting mid-size ships are prevalent within the inner estuary, which is protected from the larger Bay. Here, the waterfront is identified by huge concrete slabs stretching into the Bay (Figure 2). The slabs blur where the land actually ends and the piers begin. Rows of gantry cranes are bolted to these concrete docking stations. It is the cranes' strong visual presence – especially the rhythm of their patterned placement – that creates a sense of place and identity for Oakland.

During the Gold Rush in 1849, the role of the port of San Francisco was to transport miners from the city inland to the gold mines while providing storage and transport for necessary equipment, supplies, and food.[12] Oakland, at this point in time, was simply called the *contra costa*, or opposite shore.[13] As a Gold Rush town, its role was to facilitate the transport and support of miners and goods. With the completion of the transcontinental railroad in 1869 and the Panama Canal in 1914, San Francisco became the major port of the West Coast, with Oakland as a close second. The outer harbor utilized long docks to access larger ships in deeper water, while the natural estuary between the island of Alameda and Oakland provided protection and calm waters for smaller vessels. This inner harbor area was the location of Jack London Square which consisted of a fishing wharf, a wholesaling and warehouse district, and working class amenities.[14]

Influenced by the City Beautiful movement in the early 20th century, San Francisco built their city, from the civic center to the waterfront, in grand, neoclassical style.[15] Even the industrial shipping piers had a Beaux-Arts facade. Shipping in the early 1900's was done through break-bulk cargo, meaning cargo that is broken down into small units.[16] This inefficient and costly method of shipping changed in the middle of the century. During World War II, the military had a heavy presence on San Francisco's waterfront which made expansion of harbor industries difficult, especially reconstructing the piers to accommodate this new form of shipping. The intermodal system of shipping was developed in the 1950's in order to "link various modes of transport into one integrated system."[17] Standardized steel containers packed with goods and materials were carried by ship, train, and truck. By the late 1960's, Oakland surpassed San Francisco as the largest port on the Bay with total annual cargo of 2.5 million tons, and by the 1980's, almost all available waterfront land had been redeveloped to accommodate container shipping. Oakland had an obvious geographical advantage over San Francisco for this form of shipping, since the intercontinental railroad terminated at the Oakland waterfront and many major highways were easily accessible from the city.

Due to the decline in industrial waterfront activity and the presence of the Embarcadero Freeway—an elevated highway which cut off the city from its waterfront because it spanned the entire length of the waterfront—the San Francisco harbor was relatively unused for several decades in the late 20th century. Demolition of the Freeway in 1992 and recent redevelopment projects have sought to reconnect the public with the water while maintaining its historic character. On the other side of the Bay, Oakland is the fourth busiest port in the United States which makes commercial redevelopment of the waterfront costly and challenging for the city.

In San Francisco, Piers 1 ½, 3, and 5 occupy a single structure on the waterfront just north of the Ferry Building, adjacent to the city's Financial District (Figure 3). Piers 1 through 5 are considered part of the Ferry Building neighborhood and share its Beaux-Arts architectural style and monumental presence. This area has specific design criteria to ensure continuity of urban space, including roof height standards and maintaining its historic character.[18] Originally built in 1919, the Piers were redeveloped in 2003 as a single project by the development firm Pacific Waterfront Partners, creating high-end office space, several restaurants, and public waterfront access.

On the other side of the bay in Oakland, located where Broadway meets the estuary, Jack London Square has always been the face of Oakland's waterfront (Figure 4). The Square is more than a traditional plaza: it is a neighborhood around 7 blocks long and 2 blocks wide. In the 19th century, it was a bustling, working waterfront and the site of the first regular ferry service to San Francisco. In 1950, the Square was named after Jack London (1876-1916), the famed author, socialist, and Oakland

Figure 1. San Francisco's waterfront is lined with finger piers. Photo courtesy of Christian Abend.

Figure 2. Oakland's port is dotted with the iconic gantry cranes. Photo courtesy of the Smithsonian Institute.

resident.[19] The area started to accommodate tourism in the 1930's when the wharf provided berths for commercial fishing, a fish market, and a seafood restaurant.[20] However, it was in the 1950's that Jack London Square took on the form that is recognizable today. Nevertheless, in the following decades, Jack London Square would slowly lose its visitors, tenants, and vibrancy. In the early 21st century, the development firm Ellis Partners began a phased redevelopment process for the area through the creation of significant exterior space, retail and office space, restaurants, and other public amenities.

The waterfront sites in each city were originally chosen for this study because of their linked industrial histories, but close analysis showed that they treated their industrial heritage in very divergent ways. San Francisco's waterfront has shifted its industry to less visible locations along the southern waterfront.[21] Oakland, on the other hand, continues to embrace industry, and thus, showcases its machinery in the design of the waterfront. Since San Francisco's shipping industry is now practically non-existent, displaying that heritage would be nearly impossible. Instead, San Francisco's waterfront embodies its current role as a cultural, political, and tourist destination. The waterfront is filled with neoclassical buildings, such as the Ferry Building, and it offers sweeping views of the city of San Francisco (Figure 5).

In contrast, Jack London Square, which itself is no longer industrial, frames views of flourishing industry as a proud icon of the city of Oakland (Figure 6). One finds that restaurants on the Square, such as Il Pescatore, brag about their waterfront location with great views of the estuary and gantry cranes. These eye-catching structures are representative of what Oakland has become: hard-working, globally relevant, and prosperous. San Francisco altered its waterfront to accommodate tourism and small-scale industry, while Oakland is developing its waterfront to enhance its shipping industry and to optimize areas of the waterfront for commercial real estate.

City Beautiful versus City Green

San Francisco's waterfront design is deeply indebted to the City Beautiful movement of the early 1900's, in that the harbor consists of monumental buildings in a neoclassical style and streets with sweeping views.[22] Even the water's edge has been designed, constructed and redeveloped to enhance this style of city building. The recent redevelopment of the Ferry Building Area, including Piers 1 ½, 3, and 5, perpetuated this design ethos while modernizing and adaptively reusing the neoclassical structures.

Originally, the City Beautiful movement encouraged monumentality and beauty for the sake of the public; the city's beautification was expected to improve the quality of life for all citizens. Piers 1 ½, 3, and 5 lay derelict for a large part of the late 20th century. While being a product of the 21st century, their redevelopment in 2003 is actually a very "City Beautiful" response to a contemporary problem. The redevelopment restored the structures to their original grandeur, improving the quality of the waterfront for the use of the public. Taken together, the Piers and the Ferry Building, which was also restored in 2003, serve as a small scale version of what the City Beautiful movement strove to do: enhance the aesthetics of structures to improve the public's well-being and to foster pride in their city.

A century after the City Beautiful movement and on the other side of the Bay, Oakland's waterfront redevelopment has been guided by a different kind of movement – the Green Movement.[23] Parallel to the changes that occurred in the early 1900's, the

phenomenon of creating a more inhabitable city accelerated again at the turn of the 21st century. The Green Movement advocates increasing green space, reducing pollution and greenhouse gas emissions, building sustainable structures, encouraging exercise, and using environmentally-friendly products. Influenced by the

Figure 3. San Francisco's Pier's 1 ½, 3, and 5 and its surrounding area. Photo courtesy of Austin Aerial Photography. Photo Illustration by author.

Green Movement, the Ellis Partners, developers of Oakland's Jack London Square, have addressed this contemporary trend in land development and city building to some extent.

A close examination of the Port Authority's master plan and development goals affirms that the majority of Oakland's commercial redevelopment efforts in the past decade have been directed at creating more open, green space for the public in the form of parks and trails.[24] Oakland is constructing paths that contribute to the Bay Trail project which involves encircling the Bay's waterfront with a 500 mile biking and walking trail.[25] This trail system enhances public outdoor space used for leisure. Facilitating access to venues for outdoor recreation and physical activity is an aspect of the Green Movement which distinguishes it as a social movement, not simply a development strategy.

Since Jack London Square is largely a collection of new buildings and renovated older structures, Oakland, unlike San Francisco, did not face pressure to preserve a distinct architectural flavor. The keystone building of the project, the Jack London Market building (Figure 7), is certified LEED silver, the third highest possible sustainability certification.[3] All of the structures on Jack London Square, old and new, embrace variations on modern design rather than emulating the character of older surrounding buildings. Identifying the "look" of Green Movement buildings is much more challenging. Due to modern design criteria, cities do not seek the regularity and replication of neoclassical buildings and city design. Modern designers are less constricted by rules and canons, so they are able to design more freely. However, when designing buildings for LEED certification, geographical factors and climate limit the freedom of the designer, but in the process may fashion a local visual identity or "style." Hence, while the City Beautiful movement's stylistic qualities are recognizable anywhere in the country, buildings reflecting Green Movement ideals are more linked to individual regional

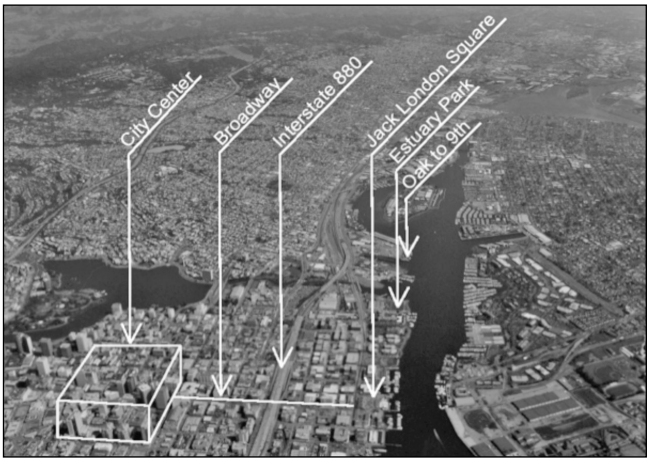

Figure 4. Oakland's Jack London Square and its surrounding area. Photo courtesy of Derrick Coetzee. Photo Illustration by author.

contexts. In the Bay Areas, the City Beautiful movement and the Green Movement have produced distinct spaces in similar settings less than ten miles apart.

Urban Design at the Waterfront and Beyond

In defining the spaces of a leisure-based urban shoreline, the Bay Area cities provided distinct solutions: a corridor-like, linear arrangement in San Francisco versus a series of outdoor rooms in Oakland. While these architectural designs stand in strong contrast with one another, their programs are comparable. Like other industrial harbors converted into recreational urban waterfronts, they favor mixed-use developments with significant exterior public space.

Figure 5. San Francisco's neoclassical building style. Photo by author.

What makes portside development at the Piers and Jack London Square attractive is the water. It is imperative that architecture and exterior spaces are oriented towards it. Visual documentation of the two sites showed that, while their structures act as a boundary between the water and the rest of the city, once

Figure 6. Oakland's iconic gantry cranes.
Photo courtesy of David Sanger.

inside the projects, the focus is on the water's edge. Oakland's site sets up a plaza-like exterior, surrounded by buildings with swaths of windows facing the water (Figure 8). Views are not only framed by glazing within buildings, but also by the spaces between buildings which allow glimpses of the estuary. The streets in Jack London Square's neighborhood are in a strict grid pattern, creating blocks of open space, rather than lines of space. San Francisco's edge is much more linear, a corridor echoing the Embarcadero, the expansive boulevard that connects one end of the waterfront to the other. The Piers' bulkhead building is simply a voluminous extension of that linear corridor, which simultaneously creates a threshold or buffer between the bustling financial district and the calm bay (Figure 9). Thus these different building strategies – room versus corridor – create experientially distinct spatial configurations which are suggested by surrounding circulation and street patterns.

All cities along the San Francisco Bay appreciate the value and appeal of access to the waterfront. Oakland's and San Francisco's recent development efforts are designed for visitors to have direct contact with water. Careful observations of day-to-day activities at the ports suggested that the new developments deliberately encourage recreational boating, not just commercial or industrial shipping, by providing public docks and marinas. Giving the public the option to be on top of the water, rather than just looking at it from the shore, is a key component to urban waterfront redevelopment. Hence, in a sense, both cities have made the water part of the land, extending the space in which activities take place.

Simon Snellgrove, developer of the Piers project in San Francisco, pointed out that a central reason for the success of the Ferry Building Area is its close proximity to the city's financial district and to many modes of transportation.[26] Oakland's downtown is not directly on the waterfront; it is one mile up Broadway from the estuary. Addressing the issue of location is one of the greatest challenges for Jack London Square's revitalization. Optimists, such as architect Steve Worthington, believe that the excitement and success of the revitalization will naturally bring about developments along the Broadway corridor, which will link the activities of downtown to those at the waterfront.[27] This may be true, but his assumption relies on the premise that Jack London Square will be successful first, with or without a thriving corridor connecting it to the city center.

In order to truly evaluate the success of any city revival project, one must determine the degree to which a project is self-contained as well as how it affects adjacent neighborhoods. The analyses in this case study provide new insights concerning how the proximity of a harbor to a city center affects waterfront redevelopment. San Francisco's Ferry Building Area, being adjacent to the financial district, has never really lost traffic. Even when the Embarcadero Freeway cast a shadow over the area during the last half of the 20th century, the bustling business district flourished just a few blocks away. When industry was relocated away from the core of the port, San Francisco did not need to make a case for the area, as it was already central to the city, even if it was underutilized. Jack London Square, whose relevance to Oakland has always been acknowledged, has nevertheless lacked a significant connection to the city's bustling downtown. Rather than stumbling upon Jack London Square, a visitor must intentionally venture to Oakland's waterfront in order to enjoy it. Oakland recognizes this and has attempted to market Jack London Square as a destination by providing substantial parking infrastructure and creating the free "B" shuttle, a bus which runs between downtown and the Square.[28] These initiatives solve some of the connectivity dilemmas, but they do not change the fact that visitors must already be aware of the existence of Jack London Square.

When there is a need for area-wide revitalization, as there is in Oakland, a waterfront project is potentially a catalyst for growth. Since the edge of San Francisco's financial district has been heavily inhabited for decades, the Piers project was not burdened with the responsibility of fueling redevelopment in the surrounding area. The Piers are more of a model project for future port renovations in San Francisco than a vehicle for neighborhood revitalization. Jack London Square, in contrast, is surrounded by property in need of rehabilitation in order to foster a more cohesive neighborhood. The Square may, in fact, transform its neighborhood more than the Piers redevelopment influenced its surrounding area, but the need for change is greater in Oakland.

Place-Making

In terms of place-making, theorists tend to be in agreement with the basic principle that the natural environment, history, and

Figure 7. Oakland's Jack London Market building. Photo by author.

culture of an area are key to distinguishing one place from another and providing each with a unique identity.[29] At the waterfront, reverence for locality is particularly crucial. The environment is fragile, and a port is often home to rich histories of a city. Both Oakland and San Francisco address the past by preserving historical buildings and creating educational itineraries throughout the neighborhoods. San Francisco's "History Walks," which provides historical information on plaques, is a fitting example, as are the many references to author Jack London in Jack London Square. However, more often than not, the two cities differ in the manner in which they address culture and the environment.

Planning movements can shape a city's identity. San Francisco's waterfront, as a product of the City Beautiful movement, emerges as one extremely conscientious of the public's aspirations to shape society. The monumental buildings designed in the City Beautiful era do not necessarily mirror the existing culture; instead, they seek to image a better society for the future. As a city known for its social activism and radicalism, the City Beautiful movement's desire to change the very structure of society is telling of the culture of San Francisco in the 20th century. The most recent redevelopments – like the Piers – aim to modernize the City Beautiful port.

The Piers renewal strikes a delicate balance between preserving the city's history and modernizing its structure to accommodate today's urban culture. It is the tenants, not the architectural surroundings of the port, which reflect the current culture of San Francisco.[30] The city is particularly known for its strong views on environmental and social integrity. So, even though the Piers project is not an LEED certified building or an environmental education site, it does successfully represent key aspects of San Francisco's culture, thereby helping to give the city a unique sense of place as a progressive, diverse community with a strong appreciation for its dynamic history.

Figure 8. Jack London Square's plaza-like exterior. Photo courtesy of the Ellis Partners.

Figure 9. The Piers' corridor-like waterfront designPhoto by author.

In contrast to the City Beautiful movement, the Green Movement actively addresses environmental concerns as a means of place-making. While Jack London Square was not designed to be a model project for this movement, it has been heavily influenced by it. The desire for LEED certification can be as much a response to societal demands as it is the developer's feeling of obligation to the environment. Enhancing outdoor recreational facilities is a facet of the Green Movement which promotes an active lifestyle while fostering appreciation for nature. The Green Movement is a multifaceted cultural movement in itself, one that includes goals for the natural environment, urban design, and social welfare.[31] It strives for a more responsible, less wasteful population which, by being aware of its environmental impact, becomes more conscious of the uniqueness of place.

Jack London Market, the LEED certified anchor building of development, is the center of Oakland's socially sustainable food movement, the activities of which have been well documented in the Oakland press.[32] Jack London Square, the third corner of an emerging "culinary triangle" consisting of Oakland, San Francisco, and Berkeley, reinforces the avid food culture of the Bay Area.[33] Food is obviously a necessity to all humans, but the plethora of fresh, local ingredients, acclaimed restaurants, and diverse populations, echoes the culture and environment of northern California. Based on current theories of place-making, this case study argues that providing locations for dining near the sea and the land that produced the food, as Oakland does, reinforces a sense of place.[34] By addressing the Bay Area food lifestyle, both Jack London Square and the Piers offer a unique juxtaposition of contemporary and historical culture, nature, and commerce.

When analyzing the success of a city's redevelopment project, the most important, yet complex, variable to consider is the context from which a project emerges. San Francisco's Piers 1 ½, 3, and 5 and Oakland's Jack London Square do not differ substantially from one another in program, climate, or motive, yet the public views them as unrelated projects due to the cities' reputations.[35] The real distinction between the two projects is temporal. San Francisco's efforts have perpetuated an image based

on the port's historical, early 20th century design. Oakland's port revitalization, on the other hand, is almost entirely contemporary. It is currently in the *process* of rehabilitating the estuary shore while establishing a waterfront identity. What makes the case study comparing San Francisco's Piers and Oakland's Jack London Square so compelling is that, while the two cities share a close history, their waterfronts are products of two different centuries. Hence, the city of Oakland must proceed discerningly when considering San Francisco as a model for its own port revitalization.

Points of Action

This comparative analysis of the Piers in San Francisco and Jack London Square in Oakland suggests a need to reassess Jack London Square's development plan in order to ensure that the city maximizes its potential as a revered waterfront destination on the San Francisco Bay. Given that the redevelopment project is not yet complete, the outcome of this study can be formulated as three points of action which revolve around some of the principles of the Green Movement that will facilitate the successful transformation of Jack London Square into a vital nexus of urban life.

Point of Action #1. Driven by society's demand for monumental civic buildings and spaces and grand boulevards, the success of the City Beautiful movement nationwide stems largely from its role as a significant social movement. In San Francisco, it created much of the layout of the city's urban fabric and filled it with notable edifices. Preserving these early 20th century buildings has become an integral part to every redevelopment initiative in San Francisco, even along the waterfront. The movement bestowed a unique character on San Francisco's port, which is a source of pride to San Franciscans and interest to visitors. The first point of action for Oakland in its bid to successfully create a vibrant, unique recreational waterfront at Jack London Square is to acknowledge and harness the immense power of a movement which links social idealism to built forms.

The Green Movement has already influenced certain aspects of Jack London Square development (e.g., the design of the Jack London Market building), but the city of Oakland needs to embrace the movement as a total urban reform. The Green Movement has the capacity to improve cities as effectively as the City Beautiful Movement. Indeed, a full-fledged commitment to an integrated program of reform is necessary for Jack London Square, because the Square alone is widely viewed as the catalyst for the future revitalization efforts at the Port of Oakland.[36] By contrast, the City Beautiful movement in San Francisco shaped many neighborhoods in the urban fabric, so that the Piers renovation project is not solely responsible for its own success or failure, or that of the surrounding district. If Oakland develops the project through the social and built environment ideals of the Green Movement, the chances of Jack London Square becoming and remaining a vibrant and relevant neighborhood in the decades to come is very high.

The very fact that Oakland chose to redevelop Jack London Square – an environmentally abused area lacking in social or economic activity - was in and of itself already a quintessentially "Green" act. The area was a drain on the city of Oakland instead of an asset. Harnessing the Green Movement in all of its facets would make Jack London Square a superior example of a 21st century mixed-use development, one that embodies environmental concerns, social health, and economic strength. The Ellis Partners' current development strategy attempts to address some aspects of these issues, but it lacks consistency. Several buildings have been LEED certified but others have not. Outdoor spaces encourage physical activity but they are not yet well-integrated with nearby city neighborhoods. Implementing the plan through phases is more sustainable in an uncertain economic climate, but the lack of short-term investment poses the risk of the project never being complete.

To truly harness the Green Movement, the developers of Jack London Square need to continue to find ways of salvaging what remains in the area, whether that be existing culture, architecture, building materials, or businesses. In some ways, the creation of food as a theme, with Oakland as the third vertex of the Bay Area's culinary triangle, does attempt to do this, but it is a very small niche in a much larger societal movement. To avoid being gimmicky or creating the impression of a fabricated tourist trap, Jack London Square has to do more than simply display signs about LEED certification and the benefits of eating organic, local food. It must *realize* Green ideals by producing space for them rather than merely proclaiming them in plaques and posters. Extending the waterfront bike trail, for example, is integral and a significant step in the right direction. It highlights the juxtaposition of nature and the constructed environment, while expanding the accessibility of Jack London Square to other communities along the shore. If the developers can continue to make efforts that nurture Green culture, Jack London Square will become truly sustainable – socially, environmentally, and economically – and an enduring piece of Oakland's dynamic urban mosaic.

Point of Action #2. In contrast to the Piers of San Francisco, Jack London Square lacks a strong sense of place. Its mixed-style buildings and open-air plan are preferable to the monotony of many contemporary developments, but this ad hoc mixture of colors, patterns, and incongruous buildings lacks an identifiable character. The look of the area is not deeply rooted in a single movement of the past, like the City Beautiful movement, so the Port of Oakland must take an active role in cultivating the Square's identity. Using the Green Movement as a vehicle, Oakland can present the waterfront in a more distinctive light.

With a heavily industrialized warehouse district surrounding it, Jack London Square should integrate the nearby buildings and activities they house with the natural environment, both the water and the land. Simply preserving green space or renovating buildings will not substantially change the character of the area unless those spaces are experienced by citizens. With bike trails and a multitude of water sporting activities, Jack London Square is not merely a leisure waterfront for passive enjoyment. It is also becoming an actively recreational harbor. Even a proposal for the new market building does not simply provide a place to dine or shop; it also offers visitors cooking classes. By distinguishing itself as a generator of active social engagement, rather than a passive vessel for non-working time, Jack London Square can achieve a greater sense of place without succumbing to superficial gestures.

Unlike many other waterfronts where consumption is the main activity, Jack London Square has the space and the time to establish itself as an everyday gathering place. It does not require a substantial amount of money or status. Distanced from downtown, it needs to provide more than just dining options. It must supply a distinctive experience. To create a place of meaningful activity is consistent with the principles of the Green Movement. Spending money on an experience, rather than on the consumption of goods, Jack London Square would produce less waste and discourage mindless spending, becoming a more environmentally and economically sustainable place in the minds of Bay Area citizens. One basic principle of the Green Movement is to "think globally, act locally."[37] If a visitor familiarizes him or herself with Jack London Square through personal interaction and purposeful skill-building, the area is remembered for what it offered. By fostering a connection between Jack London Square and its visitors, more meaningful than simply a meal or a shopping bag, those developing the Port of Oakland can better formulate exactly how they want Jack London Square to be experienced.

Point of Action #3. The problem of connectivity is perhaps more threatening to the sustainability of Jack London Square as an Oakland waterfront institution than any other concern, including the worldwide economic recession. The fact that the Square is a mile from the downtown is not an inherent predicament, because many city centers have developed away from prominent leisure locales. The problem is that in a dense, urban environment such as the Bay Area, a development hoping to become a destination must be linked to other nodes of activity. Particular focus must be concentrated on the one-mile stretch of Broadway connecting downtown Oakland with the bay.

Large sites for non-working time such as stadiums, zoos, or theme parks, are typically distanced from substantial urban activity because of the extensive parking and amenities necessary to accommodate a large number of guests. Patrons generally make an event out of these activities, perhaps spending a full-day enjoying the offerings. A marked difference between these sorts of developments and Jack London Square is that the latter provides both leisure and recreation, but at a smaller scale. Hence, people must be able to access the area easily, whether that be for a quick lunch or a half-day visit.

Due to the crime rates and public image of downtown Oakland, distancing the development from the center of activity is not inherently a bad formula. The Port and City of Oakland should, however, be able to link the two areas through varied modes of transportation, not simply the free "B" shuttle. This is another facet of the Green Movement which, if embraced fully, would strengthen the development as the physical manifestation of a social ideal. Oakland could do this by integrating the existing bike trail system, which is currently limited to the Bay shore, into the city fabric. Providing a safe and scenic transportation option – one which is also a recreational activity – should highlight Jack London Square as a destination in the planned 500-mile Bay Area trail network.

Data gathered in this study support the premise that connectivity within Oakland could also be enhanced through a more thoughtful development of Broadway. In the city center, restaurants, shops, offices, and other necessities line the middle of Broadway. If Broadway could be enhanced as a transitional corridor from a typical downtown street to the recreational waterfront at Jack London Square, the Square would not feel as cut off and separated from downtown as it is now. This sense of insuperable division is largely due to the presence of Interstate 880 overpass which bisects Broadway between the city center and the waterfront. By altering the passage under this overpass so that it becomes an appealing place to drive, bike, or walk, this immovable obstacle will feel less formidable. A renovation could be as simple as displaying public art, installing proper lighting, or ensuring that adequate safety precautions are visible. Making Jack London Square a distinct yet linked part of Oakland's physical form will enhance its sense of place while perpetuating the Green Movement as a city shaper.

Conclusion

Through the conduct of this study, I discovered that the two cities have faced similar challenges with different limitations when altering their waterfront. Though San Francisco is the identifiable destination of the area and Oakland is simply the *contra costa*, the desire to create an urban waterfront which locals and visitors alike could enjoy is a central motive for both cities' revitalization efforts. Both waterfronts boast unique culinary experiences, views of the Bay, and enjoyment on the water. The offices of the Port Authority both reside in these high-profile areas. Programmatically, market buildings in each, combined with weekly outdoor markets, form the centerpiece building. While this research has shown that the parallels between Oakland and San Francisco's waterfronts are numerous, it is impossible to ignore the stigmas affecting Oakland and larger long-term issues affecting both cities. Crime rates, industrial processes, and transportation concerns could hinder the success of Oakland's Jack London Square, while high-priced restaurants, limited open space, and high-levels of tourism potentially pose problems for the Piers in San Francisco. Further, both cities have been grappling with the difficulties of waterfront building and the most recent economic recession.

It is my hope that this study can provide the impetus for further investigation of how these cities and others can successfully redevelop their waterfronts, whether they consist of historic structures or still boast an active working shipping industry. San Francisco's preservation of its monumental City Beautiful buildings was central to the redesign of the Piers. How societal movements, such as the Green Movement, impact current redevelopment efforts is one area of further study. The burgeoning Green Movement is a driving force for many cities' urban revitalizations, due to the environmental benefits of density and infill. Similarly, investigations should be undertaken to determine how historic preservation can best be combined with adaptive reuse to produce culturally resonant, but contemporarily relevant urban neighborhoods. Further, research that identifies what type and style of building to promote when revitalizing cities, both on the water and inland, would be a resource to many cities. It is also important for future research to critically analyze the limitations of developing according to Green Movement priorities. Wisely utilizing existing features of a city to its full

potential redevelopments is key to creating or recreating a strong, identifiable sense of place in some of the country's most at risk cities.

References

[1] Peter Hendee Brown, *America's Waterfront Revival: Port Authorities and Waterfront Redevelopment* (Philadelphia: University of Pennsylvania Press, 2009). Also see, Carol Berens, *Redeveloping Industrial Sites: A Guide for Architects, Planners, and Developers* (Hoboken, New Jersey: John Wiley & Sons, Inc, 2011) and Henry Reader, "The City at the Edge," *Arcade* (Fall 2000): 18-19.

[2] Robert K. Yin, A *Applications of Case Study Research* (Newbury Park, CA, SAGE Publications, 1993). Yin is a commonly referenced primary resource for case study methodology.

[3] Linda Groat and David Wang, *Architectural Research Methods* (Canada, John Wiley & Sons, Inc., 2002). These characteristics are unique to a case study methodology as well as directly applicable to the built environment.

[4] Adriana Araujo Portella, "Evaluating Commercial Signs in Historic Streetscapes." Ph.D. in Urban Design dissertation. (Oxford Brookes University, Oxford, England, United Kingdom, 2007). A matrix linking research questions, objectives, and tactics as seen in Portella's dissertation.

[5] Barbara A. Kayzar, "Analyzing the Revitalization Outcomes in Downtown San Diego." Ph.D. dissertation. (University of California, Santa Barbara and San Diego State University, 2006). The term "actors" as used for identification of interviewees is used within the conext of actor network theory (ANT).

[6] J. Amos Hatch, *Doing Qualitative Research in Education Settings.* (Albany: State University of New York, 2002), 72-116. Essential questions are considered the main focus of the study. Supplementary questions are defined as questions that relate to essential questions, but come from a slightly different angle. Probing questions are designed to persuade interviewees to talk about something specific.

[7] According to Hatch, bracketing includes personal thoughts and opinions to supplement the objective observations

[8] According to Hatch, organizing comparable interview data into a common form creates a more efficient method for triangulation. Ibid.

[10] Michael R. Corbett, *Port City* (San Francisco: San Francisco Architectural Heritage, 2010).

[11] Oakland's history

[12] Port of San Francisco, "Chapter 1: Waterfront Form," in the *Waterfront Design & Access Element* of the *Waterfront Land Use Plan*, http://www.sf-port.org/ftp/ uploadedfiles/about_ us/ divisions/planning_development/WaterfrontForm.pdf (accessed January 30, 2011). Finger piers are defined as piers which extend from the land surface into the Bay.

[13] According to the history in Corbett's *Port City*. Ibid.

[14] Woodruff Minor, *Pacific Gateway: An Illustrated History of the Port of Oakland*, Oakland: Port of Oakland, 2000.

[15] According to Minor in *Pacific Gateway*. Ibid.

[16] According to Corbett, the City Beautiful movement is defined as a general improvement effort for American cities which began with the World's Colombian Exposition in Chicago in 1893. Specific qualities of the City Beautiful movement include "ornamental streets, established cornice heights, monuments and fountains, and monumental public buildings." Ibid., 152.

[17] For example, paper would be shipped in rolls or reams. Fruits and vegetables were shipped in manageably sized cartons.

[18] According to Minor. Ibid.

[19] *Design and Access: An Element of the Waterfront Land Use Plan* (San Francisco: Port of San Francisco, 1997), 92.

[20] Daniel Dyer, *Jack London: A Biography* (New York: Scholastic Press, 2001).

[21] According to Minor in *Pacific Gateway*. Ibid.

[22] Jasper Rubin, *A Negotiated Landscape: The Transformation of San Francisco's Waterfront since 1950,* quoted in Corbett's *Port City*. Ibid.,168. The available northern waterfront sites were considered too "complex and restrictive" to be able to adequately adapt them for modern industrial needs

[23] Daniel M. Bluestone, "Detroit's City Beautiful and the Problem of Commerce," *Journal of the Society of Architectural Historians*, Vol. XLVII, No. 3 (1988): 245-62. Also see, William H. Wilson, *The City Beautiful Movement (Creating the North American Landscape)* (Baltimore: The Johns Hopkins University Press, 1989).

[24] Jerry Yudelson, *The Green Building Revolution* (Washington DC: Island Press, 2008) 1-12. Also see, Philip Shabecoff, *A Fierce Green Fire* (Washington DC: Island Press, 2003).

[25] Omar Benjamin, "Building Oakland" (speech, San Francisco Business Times Oakland Structure Event, Oakland, CA, December 1, 2006).

[26] The Bay Trail Project, http://www.baytrail.org/baytrailplan. html#plansummary (accessed February 20, 2011).

[27] Simon Snellgrove (founder, Pacific Waterfront Partners, LLC), in discussion with the author, January 2011.

[28] Steve Worthington (architect, RMW Architecture), in discussion with the author, January 2011.

[29] Chris Metinko, "Free Downtown Oakland Shuttle Unveiled," *Contra Costa Times*, August 5, 2010.

[30] James Howard Kunstler, *The Geography of Nowhere* (New York: Touchstone, 1993). Christian Norberg-Schulz*, Genius Loci* (New York: Rizzoli, 1979).

[31] Two of the three restaurants tout local, sustainable menu options, a growing social movement that has had a strong presence in California. The third restaurant, La Mar, offers Peruvian dishes, mirroring San Francisco as a melting pot of cultures from around the world.

[32] Jerry Yudelson, *The Green Building Revolution* (Washington DC: Island Press, 2008) 1-12.

[33] Jonathan Kauffman, "Jack London Square Courts Foodies; But will Harvest Hall be a destination or a food court?" *East Bay Express*. November 24, 2004. Angela Woodall, "New Plans for Oakland's Jack London Square," *Contra Costa Times*, December 3, 2010.

[34] James Temple, "Developers Roll Dice on Oakland, California's Retail Draw," *Contra Costa Times*, November 17, 2004.

[35] Michael Hough, *Out of Place* (New Haven: Yale University Press, 1990).

[36] The City of Oakland, itself, recognizes its reputation of "high crime and underperforming schools" which makes "business attraction a long-standing challenge." Build a Thriving Economy, http://www2.oaklandnet.com/Government/o/CityCouncil/o/District4-LibbySchaaf/s/EconomicDevelopment/index.htm (accessed March 1, 2011).

[37] Jack London Square's notability as a catalyst development is reaffirmed by remarks by the Executive Director of the Port of Oakland, Omar Benjamin. Ibid.

[38] Patrick Geddes, *Cities in Evolution* (New York: H. Fertig, 1968). This is the first work to use the phrase "think globally, act locally."

Mentor Comments: Because Annie's complete thesis could not be published, Professor Kim Sexton's comments provide an overview of the more comprehensive project that led to this article.

Annie Fulton's research on the contemporary state of the ports of San Francisco and Oakland is both topical and incisive. In this article, which is the outcome of her Honors thesis, this senior architectural studies major asked two overriding questions: how it is that the ports of two great American cities of about the same age and on the same West Coast bay have come to utilize their waterfronts so differently, and in what ways could the successful redevelopment of the port of San Francisco serve as model for the port of Oakland. At first glance, the answers might seem to be predetermined from the start: Oakland's notoriety as a dangerous and blighted city would seem to doom any revitalization initiative before it began, with or without the exemplar of the shining city of San Francisco across the bay. But, given her training in architectural studies, as well as her minor in environmental sciences, Ms. Fulton would not accept popular misconceptions at face value. With her academic focus on interfaces between the natural and the urban, as well as her keen interest in the San Francisco Bay Area, she proceeded with a scientific case study of the ports of San Francisco and Oakland, traveling to the Bay Area in summer 2010 and again over the holiday break in December. Ms. Fulton and I express our appreciation to the University of Arkansas Honors College, which awarded her two Undergraduate Research Grants and one Honors College Travel Grant, to assist her in completing her investigations in California.

Armed with well-developed criteria and questionnaires, she interviewed city planners, port commissioners, architects, and developers involved with the port projects. She logged on-site observations about daily use of the ports by inhabitants, including circulation patterns and activities. Visual documentation focused on specific areas of the ports: the Piers in San Francisco and Jack London Square in Oakland. While many professionals interested in the re-development of city ports are typically concerned with commerciability, Ms. Fulton's approach was distinctive in that she investigated the degree to which harbor settings form part of a city's identity, and on the roles nature and culture have played, and will continue to play, in the successful conversion of industrial zones into liveable places.

The conclusions of her study culminate in three points of action for Oakland's Jack London Square. Her first and most innovative point is urging the port authority of Oakland to embrace the Green Movement as a catalyst for urban development in much the same way that San Francisco had utilized the City Beautiful reform philosophy in the early 1900s (and, surprisingly, as Ms. Fulton demonstrated, in the late 1900s!). Secondly, she offers a creative proposal for replacing a trend toward frankly ingratiating tourism in Jack London Square with a strategy for fostering an authentic sense of place for residents and visitors alike. Lastly, she details steps to be taken to reconceptualize Broadway, a largely deserted connective thoroughfare between the port and downtown Oakland.

As a mentor, I was very impressed by the initiative Ms. Fulton exhibited not only in formulating her project but in conducting research independently and far from campus. Due to the inherently transdisciplinary character of the project, this researcher had to overcome many conceptual and practical difficulties on her own in order to bring her work to a successful conclusion. Because the subject is so topical, she had few precedents to follow. Studies like it are part of global efforts of the design professions, partnering with hard sciences and social sciences, to improve and save "obsolete" areas of cities and towns. In fact, just last summer, the Museum of Modern Art in New York featured an exhibition entitled, "Rising Currents: Projects for New York's Waterfront," which, like Ms. Fulton's thesis, imagines new ways to occupy a harbor. In many such proposals, "soft" infrastructures (public interfaces, computer technologies) meet the old-fashioned, hard infrastructure to serve the demands of sound social and natural ecologies. Her thesis – as well as the 2011 University of Arkansas Undergraduate Research Award – makes her a competitive candidate for a wide range of graduate programs with their growing emphasis on interdisciplinarity in professional education. I am confident that Ms. Fulton will one day be in a cadre of professionals whose creative solutions dramatically improve the relationship between people and their natural and cultural environments.

IMPLEMENTING A FOOD WASTE TO COMPOST PROGRAM AT THE UNIVERSITY OF ARKANSAS: AN ECONOMIC FEASIBILITY ANALYSIS

By Zoe Teague
Department of Crop, Soil, and Environmental Sciences

Faculty Mentor: Dr. Jennie H. Popp
Department of Agricultural Economics and Agribusiness

Abstract

The University of Arkansas Fayetteville (UAF) is actively pursuing ways to increase sustainability on campus. Through the establishment of the Sustainability Council and campus centers, multiple projects are attempting to reduce the carbon footprint at UAF. One particular study is designed to eliminate food waste on campus through composting. The purpose of this study was to evaluate and project the economic savings of implementing a food waste composting system using Earth Tubs. Earth Tubs are an in-vessel electrical composting system capable of diverting up to 150 pounds of organic material daily with minimal odor. Results suggest that composting food waste from one dining hall only over the 15-year life of the project will likely result in an overall increase in food waste disposal costs. However composting waste from all three resident dining halls will likely reduce food waste costs for UAF over the life of the project.

Introduction

In February of 2007, the University of Arkansas Fayetteville (UAF) signed the American Colleges and Universities Presidents' Climate Commitment Plan (University of Arkansas, 2007). As part of this plan, the University Sustainability Council has actively searched for ways to reduce the negative environmental impact of the campus. Many efforts have been made in pursuing this goal, and managing food waste has been one suggested area of improvement.

As far back as can be verified, all food waste generated by the UAF dining facilities has been sent to landfills. This contributes to two types of negative externalities. An externality is a spillover effect that extends to a third party outside of the market, in this case UAF. Negative externalities generate costs to a third party or society (Callan and Thomas, 2007). First, the transportation of wastes to a landfill creates carbon dioxide emissions. Second, methane is generated when the food decomposes in the landfill. Methane is a by-product of microbial activity released when food waste breaks down (Lundie and Peters, 2005). One way to reduce the occurrence of these negative externalities is to implement an onsite-composting program for dining facilities' food waste. However, research related to the costs and benefits of this alternative waste disposal system is needed in order to consider a change of practice across campus. The purpose of this study was to provide an assessment of the economic costs and benefits associated with the current food waste disposal program on the UAF campus as compared to those of an on-site composting system.

Background

A Student-Led Feasibility Study – Earth Tubs for Composting

In Fall 2008, a team of UAF students conducted an initial feasibility study for composting pre-consumer food waste from the UAF dining halls. This study consisted of research into similar institutions and their food waste diversion efforts and determination of the most environmentally and economically sound method of food waste diversion for UAF. Several different options were explored, and it was determined that "Earth Tubs" provided one low-cost means of composting food waste on our campus. With student assistance at the conclusion of this study, the low cost purchase of two "Earth Tubs" to be used to implement this program was secured.

Earth Tubs are large self-contained, electrically powered composting tools (Green Mountain Technologies, 2006). Each Earth Tub has the potential of diverting 150 pounds of organic material daily with minimal odor (Green Mountain Technologies, 2006). Earth Tubs are 3 cubic yards in volume and have an electrically powered auger motor in the middle that moves throughout the tub to turn the compost and allow proper aeration. The tubs contain a bio-filter (Figure 1) to filter exhaust and liquid leachate (liquid run-off from the food waste in the tubs) from the Earth Tubs. The bio-filter contains dry organic matter and is used to control odor (Arnold, 2010).

To determine the optimal food waste diversion method for the UAF, composting initiatives at other universities were studied. Several other peer (in size) institutions such as University of California Santa Cruz (Grobe, 2001), University of Montana (DeLuca, 2004), and University of Oregon (Sims, 2004) have successfully implemented Earth Tub composting systems.

The University of North Carolina at Charlotte (UNC-C) is a campus of over 26,000 students. Earth Tubs have been in use there since 1999 using the same model of Earth Tubs as UAF. This operation was visited in the Fall of 2010 to observe operations and management logistics. At the highest volume, their Earth Tubs were able to accept 300 pounds of food waste per day (Arnold, 2010). To compost more efficiently with an uninterrupted stream of food waste, it is necessary to have two Earth Tubs, so the food waste can be rotated between the tubs. At 300 pounds per day, the Earth Tubs operate on an 18-21 day cycle with 9-10 days of filling Earth Tub A followed by 9-10 days of filling Earth Tub B while Earth Tub A "cures." It was determined that the UAF Earth Tubs would be able to operate on a similar cycle since the models were identical.

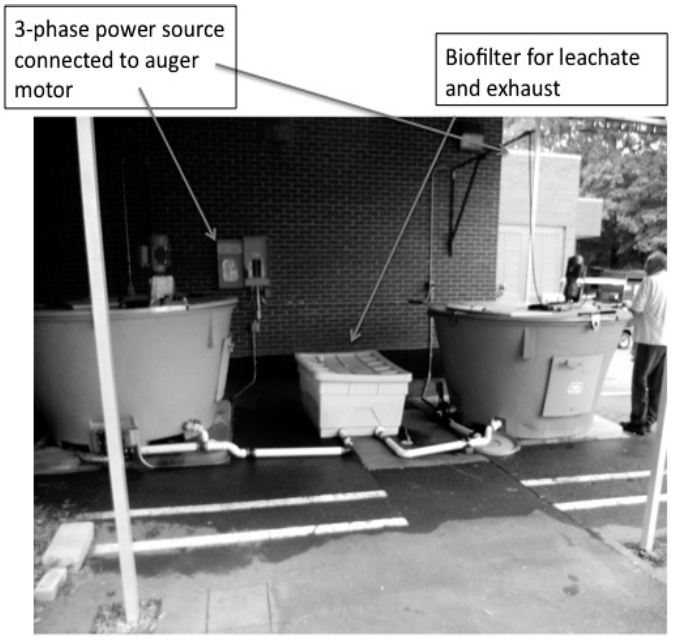

Figure 1: Earth Tub operation at UNC-C. October 2010.

Current Food Waste to Compost Pilot Project

After the Fall 2008 study, the various stakeholders – Chartwells, Facilities Management and the Division of Agriculture – met to discuss logistics, responsibilities and timelines for implementation of a pilot project using Earth Tubs for composting. Many challenges arose including 1) identification of Earth Tub installation location, 2) transportation of food waste to compost vessels, 3) labor to dedicate to the project, and 4) adequate funds to cover costs of project start up. Most challenges were overcome with the exception of funding. Without adequate financial support, the project stalled. In the Summer 2010, after active fundraising efforts, funds were collected from the Associated Student Government Executive Budget, the Associated Student Government Senate, the Residents' Interhall Congress Senate, the Office of Student Affairs, Facilities Management, the Office of the Provost, and the UA Division of Agriculture. Financial support from student-supported groups totaled over $10,000; all funds collected totaled over $16,000.

The current food waste to compost project entails the collection of food waste from the largest dining hall on campus, the Northwest Quad (NWQ). The UAF Campus has coordinated composting efforts through several organizations on campus including Chartwells Dining Services, Facilities Management, and the UA Division of Agriculture. The project began in April 2011 as a pilot study to identify the operating efficiency of working with the Earth Tubs, including transportation, the input ratio of food waste to dry carbonaceous material, and the demonstrated need of the end compost result as a soil amendment. If the pilot project is economically efficient, food waste from the two other dining facilities on campus (Brough Commons and Pomfret Dining Hall) will be included.

These three facilities produce approximately 95% of campus food waste (Chartwells, 2011). Of that quantity, approximately 90% is post-consumer food waste. Post-consumer food waste is defined as all waste that has been served to a customer, but not consumed (Arnold, 2010). The remainder of food waste is pre-consumer, mostly kitchen preparation waste such as potato peelings, lettuce clippings, etc. (Zemke, 2008). Pre-consumer food waste has not been served to customers.

The majority of institutions with an Earth Tub Composting system install Earth Tubs on food service sites. However, due to space restrictions, Earth Tubs at the UAF have been installed at the UA Division of Agriculture, about 1.5 miles north of the main campus. At the start of the pilot project, pre and post-consumer food waste is being collected from the Northwest Quad Cafeteria only by Chartwells staff and is placed in sealed 5 gallon buckets.

This food waste is taken from the Northwest Quad 3 days a week to the Farm, the UA Division of Agriculture Research Facility on Highway 112 (approximately 1 mile north of UAF Campus) (Brown, 2011). The estimated mileage spent per week in this activity is 30 miles (Brown, 2011). At the Farm, the Composting Coordinator (20 hours per week position) is responsible for mixing the food waste with the dry carbonaceous material (initially, sawdust from the School of Architecture) and collecting input-data to determine the optimal ratio of food waste to dry carbonaceous material (FW: DCM). Once the appropriate composting technique is identified, it is expected that pre and post-consumer food waste will be collected from all three dining halls: Pomfret Dining Hall, Northwest Quad Cafeteria, and Brough Commons.

While this current project focuses on waste from campus dining halls, there is other food waste production on campus at Greek houses, the Arkansas Student Union, athletic events, and other events catered by Chartwells. Earth Tubs are merely a starting point for developing a sustainable composting system for all food waste, because coordinating the logistics of food waste transport with these other entities has not yet been arranged. The ultimate goal of the UAF is to become a zero-waste institution. This would be consistent with the American Colleges and Universities Presidents' Climate Commitment Plan, which requires the diversion of 100% of food waste.

Cost-Benefit Analysis

Cost benefit analysis (CBA) is a tool that is used to evaluate benefits and costs to a society, in this case, UAF as a whole (Callan and Thomas, 2007). The United States federal water agencies, principally the Bureau of Land Reclamation and the U.S. Army Corps of Engineers, were among the first to make use of CBA in water-related projects. The Federal Interagency River Basin Committee produced the first guide to CBA in 1936 with the Flood Control Act, describing the costs and benefits related to flood control projects (Hanley & Spash, 1993). In 1952, a similar document was produced with the aim of replacing the Flood Control Act called Budget Circular A-47. These two publications were the first documents inspiring academic interest in developing CBA for projects suggesting environmental improvement (Eckstein, 1958). In 1981, Presidential Executive Order 12291 was devised; it explicitly required the application of CBA to all new environmental regulations in the U.S. (Hanley and Spash, 1993). CBA can capture and express in a single dimension (monetary

units) many, but never all, of the effects of environmental projects (Johanesson, 1993).

A full CBA would include both explicit (monetary) and implicit (non-monetary) costs and benefits (Callan & Thomas, 2007; Field, 1997). Explicit, or market value, costs and benefits are those to which a monetary value can be assigned. An example of typical explicit costs associated with a food waste to compost system could include installation of an in-vessel composting unit. An example of a typical explicit benefit could be cost savings incurred from landfill tipping fee avoidance. Implicit costs and benefits are both difficult to fully identify and to place into monetary terms. Examples of implicit benefits and costs respectively include the reduction in carbon and methane emissions achieved by diverting food waste from the landfill and the reduced convenience for dining hall staff. In CBA, a discount rate is used to place all costs into their present value so that total costs of each program can be compared. The discount rate was determined based on projects of similar nature. The present value formula is expressed as:

$$NPV = \sum_{t=1}^{T} PVB - PVC \quad [1]$$

$$PVB = \sum_{t=1}^{T} \frac{B_t}{(1+r)^t} \quad [2]$$

$$PVC = \sum_{t=1}^{T} \frac{C_t}{(1+r)^t} \quad [3]$$

where NPV is present value of net benefits, t=1 to T represents the time period, PVB is present value of benefits, B is total benefits, PVC is present value of costs, C is the total costs, and r is the discount rate.

In order to evaluate the true costs and benefits of this project, the Marginal Social Cost (MSC) and Marginal Social Benefits (MSB) must be evaluated as:

$$MSC = MPC + MEC \quad [4]$$

$$MSB = MPB + MEB \quad [5]$$

where MPC is marginal private costs, MEC is marginal external (or externality) costs, MPB is the marginal private benefits, and MEB is the marginal external benefit. Often, explicit benefits and costs are captured through marginal private benefits and marginal private costs, respectively. Implicit costs and benefits are usually captured through the marginal external costs and marginal external benefits, respectively. In the case of analyzing the economic feasibility of implementing Earth Tubs, a CBA of the explicit, or market value costs and benefits, is simpler to devise than the non-market values. If implicit costs and benefits cannot be measured economically, they must at least be acknowledged and some estimation of the value can be useful in determining overall whether or not total benefits (explicit and implicit) outweigh the total costs of the project. The benefits of the earth tub project will outweigh the costs if the following statements hold true:

$$NPV \geq 0 \quad \text{or} \quad [6]$$

$$PVB/PBC = 1 \quad [7]$$

An interactive spreadsheet (Rice University, 1998) was also used in the calculation of the CBA. The workbook divides the costs and benefits of the composting program into four categories: 1) Start-up Costs - one time costs associated with the acquisition and installation of the Earth Tubs); 2) Recurring Costs - costs to operate and maintain the Earth Tubs over time; 3) One-time Benefits – one time savings associated with the Earth Tubs; and 4) Recurring Benefits – labor, waste disposal and other costs that are avoided annually due to Earth Tub activities. The workbook also shows the mechanics of the Net Present Value Calculation considering these categories, which is useful in estimating value of the project over the expected life of the Earth Tubs.

Methods

Cost-Benefit Analysis

The first step in this project was to perform a cost benefit analysis. The following assumptions were made to conduct the analysis:

1) As Earth Tubs are expected to last 15 years, the projected life of the project is from 2011to 2026 (Arnold, 2010).
2) Earth Tubs are assumed to be operational for 42 weeks of the year based on peak student presence on campus (Harrel, 2011).
3) The amount of food waste generated remains steady across the 15-year period. While student numbers are expected to increase, efficiencies in food waste management are expected to improve as well.
4) Two scenarios were considered. In the first, the total amount of estimated food waste from the three dining halls – 250,000 pounds annually – is assumed to be composted. In the second, only 100,000 pounds annually is composted, as this is the maximum amount that can be composted without a permit from the state (Brown, 2011).
5) Many of the operational costs will not vary by pounds of food waste diverted (e.g., energy is still needed to operate the earth tubs and labor is still needed to transport food waste and operate the tubs, regardless of how much is composted). Therefore, most costs (with the exception of mileage traveled due to additional pickups) are assumed constant across both food waste input rates (scenarios one and two). These constant costs represent a small percentage of overall costs of the project.

In the CBA, all costs and benefits are compiled and divided into market values and non-market values. Not only does disposal of the waste via landfills add costs to UAF, it also results in a missed opportunity for grounds management. The UAF campus spans 345 acres in Fayetteville including the University of Arkansas Agriculture Experiment Station. These grounds constitute an ongoing need for compost and fertilizer for seasonal landscaping and agricultural research plots. The compost produced by the Earth Tubs is expected to be used primarily by researchers on the Arkansas Agriculture Experiment Station.

Costs: Market Value

Full market value costs for implementing the Earth Tubs can be divided into four subsections: initial installation, operations/ maintenance logistics, compost curing, and transportation of compost to final destination. *Initial installation costs* include the procurement of the Earth Tubs and their installation (labor, water/ sewer utility access, electricity access) in their final location. *Operations/maintenance costs* include 20 hours/week labor and electricity costs. *Compost curing costs* include transportation of compost from Earth Tubs to covered curing location (6 month curing period), labor for turning of compost with shovel at 3-month period, and testing of compost before final use. Finally, *transportation of compost to final use location costs* include transportation of compost from curing location to final use location (either on UAF campus or to UA Farm research plots).

Because the plot of land used for the Earth Tubs was so small in size compared to the entire UA Farm space, the opportunity costs of this land area were not considered in this study. Identification of all costs was acquired from various departments of Facilities Management, Chartwells Food Service, and Environmental Sciences professors.

Costs: Non-Market Value

The only non-market value cost associated with this project is a reduced convenience for dining hall staff imposed by the new protocols for disposing of food waste. Disposing of food waste via landfill is much more convenient for dining hall and waste management teams.

Benefits: Market Value

The addition of full market value benefits includes cost savings from reduced landfill tipping fees and reduced compost purchases for UAF Grounds. While other studies cite some labor savings, this is not expected for the compost project. Any labor savings in waste disposal, for example, are expected to be offset in labor needed (if any) to divert food waste to the bucket containers. The quantity of compost and water saved as well as the dollar value of all benefits was acquired from the involved stakeholders, including Chartwells, UAF Facilities Management and UAF Grounds Management. Chartwells' estimates of annual food waste were used for 2011-2026 (Zemke, 2011). Average landfill tipping fees for 2005-2010 were combined with food waste projections to estimate in part future tipping fees. These and all costs were inflated annually using a five-year average inflation rate of 2.11% (Bureau of Labor Statistics, 2010). A discount rate of 5% was also assigned based on previous studies (Rice University, 1998).

Benefits: Non-Market Value

The general environmental benefits include reduced carbon emissions and methane emissions generated by diverting food waste to the landfill. The non-market values were not projected explicitly in this study. However, these benefits are discussed qualitatively in the CBA.

After the two CBAs were conducted, sensitivity analyses were run to determine: 1) the year in which a permit must be acquired (if any) to compost all food waste such that the NPV of the project is positive; and 2) the allowable cost of the permit process over the life of the project that would allow maximum benefits of a composting project.

Results of Cost-Benefit Analysis

This section presents the results of the cost benefit analyses under the two scenarios. Scenario one assumes 250,000 pounds of food waste are composted annually. Scenario two assumes only 100,000 pounds of food waste are composted while the rest is land filled, as this is the plan for the first year of the project.

Start-Up Costs

The start-up costs for this project included procurement, electrical installation, site preparation, and plumbing (Table 1). Labor costs were factored into these categories, but due to accounting methods practiced by Facilities Management, it was not possible to break them out individually (Conroy, 2011). Procurement costs included the purchase and transportation of the Earth Tubs to their location at the Farm as well the architectural design fee for the concrete slab and electrical connections. Total start-up costs were $4,430. Electrical installation included installing the electrical connects and locating fees for a total of $7,146. Site preparation costs of $9,076 consisted of dirt and concrete work at the site of the Earth Tubs. While the CBA spreadsheet allows for water sourcing costs, water source was already present at this site and therefore there were no additional water sourcing costs associated with this activity. Plumbing costs of $6,213 included location, materials and sanitary sewer installation. Start-up costs totaled $26,867 (Table 1). Because these start up costs are not related to food waste amounts, they are the same for both scenarios.

Table 1: Start-up costs for both scenarios one and two.

Start-Up Costs		Monetary		Notes
Earth Tubs				
	Total Cost for 2 Earth Tubs	$3000.00		
	Procurement	$953.51		
	Design	$477.09		
	Total		**$4,430.60**	
Electrical Installation				
	Locator	$274.11		
	Electrical Service	$6,871.94		
	Total		**$7,146.05**	
Site Preparation				
	Dirtwork	$4,163.49		
	Concrete work	$4,913.32		
	Misc.	-		
	Total		**$9,076.81**	
Water Source	Cost of water source	$0.00		
	# of sources needed	$0.00		
	Total		**$0.00**	already present
Plumbing				
	Locator	$223.28		
	Materials	$2,505.34		
	Sanitary Sewer	$3,485.09		
	Total		**$6,213.71**	
Total			**$26,867.17**	

Operational Costs

The annual operational costs (Table 2) for this project include the electricity costs and maintenance labor. Electricity is needed to run the auger and the blower. Based on Facilities Management and University of North Carolina at Charlotte estimates, annual electricity usage over the 42 active weeks is approximately 374 kwh for a cost of $22. Labor costs were calculated at 20 hours a week for 42 weeks ($6720). In scenario one, transportation costs totaled $25 per year. However with the reduced food waste collection for scenario two, transportation costs fall to $12 per year. Total operational costs are $6768 for scenario one and $6755 for scenario two. Combining start up costs and operational costs, the total estimated costs of this project in year one are $33,609 for scenario two and $33,622 for scenario one.

Table 2: Operational costs for both scenarios one and two, respectively.

Operational Costs		Scenario One	Scenario Two
Electricity			
	Auger consumption (kwh)	$134.19	$134.19
	Blower consumption (kwh)	$239.90	$239.90
	Total consumption (kwh)	$374.09	$374.09
	Cost per kwh	$0.06	$0.06
	Total	$22.45	$22.45
Maintenance	Labor 20 hours/week	$6,720.00	$6,720.00
	Mileage for pickup	$25.20	$12.60
	Total	$6,767.65	$6,755.05

One-Time Benefits

No benefits were deemed reasonable for the UAF campus. In some cases, it is possible that the pulper/disposal in the dining halls could experience reduced usage or be discontinued (Table 3). However, in this case, the pulpers will stay in use to reduce the amount of moisture in the waste before it is moved to the Earth Tubs. This will help to ensure a more efficient composting process.

Table 3: One time benefits for both scenarios one and two.

One-Time Benefits		Monetary	Notes
Pulper Displacement			Pulper will not be displaced; will continue use, so no benefit
	# of pulpers	$0.00	
	Cost of pulpers	$0.00	
	Tubs needed per pulper	$0.00	
	Total	$0.00	

Recurring Benefits

The annual recurring benefits for this project include the cost-savings from avoiding the purchase of imported compost.

Table 4: Recurring benefits for scenarios one and two, respectively.

Recurring Benefits		Scenario One	Scenario Two
Compost Value			
	Pounds of food waste and bulking agent	333,333	133,333
	Pounds of compost generated	200,000	80,000
	Tons of compost generated	100	40
	Cubic yards produced	133	53
	Price per cubic yard	$1.00	$1.00
	Total	$133.00	$53.00
Labor Saved			
	Food transport time	-	-
	Yard waste transport time	-	-
	Hours/week	-	-
	Total	-	-
Kitchen efficiencies			
	Labor saved with tubs	-	-
	Total	-	-
Plumbing cost avoidance			
	Monthly plumbing cost	-	-
	Average pipe breaks/year	-	-
	Average cost/pipe break	-	-
	% reduction due to composting	-	-
	Total	-	-
Dispose-all displacement			
	Cost per dispose-all	-	-
	Lifespan (years)	-	-
	Total	-	-
Disposal fees			
	Tons of food waste diverted	125	50
	Landfill cost/ton of food waste	$81.53	$81.53
	Total	$10,191.00	$4,077
Total		$10,324	$4,130

UAF receives its compost at very low cost from the City of Fayetteville, charged by cubic yard. Assuming UAF would collect as much compost as is generated by the Earth Tubs in one year, this fee would amount to $133 per year for scenario one and $53 for scenario two. The other benefit is the avoidance of landfill tipping fees of $10,091 for scenario one and $4,077 for scenario two based on an $81 per ton charge to institutions for food waste disposal (Wilkins, 2011). Other potential recurring benefits that are not relevant to UAF may include utility savings in dining halls and labor savings in waste management crews. As the program expands, these can be reevaluated in the future. The total benefits in the first year of the project are estimated to be $10,324 for scenario one and $4,130 for scenario two (Table 4).

Net Present Value

The NPV calculation includes the four categories of estimated costs and benefits: start-up costs, operational costs, one-time benefits, and recurring benefits. Based on the numbers provided previously, the net present value of the project in year one is -$23,310 for scenario one (Table 5) and -$29,492 for scenario two (Table 6). This is primarily due to the large start up costs in year one.

Table 5: NPV for scenario one.

Time	Costs	Benefits	Inflated Costs	Inflated Benefits	Net Benefits	Present Value of Net Benefits
0	$33,634.82	$10,324.25	$33,634.82	$10,324.25	$-23,310.57	$-23,310.57
1	$6,767.65	$10,324.25	$6,910.44	$10,542.09	$3.631.65	$3,458.71
2	$6,767.65	$10,324.25	$7,056.25	$10,764.53	$3,708.28	$3,363.52
3	$6,767.65	$10,324.25	$7,205.14	$10,991.66	$3,786.52	$3,270.94
4	$6,767.65	$10,324.25	$7,357.17	$11,223.59	$3,866.42	$3,180.91
5	$6,767.65	$10,324.25	$7,512.40	$11,460.40	$3,948.00	$3,093.36
6	$6,767.65	$10,324.25	$7,670.92	$11,702.22	$4,031.30	$3,008.22
7	$6,767.65	$10,324.25	$7,832.77	$11,949.13	$4,116.36	$2,925.42
8	$6,767.65	$10,324.25	$7,998.04	$12,201.26	$4,203.22	$2,844.90
9	$6,767.65	$10,324.25	$8,166.80	$12,458.71	$4,291.90	$2,766.60
10	$6,767.65	$10,324.25	$8,339.12	$12,721.59	$4,382.46	$2,690.45
11	$6,767.65	$10,324.25	$8,515.08	$12,990.01	$4,474.93	$2,616.40
12	$6,767.65	$10,324.25	$8,694.75	$13,264.10	$4,569.35	$2,544.39
13	$6,767.65	$10,324.25	$8,878.21	$13,543.97	$4,665.77	$2,474.36
14	$6,767.65	$10,324.25	$9,065.54	$13,829.75	$4,764.22	$2,406.25
15	$6,767.65	$10,324.25	$9,256.82	$14,121.56	$4,864.74	$2,340.02
				Total		$19,673.89

The net present value calculations revealed major differences depending on the amount of food waste collected. After the 15-year lifetime of the tubs, the NPV under scenario one totaled $19,673. The project breaks even in year 2019, eight years after the project begins. The majority of the savings from this project were found in the avoidance of landfill tipping fees, which averaged $10,091 annually. In scenario one, the benefits of this project outweighed the costs according to the NPV projection over the life of the project. Based on equation 6, since the NPV >0, scenario one of this project could be undertaken.

Table 6: NPV for scenario two.

Time	Costs	Benefits	Inflated Costs	Inflated Benefits	Net Benefits	Present Value of Net Benefits
0	$33,622.22	$4,129.70	$33,622.22	$4,129.70	$-29,492.52	$-29,492.52
1	$6,755.05	$4,129.70	$6,897.58	$4,216.84	$-2,680.74	$-2,553.09
2	$6,755.05	$4,129.70	$7,043,12	$4,305.81	$-2,737.30	$-2,482.82
3	$6,755.05	$4,129.70	$7,191.73	$4,396.66	$-2,795.06	$-2,414.48
4	$6,755.05	$4,129.70	$7,343.47	$4,489.43	$-2,854.04	$-2,348.02
5	$6,755.05	$4,129.70	$7,498.42	$4,584.16	$-2,914.26	$-2,283.40
6	$6,755.05	$4,129.70	$7,656.64	$4,680.89	$-2,975.75	$-2,220.55
7	$6,755.05	$4,129.70	$7,818.19	$4,779.65	$-3,038.54	$-2,159.43
8	$6,755.05	$4,129.70	$7,983.15	$4,880.50	$-3,102.65	$-2,100.00
9	$6,755.05	$4,129.70	$8,151.60	$4,983.48	$-3,168.12	$-2,042.20
10	$6,755.05	$4,129.70	$8,323.60	$5,088.63	$-3,234.96	$-1,985.99
11	$6,755.05	$4,129.70	$8,499.22	$5,196.00	$-3,303.22	$-1,931.32
12	$6,755.05	$4,129.70	$8,678.56	$5,305.64	$-3,372.92	$-1,878.17
13	$6,755.05	$4,129.70	$8,861.68	$5,417.59	$-3,444.09	$-1,826.47
14	$6,755.05	$4,129.70	$9,048.99	$5,531.90	$-3,516.76	$-1,776.20
15	$6,755.05	$4,129.70	$9,239.50	$5,648.62	$-3,590.96	$-1,727.31
				Total		**$-61,221.95**

However, in scenario two, where only a portion of food waste was composted, the NPV for the project was -$61,221. While the reduced tipping fees provided some annual benefit, they did not offset the labor costs associated with the project, thereby resulting in a net cost to the university each year for the life of the project. Without full consideration of the non-market costs and benefits, it is not possible to recommend that this project with only a partial collection of food waste be undertaken.

Sensitivity Analysis

It is clear from the above market costs and benefits analyses that composting only part of the university food waste will not offset the market costs of this project. Therefore sensitivity analyses were conducted to determine: 1) in what year a permit must be acquired to operate under scenario one such that the NPV of the project is positive; and 2) what is the maximum allowable market costs for a permit that would provide maximum project benefits to the university. Table 7 shows that, if the permit is acquired such that all food waste can be composted from the three dining halls beginning in 2014, the project will have a positive NPV, as long as the costs of the permit do not exceed a present value of $1,634 over the life of the project. Moreover, if this permit was actually acquired now, such that all food waste could be composted starting in 2012, the NPV of the project could increase to nearly $13,492 (Table 8) without consideration of the permit cost. The permitting process is complex and costly, and includes preparation of a geotech report, design and operation of services, and UA staff time to pursue the process with Arkansas

Department of Environmental Quality (Brown, 2011). If total costs of the permit are greater than $1,634 but less than $13,492, maximum market net benefits would be incurred if the permit was in place for 2012.

Table 7: NPV if permit is purchased in year 3 of the project; minimum year for purchase in order to have a positive NPV over the life of the project.

Time	Costs	Benefits	Inflated Costs	Inflated Benefits	Net Benefits	Present Value of Net Benefits
0	$33,622.22	$4,129.70	$33,622.22	$4,129.70	-$29,492.52	-$29,492.52
1	$6,755.05	$4,129.70	$6,897.58	$4,216.84	-$2,680.74	-$2,553.09
2	$6,755.05	$4,129.70	$7,043.12	$4,305.81	-$2,737.30	-$2,482.82
3	$6,767.65	$10,324.25	$7,205.14	$10,991.66	$3,786.52	$3,270.94
4	$6,767.65	$10,324.25	$7,357.17	$11,223.59	$3,866.42	$3,180.91
5	$6,767.65	$10,324.25	$7,512.40	$11,460.40	$3,948.00	$3,093.36
6	$6,767.65	$10,324.25	$7,670.92	$11,702.22	$4,031.30	$3,008.22
7	$6,767.65	$10,324.25	$7,832.77	$11,949.13	$4,116.36	$2,925.42
8	$6,767.65	$10,324.25	$7,998.04	$12,201.26	$4,203.22	$2,844.90
9	$6,767.65	$10,324.25	$8,166.80	$12,458.71	$4,291.90	$2,766.60
10	$6,767.65	$10,324.25	$8,339.12	$12,721.59	$4,382.46	$2,690.45
11	$6,767.65	$10,324.25	$8,515.08	$12,990.01	$4,474.93	$2,616.40
12	$6,767.65	$10,324.25	$8,694.75	$13,264.10	$4,569.35	$2,544.39
13	$6,767.65	$10,324.25	$8,878.21	$13,543.97	$4,665.77	$2,474.36
14	$6,767.65	$10,324.25	$9,065.54	$13,829.75	$4,764.22	$2,406.25
15	$6,767.65	$10,324.25	$9,256.82	$14,121.56	$4,864.74	$2,340.02
					Total	**$1,633.81**

Table 8: NPV if permit is purchased in year 2 of the project (2012); minimum year for purchase in order to have the maximum NPV over the life of the project.

Time	Costs	Benefits	Inflated Costs	Inflated Benefits	Net Benefits	Present Value of Net Benefits
0	$33,622.22	$4,129.70	$33,622.22	$4,129.70	-$29,492.52	-$29,492.52
1	$6,767.65	$10,324.25	$6,910.44	$10,542.09	$3,631.65	$3,458.71
2	$6,767.65	$10,324.25	$7,056.25	$10,764.53	$3,708.28	$3,363.52
3	$6,767.65	$10,324.25	$7,205.14	$10,991.66	$3,786.52	$3,270.94
4	$6,767.65	$10,324.25	$7,357.17	$11,223.59	$3,866.42	$3,180.91
5	$6,767.65	$10,324.25	$7,512.40	$11,460.40	$3,948.00	$3,093.36
6	$6,767.65	$10,324.25	$7,670.92	$11,702.22	$4,031.30	$3,008.22
7	$6,767.65	$10,324.25	$7,832.77	$11,949.13	$4,116.36	$2,925.42
8	$6,767.65	$10,324.25	$7,998.04	$12,201.26	$4,203.22	$2,844.90
9	$6,767.65	$10,324.25	$8,166.80	$12,458.71	$4,291.90	$2,766.60
10	$6,767.65	$10,324.25	$8,339.12	$12,721.59	$4,382.46	$2,690.45
11	$6,767.65	$10,324.25	$8,515.08	$12,990.01	$4,474.93	$2,616.40
12	$6,767.65	$10,324.25	$8,694.75	$13,264.10	$4,569.35	$2,544.39
13	$6,767.65	$10,324.25	$8,878.21	$13,543.97	$4,665.77	$2,474.36
14	$6,767.65	$10,324.25	$9,065.54	$13,829.75	$4,764.22	$2,406.25
15	$6,767.65	$10,324.25	$9,256.82	$14,121.56	$4,864.74	$2,340.02
					Total	**$13,491.94**

Cost-Benefit Analysis Challenges

This cost-benefit analysis could be challenged on two grounds. First, it lacks inclusion of non-market values. Second, there is no proof that the 5% discount rate is the appropriate rate for this project. These concerns are addressed below.

The values above only include market costs and benefits. A full cost-benefit analysis would also include the value of non-market costs and benefits. As mentioned earlier, non-market costs included reduced convenience to dining hall staff to separate the food. However it is not anticipated that this will pose a significant burden on the staff, particularly once the new protocols are learned. Further, the non-market benefits of this project are potentially quite large if one considers the reduced environmental impact associated with diverting the food waste from the landfill and could thereby increase the NPV of the project. Estimation of these benefits may provide a stronger argument for usefulness of scenario two.

This project adopted the 5% discount rate used by Rice University in their study in 1998. This is admittedly a dated study and therefore the discount rate may be inappropriate for this project. Since lower (smaller) discount rates will only increase the value of net benefits over time, the concern rests in identifying the discount rate that moves the NPV from a positive value to a negative value. Sensitivity analysis around the discount rate determined that, in order for the scenario one project to move from positive to overall negative net benefits, the discount rate would have to increase to close to 15.3%. For scenario two, no reasonable change in discount rate will move this project from negative to positive net benefits, given the overwhelmingly large start up costs relative to expected annual benefits. Therefore, a reasonable choice of discount rate that is different from the one used in this study is not expected to change the general results of the analysis.

Conclusions

This study marks the end of a two and half year effort to secure Earth Tubs and evaluate the feasibility of a food waste to compost project using these tubs at the University of Arkansas Fayetteville campus. Results of the analysis suggest that under scenario one (all three major dining halls participating), even without including the non-market net benefits of this project (which are expected to be large and positive), the Earth Tub project produces positive net benefits to the university over its expected 15-year life. However, more information is needed on the non-market costs and benefits associated with food waste to composting to determine whether the partial food waste collection will provide positive net benefits over the life of the project.

There are several opportunities for expansion and improvement of this project. First, a more accurate measurement of food waste and the ability to track actual labor associated with all activities is needed to identify costs better. Second, more accurate estimates of the compost usage at the UA Agricultural Research and Extension Center and UAF campus are needed. Third, estimates of the non-market benefits and costs associated with the project would provide a more complete analysis. Finally, the feasibility of moving earth tubs closer to dining facilities and incorporating the remaining 5% of food waste should be explored.

References

Arnold, F.L. (2010). University of North Carolina-Charlotte Director of Recycling. Personal Communication.

Callan, Scott J. and Janet M. Thomas. 2007. *Environmental Economics & Management: Theory, Policy And Applications*. Oklahoma City, OK: South-Western Publications.

Chartwells Dining Services. (2008) Sustainability Issues. Accessed online 30 September, 2008. http://www.myfiledock.com/pro_uploads/ChartwellsHigherEd/Savor_Newsletter_PDFs/Savor_Quarters_3-4.pdf

Conroy, William. (2011). UAF Construction Coordinator. Personal Communication.

Denise DeLuca, P.E.. Emergent Solutions. (2004). Food Waste Composting Demonstration Project - Dining Services. Missoula, Montana: Department of Environmental Quality. http://www.deq.state.mt.us/Recycle/2ndUMCompostingReport.pdf

Field, C.B. (1997). *Environmental Economics*. New York, NY: McGraw-Hill, 2nd Edition.

Green Mountain Technologies. (2006)"Earth Tubs".. Earth Tub Description. Whitingham, Vermont. http://www.gmt-organic.com/EarthTub/et-info.php

Hanley and Spash. (1993). *Cost Benefit Analysis and the Environment.* Northhampton, MA: Edward Elgar Publication Inc.

Harrel, Rachel. (2011). Manager, Northwest Quad Dining Hall. Personal Communication.

Johanesson, Per-Olov. (1993). *Cost-Benefit Analysis of Environmental Change.* New York, NY: Press Syndicate of University of Cambridge.

Karin Grobe. Organic Recyclers Anonymous. (2001). California Grey Bears Food Scrap Diversion Project FINAL REPORT. Santa Cruz, California: University of California at Santa Cruz. http://www.ciwmb.ca.gov/foodwaste/CaseStudies/Contracts/2000/GreyBears2.pdf

Lundie, Sven, and Gregory Peters. (2005). "Life cycle assessment of food waste management options." Journal of Cleaner Production 13 (3): 275-286.

McGlaughlin, Harold. (1992). *The Entrepreneur's Guide to Building a Better Business Plan.* New York, NY: Jon Wiley and Sons Inc.

Michael Sims, et al. University of Oregon. (2004). An Environmental Studies Service Learning Program Project in Cooperation with: The Erb Memorial Union University of Oregon Campus Recycling. Eugene, Oregon: University of Oregon. http://www.uoregon.edu/~recycle/PDFdocuments/EMUfinalReport.pdf

O'Hara, Patrick. (1995). *The Total Business Plan.* New York, NY: John Wiley and Sons Inc.

Purdy, Warren G. (1996) The Service Business Planning Guide: The complete handbook for creating a winning business plan for any service company. Boston, MA: INC. Business Resource

Rice University. (1998). Composting Pilot Project Accessed online 11 January, 2011 http://www.ruf.rice.edu/~envintrn/report99/enviroreport-body.html

University of Arkansas. (2007). "Climate Action Plan" (11 April, 2011). http://sustainability.uark.edu/University_of_Arkansas_Climate_Action_Plan.pdf

Zemke, Bill. (2011). Chartwells Manager. Personal Communication.

Mentor Comments: Although Zoe's article focuses primarily on the cost-benefit analysis she conducted for her honors thesis research, Professor Popp's comments place her work in the much broader context of a long-term commitment to exploring sustainability on campus through management of food waste.

This article is the culmination of a two and a half year research project focused on developing a food waste to compost program at University of Arkansas Fayetteville (UAF). In fall 2008, under Division of Agriculture faculty leadership, Zoe Teague and four other undergraduate students assessed the feasibility of composting food waste at UAF. During the semester long endeavor, they explored composting techniques used at peer institutions, spoke to local waste management officials, and gathered information related to UA cafeteria food waste volumes, weights, disposal costs. In the course of their investigations, the students found two idle Earth Tubs (composting vessels) at a Northwest Arkansas solid waste division and convinced the organization to sell those tubs to UAF at a fraction of their worth for use in a pilot UAF compost program. The students concluded, based on a preliminary analysis of food waste volumes and project costs, that a food waste to compost project utilizing the Earth Tubs could be a viable way to reduce campus waste and promote sustainability on campus and recommended a pilot project be initiated by the UA Sustainability Council in Fall 2009. Zoe opted to continue on with the project as the focus of her honors college thesis.

Financial and logistical constraints delayed the project. But Zoe, serving as student representative to the UA Sustainability Council, worked closely with others on campus (in Facilities Management, Chartwells Food Service, University Housing and the Division of Agriculture) to help identify a location for the composting vessels and facilitate coordination among the various entities that would be involved with the project. Additionally, after determining there was a $13,000 shortfall to support the installation, maintenance and operation needs of the project, she worked with student government, local businesses, faculty, as well as Division of Agriculture and campus administrators to raise the needed funds. She used her research funds to travel to an Earth Tub user for many years - the University of North Carolina Charlotte - to learn everything about the Earth Tub systems, from construction to waste collection, to compost generation, and their associated costs and benefits. This information guided much of the Earth tub installation at UAF. The pilot project, albeit smaller in scope (collecting 100,000 pounds of food waste, not the 250,000 pounds available), commenced in April with food being collected from one dining hall.

This manuscript focuses on a cost-benefit analysis that compares the benefits and costs of composting two different

amounts of food waste (that from one UAF student dining hall and that from all three dining halls) to landfill of the same food waste. While cost-benefit analysis is straightforward in theory, collection of the value of the costs and benefits associated with a program that has never before existed on campus. Zoe worked for weeks with Facilities Management, Campus Housing, Chartwells, Walmart, the City of Fayetteville and others to place dollar values on market costs and benefits and to identify on a qualitative basis the non-market costs and benefits. To do this required knowledge and skills in areas of economics, environmental science and even engineering. Her work is truly multidisciplinary and highly collaborative. Furthermore, as her analysis suggests, should University of Arkansas implement a compost project that utilizes all the food waste from the three dining halls on campus, the university not only can help reduce its negative environmental impacts but also can save money as well.

IMMIGRATION AND THE EXTREME RIGHT: AN ANALYSIS OF RECENT VOTING TRENDS IN WESTERN EUROPE

By Andrew Walchuk
Department of Political Science

Faculty Mentor: Jeffrey R. Ryan
Department of Political Science

Abstract

Western European politics have been marked over the last couple of decades by a fierce debate about the place of Europe's increasingly large immigrant population in society. Across the continent, far-right parties campaigning on nationalistic platforms opposing immigration have seen great electoral success. The debate is undoubtedly becoming more heated as more immigrants pour into the area, and these anti-immigrant parties seem to have established themselves in the political arena. Immigration does not appear to be slowing down at any point in the near future, so what is going to happen to these far-right parties as we move into the future? My research sought to answer this question and offer a more optimistic outlook on the situation. The most popular opinions view the relationship between immigrant population size and anti-immigrant electoral support as a simple positive linear correlation, meaning that there is little hope that the existing enmity will do anything but increase. I hoped to show that the relationship is, in fact, curvilinear. In the case of these immigrants, a curvilinear relationship would indicate strong xenophobic voting until the immigrant population becomes so large that the non-immigrants become more accustomed to the presence of those that they formerly viewed as "outsiders." What I discovered was that an alternative hypothesis provided the best description. As the immigrant population increased, the support for the far right actually decreased. This "contact hypothesis" shows that the increased population leads to increased interaction with immigrants and the weakening of stereotypes perpetuated by the extreme right.

Introduction

As Europe moves forward into the 21st century, it faces a stark new reality. The end of the Cold War, combined with the burgeoning integration that would lead to the European Union as we know it today, raised hopes of a more peaceful and successful Europe for the new millennium. However, issues of migration did not take long in exposing deep fault lines in this new, unified European community. Conflicts are no longer along ideological lines of capitalism versus communism, but rather along lines of ethnicity and religion. Strong national allegiances are slowly giving way to concerns and questions about the very nature of the nation's identity. The undeniable truth of the past several decades is that the face of Europe is changing, facilitated in part by historically low birth rates among so-called "ethnic" Europeans.

Responses to these demographic shifts have varied, with some viewing them as an opportunity for further development, and others seeing them as a challenge to perceived European values. Some of the most vehement reactions come from far-right anti-immigrant political parties. Though these groups have yet to achieve governing status in most governments, their voices have proven to be very influential in the immigration debate. A mere glimpse of recent headlines shows this to be true, as a series of measures have been implemented that disproportionally affect immigrant communities.

In recent years, European immigration research has focused on the motivations for anti-immigrant attitudes. Existing studies have examined the relationship between these attitudes and the size of the outgroup, in this case, immigrants. This relationship is typically explained as a result of one of two phenomena: competition or contact theory, each of which is discussed further. My aim was to propose and subsequently test a set of hypotheses which reconcile these two theoretical approaches by incorporating elements of both into a single parsimonious model. At the center of my proposed model and the innovative aspect of my research, is the replacement of the linear models used in both contact and competition theories with a curvilinear description of the research question proposed here: what is the relationship between levels of electoral support for far right anti-immigrant parties and the size of the immigrant population? I turn first to a discussion of the patterns of migration in Europe and then of the political responses to those patterns.

History of the Migrant Influx

The massive migration that marked the second half of the 20th century in Europe was born out of the rubble of the Second World War. The reconstruction of a continent ravaged by war required more than the mere replacement of damaged and destroyed buildings. Entire economies and societies had to be rebuilt. While much of the money for the reconstruction efforts was supplied by the United States through the Marshall Plan, there was not enough labor to support the rapidly growing economy of the reemerging Europe. As a result, many countries began to look beyond their borders to find new workers, actively recruiting through two primary methods: guest worker programs and colonial migration regimes.

The clearest example of a nation that used the guest worker approach is Germany, whose program for *Gastarbeiter* brought in workers from southern Europe and beyond, particularly Turkey. The government established a series of bilateral agreements with each country to allow workers to move to West Germany in order to support and drive the economic boom. Between 1955

and 1973 alone, the West German government recruited over 2.5 million of these guest workers (Boswell, 2005). Under the plan, workers were to return to their home countries during economic slowdowns, with the hope of returning to Germany once the economy rebounded. Initially, the *Gastarbeiter* program saw spectacular success, and during the first major postwar recession, many did return to their homelands (Hansen 2003).

The great colonial powers of the late 19th and early 20th centuries faced many of the same issues as Germany after the war, but approached the recruitment of labor in a different way in order to take advantage of the resources provided to them through the territories still under their rule. Among these were Great Britain, Belgium, and France. Many of their economies were not seeing the rapid growth of the Germans or other European powers, and were thus less attractive to prospective workers. Rather than initiating bilateral agreements, these countries instead made all inhabitants of their colonies full citizens (primarily as a result of other political pressures), granting a host of unskilled laborers unrestricted movement to the home country (Hansen 2003). Soon South Asians were pouring into Great Britain, as France saw similar movement from Algeria, which was technically a part of the French state rather than a colony.

With the global economic slowdown resulting from the 1973 oil crisis, the vast majority of economic and labor immigration ground to a halt. However, rather than stopping the migrant flow into Europe, this halt simply shifted the reason for movement. Governments began limiting the influx of workers and implementing measures to encourage existing workers to move back to their native countries. However, these measures had the unintended effect of solidifying the presence of existing workers. Business owners did not want to lose well-trained and experienced labor without the hope for replacements willing to work for low pay. The immigrants themselves were hesitant to leave, fearing that they would not be able to return once the economy had regained speed (Lucassen, 2005).

The Germans went so far as to limit the amount given as family allowances for children abroad, but instead of forcing the workers to return home, their children came to Germany (Lucassen, 2005). Across Europe, the primary reason for migration became family reunification, and the wives, children, and parents of immigrant workers began to move to rejoin the young males that had moved to find work. Early attempts by European governments to limit family immigration were met with stiff human rights opposition and were often foiled in courts, thus allowing reunification to move forward. During this period, the labor migration that did occur was restricted to high skilled laborers (Geddes, 2003).

The shift to family reunification heavily impacted native European views of immigrants. Whereas many members of the first wave of labor immigrants had been tolerated given their contribution to economic development, the influx of non-working migrant women, children, and elderly was viewed as more of a cultural threat. It was at this point that the considerable difference in birth rates between immigrants and natives began to manifest itself. The decision of many immigrants to remain in place for the long term, coupled with the arrival of their families (and the resulting offspring), produced a rapidly expanding immigrant population while native populations stagnated (Statham 2003).

The changing face of Europe will have major consequences for the future, especially in the area of religion. What was once a homogenously Christian (overwhelming Roman Catholic) Europe has already begun to disintegrate, as the major influxes of non-European immigrants come from regions of Africa, the Middle East, and South Asia with predominantly Muslim populations. The growth of Islam across Europe is one of the greatest lines of conflict that has been established between immigrants and native Europeans. It is a trend playing out across the continent. While ethnic European birthrates plummet, Muslim immigrant birthrates remain very high. The total Muslim population of Europe is projected to double by 2015, while ethnic Europeans are likely to decline by 3.5 percent. The trend is even larger in cities, many of which are expected to be half foreign or more within the century (Shore, 2006).

The Political Response

The growth in immigration has been mirrored in many areas by a rise of numerous far right anti-immigrant political parties that have capitalized on a spreading xenophobia within Europe. These parties are not geographically constrained to a single country and have gained toeholds in a number of nations that have long been heralded as examples of liberalism and tolerance. In fact, one of the most successful examples of this phenomenon is the *Schweizerische Volkspartei* (SVP) of Switzerland. In the 2007 federal elections, the SVP was able to garner 28% of the vote, the highest vote total for any single party in Swiss history. The SVP has been able to rally support around its extremely restrictive immigration policies, including a controversial ban on the construction of minarets that was approved via national referendum in late 2009. At the time of the vote, there were only four minarets in the entire country, none of which were used for a call to prayer (Erlanger, 2009).

Another famous example of a far right party that has thrived on its anti-immigrant positions is seen in France. The post-crisis era saw the rise of *Front National*, a far-right party that found its cause in the anti-immigrant movement. Led by archconservative Jean-Marie Le Pen, *Front National* saw modest electoral success, consistently exceeding 10% in multiparty federal elections, and gaining seats in the European Parliament. Le Pen's strongest support came as a result of his vocal criticism of immigrant groups. In 1984, 39% of the National Front voters cited immigration as their primary concern, and in 1986, this number jumped to 60% of the same voting group (Golder, 2003). Today, *Front National* advocates for the cancellation of family reunification immigration, shortening the permitted stay from 10 to 3 years, and sending criminals back to the country of origin (Front National, 2010).

The *Freiheitliche Partei* Österreichs, Austrian Freedom Party, traces its roots all the way back to the Nazi occupation of Austria. Though it was not officially formed until 1956, as the conglomeration of three different right-wing groups, it was strongly associated with the fervently nationalistic and

conservative positions of the Nazi party. It saw little success for most of the Cold War, typically garnering just 6-7% of the national vote. By the early 1980s, the party was beginning to splinter, as many of the more conservative elements were unhappy with the increasingly liberal leadership of Norbert Steger.

Both the party's goals and its subsequent fortunes underwent dramatic shifts in 1986 when Jörg Haider supplanted Steger as head of the party. It was at this point that the FPÖ began taking on a more stridently anti-immigrant image, a perception that Haider readily fostered and used to help boost the party to nearly 10 percent of the vote in November of the same year. Just over a decade later, the Freedom Party had become a force to be reckoned with in Austrian politics. It shocked outside observers by capturing almost 27 percent of the vote in the 1999 federal elections, enough to push the party into second place and into part of a governing coalition with the center-right Austrian People's Party. Though few parties outside of the government were willing to deal with the Freedom Party, it managed nonetheless to legislate a more restrictive immigration policy that ultimately cut asylum applications by more than a half (Luther, 2004). The following years saw a tapering off of support for a party that best functioned as a voice of opposition, and support was further deflated when Haider himself died in a car accident in 2008.

Interestingly, the United Kingdom and some countries of Southern Europe have not seen comparable political movements against immigration. While parties espousing such positions certainly exist, they have not come close to replicating the success of Front National or the FPÖ. The reason for this lack of success is unclear. It may be a result of any number of differences across European nations, ranging from structural factors, like minor party access to the ballot, to individual level factors, such as voter tolerance or lack thereof.

Several existing studies analyzing support for extreme right parties (ERPs) at the individual level, for example, have pointed out the strong positive correlation between anti-immigrant or xenophobic attitudes and a voter's likelihood to support an ERP candidate (Lubbers, Scheepers and Gijsberts 2002; Knigge 1998). As Kessler (2005) points out, the relationship is rather self-evident: "These prospective extreme right voters express a host of imagined or real grievances, blaming migrants for perceived reductions in the quality of children's education, abuse of the welfare system, increases in unemployment, and rises in crime, violence, and delinquency" (273).

One key analytical advantage that researchers in the area are presented with is the aforementioned variability across European countries in terms of ERP support, since it allows us to hold certain variables relatively constant while others vary. I return to this theme in my research design section, which follows a discussion of current theoretical explanations for the growth in anti-immigrant sentiments.

Theoretical Perspectives

Competition Theory

Currently, of the two common explanations for anti-immigrant attitudes, the predominant one is the idea of ethnic competition (Knigge 1998, Lubbers *et al.* 2002, Scheepers *et al.* 2002, Alexseev 2006). It is based in the concept of realistic group conflict theory, which seeks to explain the tensions between groups seeking resources and power in a society (Coser 1956, Duke 1976). Essentially, when one group has access to limited resources, any increase in demand for those resources (i.e. the arrival of an outgroup) becomes a threat to those that originally had access, the ingroup. The closer the relationship between the two groups, the more vigorous the competition between them becomes. Thus, as the size of an outgroup increases, the contact that individuals in the ingroup have with them increases as well. Elevated awareness of the existence of the outgroup in turn leads to an escalation in the level of competition, manifesting itself in increased hostility towards the newcomers (Banton, 1983).

According to competition theory then, migration directly results in an antagonistic relationship between ingroup and outgroup. The basis upon which members of each group delineate themselves from the 'other' may be language, ethnicity, or religion. Distinctions such as these help to clearly delineate the boundaries between ingroup and outgroup, thus eliminating the possibility of boundary dissolution over time.

The question of ethnic competition then turns to the matter of the resources that are being fought over. Some studies have focused primarily on competition for basic needs and resources. Included in this grouping would be issues such as employment and access to education, among other government provided services (Campbell 1965; Sherif 1966). A less tangible but no less potent resource may be that of culture and identity (Tajfel and Turner 1979).

France's long simmering immigration debate has featured both of these types of resource conflicts, laid bare with tragic consequences in the tumultuous autumn of 2005. In that year, the deaths of two immigrant teenagers sparked a series of riots around Paris and across the country. Thousands of cars were burned by rioters that were predominantly young immigrant men. What had started as anger over the deaths boiled over into a national crisis as the riots became an outlet for many of these working-age men to express their frustrations at the lack of employment opportunities available to them. According to Ford, immigrant rage at pernicious discrimination and dismal job prospects provides an unequivocal example of materialistic competition (Ford, 2005).

Equally contentious was the issue of the 2004 ban on the wearing of headscarves in public schools. Some native French view the headscarf as a symbol of outsiders amongst them, fearing a loss of identity as that population grows. Regardless of the source of inter-group competition, the consequences are similar if not identical.

Thus, according to competition theory, increases in the size of the outgroup, in this case immigrants, will coincide with proportional increases in electoral support for ERPs as a result of increased threat to the ingroup's resource pool. The resulting relationship will be a positive and linear.

Contact Theory

Contact theory posits the opposite effect, arguing that the size of the outgroup actually has a negative relationship with anti-immigrant attitudes. In simple terms, it is easy to vote for

parties that demonize immigrants when one has little contact with those immigrants. As an unknown specter, immigrants can take on whatever characteristics an ERP may wish to apply to them. However, once a voter has contact with immigrants, they are able to make the judgment for themselves, and their conclusion rarely coincide with public portrayals put forth by ERPs.

Williams (1947) points out that most actions undertaken to resolve intergroup conflict rest upon the assumption that increased contact results in personal connections that overcome the competition impulse. McLaren (2003) found evidence to support this theory in the case of European immigration. In her research, those who had multiple immigrant friends perceived the general immigrant community to be a lesser threat than those who had no contact with immigrants.

Early research on the contact hypothesis posited that it only applied in very limited circumstances that were rarely seen. Conditions put forth by Allport (1954) included equal status, common goals, and support for contact from authority. In many of the migration situations seen in Europe, meeting these conditions was practically impossible. Later work expanded on Allport's, saying that contact could increase anti-outgroup sentiment just as much as it could decrease it. Amir (1969) makes this point, citing some of the component ideas of realistic group conflict theory. He then develops Allport's conditions, positing that the contact must be desired, and that it can either occur between members of equal status or a member of the majority and a outgroup member of even higher social status. This difference in socioeconomic status is an important distinction in assessing the validity of contact theory. Essentially, it states that horizontal contact, such as that between a Moroccan immigrant worker and his working-class Dutch neighbor, will result in a much greater shift in attitude than the vertical contact between a wealthy Austrian family and their Turkish house workers.

However, more recent research has shown that contact does not have to occur under such stringent settings. Pettigrew (1998) found that even relatively coincidental contact could result in improved relations between ingroup and outgroup. An earlier study in German schools had found similar results, tying leisure time and the incidental contact with Turks that it provided to decreasing prejudice against the outgroup (Wagner, Hewstone, & Machleit, 1989).

A Tipping Point?

While the competition versus contact theoretical debate has been going on for some time now, there has been little research into a middle ground between the two. Both sides certainly have considerable research and evidence to back up their claims, but interaction between them is notably absent. This is particularly interesting given that both hypotheses seem to fall apart as we approach their extremes. Under ethnic competition theory, a population fully saturated with immigrants would have the highest rates of anti-immigrant voting, a clearly illogical conclusion as these immigrants would be unlikely to vote against their own interests. On the other hand, the contact hypothesis faces issues at the opposite extreme: completely homogenous communities, those devoid of immigrants, would hypothetically have the highest rates of support for anti-immigrant parties. Again, this does not follow, as the community would assumedly have very little cause to vote against a nonexistent population.

In almost all of the existing literature, the assumption of linearity seems to be taken as a certainty rather than as a part of the hypothesis. Schlueter and Scheepers (2009) even conducted a study testing both hypotheses simultaneously on the same data, finding significant support for both theories. Despite this seemingly contradictory result, the authors failed to present any challenge to the linear model. The possibility of a curvilinear relationship, made up of the simultaneously acting theories, offers a potential solution to this contradiction.

Such an idea has been put forward by Schneider (2007) but even Schneider did not seem to think that the relationship was entirely curvilinear, in that she predicted a "tapering off" of ERP voting rather than a decrease. Her study looked at the issue at the national level, analyzing 20 different EU countries. Two other authors have recently found evidence for a curve, but both are in limited settings. Rather than focusing on all non-European immigrants as the outgroup, one study zeroed in on Muslim immigrants in the Netherlands, and the other looked only at the performance of the Vlaams Blok in Belgium (Rink et al. 2009; Savelkoul, et al. 2010). Again, in both of the cases, the curve seemed to be more of a tapering off than a decrease in support for the extreme right.

Hypotheses

The first two hypotheses that I tested stemmed from the predominant theories of competition and contact. The decreasing access to resources referenced in competition theory indicates a positive linear relationship between immigrant population size and ERP voting, the relationship presented in my first hypoth esis. Contact theory led to my second hypothesis, which asserts that increasing immigrant population size will lead, in turn, to increased opportunities for contact and interaction, thus *decreasing* xenophobia and electoral support for ERPs. Whereas the first hypothesis was a positive linear relationship, this second hypothesis postulates instead a negative linear relationship.

A curvilinear relationship would indicate that ethnic competition begins as the stronger factor, driving anti-immigrant sentiment for a time, but once the outgroup population reaches a certain size, the augmented opportunities for interaction with the ingroup lead to a strengthening of the contact theory, bringing the curve back down after a maximum point of anti-immigrant voting. This curvilinear relationship became my third hypothesis to be tested, and in doing so I both incorporated existing theories and also posited a relationship that would fill a gap that heretofore has existed in the literature on ERP support and immigration.

Levels of Analysis

One of the very important matters that had to be addressed in this case was the level of analysis. In the existing literature, the scope of studies varied from continent-wide, analyzing at the national level and including various examples (Lubbers 2002), to looking at subnational units as small as counties in a single country (Alexseev, 2006). The level chosen can have a significant impact on the results, as it also indicates a shift in the resource

pool referred to for competition theory. As Quillian (1996) points out, "The correct unit at which to measure the influences is difficult to define precisely, since people probably picture relations between their own racial group and other racial groups at more than one level (city, state, region, or nation) depending on the context."

This debate also brings into account a previously mentioned issue about the contact hypothesis, and that is the question of the nature of the contact. If growing immigrant populations are confined to ethnic ghettoes, it becomes very unlikely that voters will have the opportunity for chance interactions that would hypothetically be expected to shift their attitudes. In some cases, it may even serve to intensify competition as it adds geography to the list of factors that can be used to draw the boundary between ingroup and outgroup.

A substantial portion of the existing research also looks at the issue at the individual level, examining individual socioeconomic, demographic, and opinion data to see its effect on anti-immigrant voting. For example, McLaren (2003) explores the relationship using survey responses that discuss the threat perception of individual voters, and then links it with immigrant contact and ERP support. Other studies that bring economic level and education into account have shown a significant relationship between those factors and ERP support, and unlike threat perception, these factors can be analyzed easily at a level greater than the individual, and thus were incorporated into my analysis.

In this research, data was analyzed at the first-order civil division level for each nation (the level of administration just below the central state government), as previous research has shown the effect of immigration on voting patterns to be higher when evaluated at the level of smaller units (Alexseev 2006). Additionally, subnational analysis appeared more warranted since public opinion is very rarely homogenous at the national level, but often does begin to demonstrate more convergence as the unit of analysis decreases.[1] Breaking from the typical approach taken by researchers in this field, I concentrated on the subnational analysis, but it spanned across four different case nations in order to test the hypotheses in more varied environments.

The scales and autonomy of first-order civil divisions among my cases varied substantially. The simplest measure of regions is the Nomenclature of Territorial Units for Statistics (NUTS) established by the European Union for the purposes of EuroStat, the EU statistical database. The NUTS for all EU countries are divided into 4 levels: NUTS 0 is the national level, NUTS 1 is the next largest, then down to the smallest NUTS 3 divisions. For most of these countries, NUTS 1 is simply an agglomeration of administrative regions with little meaning in the national context. In Austria, Spain, and Belgium, NUTS 2 actually corresponds directly with the first order administrative regions.

However, the NUTS designations for the United Kingdom do in fact correspond with a relevant layer of administration, namely Government Office Regions, Scotland, Wales, and Northern Ireland.[2] Furthermore, while boundaries of lower NUTS levels typically correspond with voting districts, this is not so in the UK, thus necessitating the use of the NUTS 1 level in its case. Since the data for the control variables all came from an EU database, the indicator variables are all defined within the NUTS regions and using smaller divisions than NUTS 1 would have introduced a great deal of error into the models. Therefore, I worked at the NUTS 2 level in all countries except the United Kingdom. Even given this apparent disparity, there was a rough balance across case nations as each country included between 10 and 20 regions at the specified levels. As well, there was complete balance in terms of the number of elections analyzed with two cycles examined for each of the case countries, thus yielding a total number of 100 observations.

The dependent variable in this case was the percentage of votes garnered by extreme right parties in European Parliament elections. Using the results of a survey conducted by Lubbers (2000), I was able to classify parties in each country. The survey polled 150 European political scientists, asking them to place parties on a left to right ideological scale with 1 being far left and 10 being far right, and to rank these parties by the restrictiveness of their proposed immigration policies. I focused exclusively on parties that qualify as "extreme right" on both of these measures, those with a score greater than nine on each scale.

On the basis of Lubbers' scale, I chose four countries for my analysis: Belgium, Spain, Austria, and the United Kingdom. There were actually six parties in the final analysis, given the division of Belgium between the Dutch-speaking Flanders and francophone Wallonia as well as the existence of two Spanish extreme right parties on Lubbers' scale. The parties were: *Vlaams Blok* (VP) of Flanders, *Front National* (FN) of Wallonia, the *British National Party* (BNP), *Democracia Nacional* (DN) and the *Falange Española de las Juntas de Ofensiva Nacional Sindicalista (FE de las JONS)* of Spain, and the *Freiheitlicht Partei* Österreichs (FPÖ) of Austria. Over the span of time that I measured, some of these parties saw significant organizational changes. For example, the Vlaams Blok actually became the Vlaams Belang as of late 2004 after a court ruled that the Blok had violated laws against xenophobic incitement.

Immigrant population size can be measured in a variety of ways, but for the purposes of this research, I defined that variable as the percentage of non-European Union legal residents. This is because the lack of border controls between EU countries, a result of the 1984 Schengen agreement, makes internal migration more fluid and thus more difficult to measure with precision. Also, the ethnic and cultural boundaries between groups involved in conflict are more substantial with non-EU migrants than with other EU members. While an Italian immigrant in France may face considerable difficulty with regards to language, he is still navigating in a society very similar to his own, with nearly identical values. The same cannot be said for an Algerian in

[1] Unfortunately, I did not have access to individual level data in these areas. Any analysis of the results of this research must therefore avoid the ecological fallacy, that is, using the behavior of the group as a whole to predict the action of an individual.

[2] Northern Ireland was eliminated from the analysis given that the British National Party did not run in their elections.

France. His color, accent and faith all set him apart from the rest of the "native" population, and he is much more likely to evoke a response as he is more clearly a member of the outgroup under the provisions of realistic group contact theory. While a measure of immigrant population that included illegal immigrants would be ideal, this information is understandably difficult to attain with any measure of validity.

My analysis involved model estimations using multivariate ordinary least squares regression. The models provided coefficients that indicated the relationship between the dependent variable and the independent variables. Since I hypothesized a curvilinear relationship between extreme right support and our primary predictor variable, outgroup size, I introduced a quadratic term (squaring the immigrant population size) to test for curvilinearity. While the numerical values associated with this squared term provide little useful information, the sign of the term will tell us whether or not a curve is present. A positive linear coefficient in combination with a negative quadratic coefficient indicates a curvilinear relationship of the sort predicted in my hypothesis (i.e., one resembling the classic normal bell curve).

I also tested for linear relationships with other variables, drawn from the existing research literature on the topic of extreme right electoral support, in order to account for their effect on the general trends. While education level is one of the most widely used predictors of this support, I included income level, economic status, and urbanization, as discussed in the following section.

Cases and Data

My dependent variable was the percentage vote received by the ERPs in the European Parliamentary elections of 2004 and 2009 respectively, derived using information contained in the European Election Database (Norwegian Social Science Data Services, 2011). There are two reasons that the European Parliament elections were used as valid measures of support for this study. [3]

The first is the centralization of migration-related powers that has occurred over the past two decades. The EU is seeking to and has succeeded in broadening its capability to deal with migration as a Europe-wide issue (Geddes, 2003). The immigration debate has been cast in terms of a monolithic European culture by many of the extreme right parties analyzed here. As put by Geert Wilders in a speech to the British House of Lords regarding Muslim immigration, largely Turkish and North African: "Islam means submission, there cannot be any mistake about its goal. That's a given. The question is whether we in Europe and you in Britain, with your glorious past, will submit or stand firm for your heritage" (Wilders, 2010). As the identity set in conflict with the immigrant is defined as a pan-European one with a common heritage, it would make sense that voters in perceived conflict with the outgroup would seek solutions at the Europe-wide level.

The second strength of EP election data is the increased influence that the body has wielded in the last decade. The 2004 and 2009 elections followed a period of growth resulting from the treaties of the 1990s and the early 2000s. Voting reforms had strengthened the Parliament in comparison with the powerful European Commission and Council of Ministers, with the co-decision process giving it an essential veto on many important policy matters. A turning point for the institution came in 1998 when, after years of largely rubber-stamp work, the Parliament refused the budget of EU Commissioner Jacques Santer and eventually forced the resignation of his entire commission due to allegations of corruption and gross mismanagement (Topan, 2002). With a newly empowered Parliament, it is much more likely that voters in recent years would see the body as a potential agent of change to a greater degree than they had prior to 1992.

The makeup of the non-EU immigrant populations in these countries also provided an interesting and useful comparison. The United Kingdom, as a result of its colonial legacy, is primarily a destination for South Asian immigrants. Austria has a more varied makeup. Following the example of its neighbor Germany, it recruited massive numbers of Turkish workers, but there are also sizeable numbers of former Balkan residents who moved to flee the wars there during the 1990s. Spain, unlike the others, has many immigrants from Latin America as it is a natural destination for the continent's Spanish speakers. Its geographic proximity to North Africa has also led to large Moroccan and Algerian communities in some areas. Belgium's immigrants are also primarily Moroccan, though they live alongside a considerable Turkish population as well, and were recruited as guest workers.

The four selected countries provided the opportunity to test my hypotheses across a range of demographic configurations. The proportion of immigrants of non-European origin in Belgium is only 2.9%, the lowest of the four and among the lowest in Western Europe, whereas Austria has the largest foreign presence of the four, nearly 7% of their populace (see Table 1 for descriptive statistics). The cases also show variance on the side of the dependent variable, as far-right parties like the Vlaams Blok and the Freedom Party have seen considerable success in Belgium and Austria, whereas the Spanish anti-immigrant party, Democracia Nacional, has never generated a significant amount of support.

Choosing an accurate measure of the education levels in each region proved to be a challenge. As with all of the variables, there are no individual level measures for participating voters, so I needed some contextual measure of education levels for the region as a whole. The data that I used came from the quarterly Labor Force Survey (LFS) conducted by member nations under the auspices of EU control. "The EU LFS is a large household sample survey providing quarterly results on labor participation of people aged 15 and over as well as on persons outside the

[3] European Parliament elections are under the control of member countries, but provide a more standardized measure. They enable us to eliminate variation introduced by time differences that may have occurred between individual national elections. Elections consist of national parties who then sit in large ideological coalitions once seated in Parliament. The extreme right parties analyzed here all sit as *non-inscrits*, not part of any coalition.

Table 1. Descriptive statistics for all variables included in the model.

Variable	N	Minimum	Maximum	Mean	Std. Deviation
Percent support for ERPs	100	.04	27.47	5.64	6.31
Percentage of immigrants	100	.72	13.60	4.57	3.41
Unemployment Rate	100	2.90	26.20	9.28	5.41
Percentage with Tertiary Education	100	12.52	48.54	27.52	7.53
Gross Domestic Product per capita (indexed to EU average)	100	60	256	112.05	34.10
Percentage of region with low urbanization	100	.00	1.00	.25	.24
Valid N (listwise)	100				

labor force. All definitions apply to persons aged 15 years and over living in private households" (EuroStat, 2010). The highest level of education attained was defined on the education levels of the International Standard Classification of Education (ISCED), established by UNESCO in 1997.

The LFS data aggregates these levels into three groups: respondents with only primary level education or none at all, respondents who have completed secondary education, and respondents who have completed tertiary education, be it university or some kind of professional degree. The figures used in this study represent percentages of the total respondents and exclude respondents in the 15-24 age bracket. The logic of this exclusion is that such individuals would in the first instance likely still be pursuing completion of their secondary or tertiary studies, and in the second instance, those under 18 would not have been eligible to vote in the elections being analyzed.

Two different measures were used to determine the impact of economic context upon the dependent variables. The first, unemployment rate, provided a measure of economic competition at the contextual level. Competition theory would predict a positive relationship between the unemployment rate and ERP support, as greater numbers of people looking for jobs would theoretically lead to a heightened sense of competition with the outgroup.

The other economic measure provided a sense of income distribution between regional units. This data also comes from EuroStat's Labor Force Survey, as I utilized the Gross Domestic Product per capita of each region[4]. To avoid the cross-national distortions that using raw amounts would introduce, I indexed the amounts to the average regional GDP per capita for the entire European Union, setting it equal to 100 and normalizing the other values around it. All amounts were measured in Euros to account for differences in exchange rates.

The final control variable included was a measure of urbanization. While not frequently cited as an important factor in the literature, I included it because of the role that segregation of outgroup communities can play in both competition and contact theories. As Massey and Denton (1989) find in the case of the United States, the segregation of black communities actually increased when one looks at more metropolitan areas. On a basic level, this makes sense since urban areas would be more likely magnets for immigration and thus have larger immigrant populations. The larger population can then in turn lead to a more self-sufficient outgroup community. The effect of this "ghettoization" is the same under both contact and competition theory. It both limits opportunities for contact and deepens lines of division, leading to more ERP support in both cases.

The data on urbanization levels also came from the Labor Force Survey. It provides the number of households in each region based on the population density of their immediate area. There are three levels of urbanization: densely populated (more than 500 inhabitants per square kilometer), intermediate (between 100 and 499 inhabitants per square kilometer), and sparsely populated (less than 100 inhabitants per square kilometer). To facilitate analysis, I turned each of these numbers into percentages of the total respondents divided by urbanization level.

Results

I estimated two separate models using SPSS statistical analysis software. Results are displayed in Table 2. The first model tested my first two hypotheses regarding the apparently contradictory linear predictions of contact versus competition theory. As both of these hypothesized relationships were linear, the quadratic term was not included. All of the tested variables were significant at the .01 level except for the unemployment rate. The model had a very robust adjusted R-square value of 0.489, meaning that the model could account for 48.9% of the variation across cases. The negative estimated coefficient on the predictor variable, percentage of immigrants, indicates decreasing electoral support for the ERPs as immigrant population increases, thus leading me to reject my first hypothesis. My second hypothesis based upon contact theory, by contrast, is supported by the regression analysis.

Model II introduced a quadratic term to test my third

Table 2. Regression results displaying independent variables, estimated coefficient (expressing probability to vote for an extreme right party) and standard error in parentheses; (N= 100)

Variable	**Model I**	**Model II**
Constant	10.631 (3.128)**	13.212 (3.647)**
Percentage of immigrants	-0.817 (0.196)**	-1.569 (.586)**
(Percentage of immigrants)^2		0.062 (.046)
Percentage with tertiary level education	-0.333 (0.078)**	-0.346 (0.078)**
Percentage of region with low urbanization	-8.250 (2.294)**	-8.119 (2.286)**
Unemployment Rate	-0.178 (.117)	-0.192 (0.117)
Gross Domestic Product per capita (indexed to EU average)	0.104 (.022)**	0.098 (0.023)**

[4] One important caveat to the use of GDP per capita is that, given its nature as an average, outliers, typically high outliers, can throw it off and thus it may not provide a full picture of regional income without distribution data.

hypothesis, which posits a curvilinear relationship between immigrant population size and ERP support. The adjusted R-square value was marginally higher: 0.499. In this model, we see a stronger negative correlation with the linear term, but the squared term is not significant. The results of the second model provided greater support for my second hypothesis than for either of the other two hypothesized models, including my curvilinear one.

Discussion

Hypotheses

The strong evidence for contact theory provided by my regression models was initially a surprise, as ethnic competition has been the more dominant theory in much of the existing corpus of literature on the issue. Some aspects of the predictor variable, outgroup size, may have contributed to this result.

The first of these is the matter of my definition of the variable. Due to the limitations of available data, I was unable to get a full sense of the outgroup size. For example, I could not include illegal immigrants or immigrants that have been naturalized and left their original citizenship behind. While this information is available at the national level (Schneider, 2007) and occasionally at lower levels in specific circumstances (Savelkoul, Scheepers, Tolsma, & Hagendoorn, 2010), there are no comparable data on these other segments of the migrant community at the regional level. It is quite possible that the communities with a smaller foreign national community have a large naturalized population that still functions as an outgroup, but goes unaccounted for in this model. Subsequent inquiries would be much enhanced with measurements of both the illegal and naturalized communities, as they would enable a more rigorous testing for the presence of a curvilinear relationship.

The second issue that may have contributed to my unexpected results is the absence of significant time differences in measurement. While the hypothesized curve does not include an explicit temporal measure indicator, it is possible that shifting contextual circumstances may mitigate the competition effect over time. As discussed earlier, immigration has long been framed as a Europe-wide issue, and the recession of the 1970s that began much of the backlash against immigration affected the continent as a whole. The presence of these extreme right parties, regardless of their levels of success, has been a feature of the European political landscape since that era. Ethnic competition theory proposes that increasing migrant presence increases awareness of conflict, thus deepening anti-immigrant sentiment. Given the extensive nature of anti-immigrant rhetoric that had existed for years before the elections analyzed in this study, perhaps the awareness of conflict had already been maximized, regardless of immigrant presence. Such a situation would leave decreases in anti-immigrant voting resulting from contact as the only effect significantly related with the size of the outgroup.

Other Variables of Interest

Most of the relationships with the independent control variables found in these results are consistent with the conventional wisdom of existing immigration research. I decided to use only tertiary education as the educational measure based on support in the existing literature regarding what aspects of education impact outgroup perceptions. Hainmueller and Hiscox (2007) found that "college education has far greater positive effects on support for immigration than high school education, and finishing elementary schooling actually appears to have negative effects on support for immigration" (Hainmueller, 2007, p. 424). The negative correlation coefficient on the education variable seems to support Hainmueller's finding that as the percentage of the population that has completed university or comparable studies rises, district-wide (not individual) support for ERPs decreases.

The relationship with urbanization levels also follows the expected pattern. Assuming that ghettoization could occur even in mid-sized urban areas, I utilized the low urbanization level data to explore the relationship with ERP voting. Given that the data used is a percentage that sums to one when combined with intermediate and high urbanization, higher percentages of sparsely populated area mean fewer people living in urban areas, and thus fewer opportunities for segregation. The results illustrate a very strong relationship between ERP vote and urbanization. As the proportion of the population living in sparsely populated areas increases, ERP support drops dramatically.

Unemployment was the only control variable included in the models that did not turn out to be statistically significant. In fact, this too coincides with preceding research. Numerous studies found unemployment rate to have an insignificant effect on ERP voting or threat perception (Lubbers et al. 2002; Scheepers, Gijsberts and Coenders 2002; Rink et al. 2009). However, several of these also found that, when occupational status was included at the individual level, unemployment did have a significant effect, at least on threat perception. Given that such individual measures were beyond the scope of this study, there is little alternative to accepting that at least at the regional level, unemployment is a poor indicator of community-wide anti-immigrant voting proclivities.

The coefficent associated with income, measured here using GDP per capita, presents a more complex issue. It was significant, but indicated a positive relationship. That is, as the income increased, so did the support for ERPs. Given the previously stated relationship with tertiary education, this may seem contradictory, since the wealthier are typically better educated. In fact, though, it does fit with the tenets of contact theory. Recall that the literature indicates that there exist two kinds of contact. Ameliorative effects only derive from horizontal, not vertical, contact. As Amir (1969) emphasizes, the equal status of those involved in contact is essential. As income rises, one is less likely to encounter an immigrant of equal socioeconomic status, since most immigrants initially enter in pursuit of low salary work. Under such conditions, the contact becomes increasingly vertical with increasing income, and thus less effective. As we have already found contact theory to be the dominant phenomenon at play in this case, the income relationship ultimately does comport with expectations.

Conclusion

Though the hypothesized curve did not find support in this study, the results still provide considerable reason for optimism in

Europe's coming years. The dominance of contact theory, whether it is in fact simply the downward portion of a curve that reached its maximum in the past or if it is truly the stronger phenomenon at play, is encouraging. The migrant influx shows no real signs of slowing, and Europe will be required to adapt to the presence of this new community as the community itself adapts to its new surroundings. My findings indicate that they are doing just that.

Though further research will be required to discover if national general election data matches that of the European Parliament elections analyzed here, the trend is occurring as the EP grows in influence and capacity. My results may not inform the impending policies of individual nations, but as the European Union is taking on a more active role in the integration of the immigration regimes of member nations, it seems that restrictive anti-immigrant parties will hold less sway in the creation of the common policy. These results are also important for those ultimately charged with the creation of such policies. While electoral support of ERPs is just one of many measures of xenophobia, this study indicates that programs that encourage contact may aid in integration of immigrants. Irrespective of the national milieu, environs that facilitate greater contact between natives and migrants, particularly horizontal contact, will coincide with decreases in support for those who use xenophobia as a political cudgel in pursuit of elected office.

Works Cited

Alexseev, M. (2006). Ballot-Box Vigilantism? Ethnic Population Shifts and Xenophobic Voting in Post-Soviet Russia. *Political Behaviors*, 211-240.

Allport, G. (1954). *The Nature of Prejudice.* Reading, MA: Addison-Wesley.

Amir, Y. (1969). Contact Hypothesis in Ethnic Relations. *Psychological Bulletin, 71*(5), 319-342.

Banton, M. (1983). *Racial and Ethnic Competition.* Cambridge: Cambridge University Press.

Boswell, C. (2005). Labor Migration Programs in Europe. In H. Henke, *Crossing Over: Comparing Recent Migration in the United States and Europe* (pp. 223-234). Lanham: Lexington Books.

Campbell, D. T. (1965). *Ethnocentrism and other altruistic motives.* Lincoln, NE: University of Nebraska Press.

Coser, L. A. (1956). *The Functions of Social Conflict.* Glencoe, Illinois: Free Press.

Duke, J. T. (1976). *Conflict and Power in Social Life.* Provo, Utah: Brigham Young University Press.

Erlanger, S. (2009, 29-November). *Swiss Ban Building of Minarets on Mosques.* From New York Times: http://www.nytimes.com/2009/11/30/world/europe/30swiss.html

EuroStat. (2010, April 10). *European Union Labor Force Survey*. Retrieved from http://epp.eurostat.ec.europa.eu/portal/page/portal/microdata/lfs

Evan-Pritchard, A., & Clements, J. (2003, 28-March). *Fortuyn killed 'to protect Muslims'.* From The Telegraph: http://www.telegraph.co.uk/news/worldnews/europe/netherlands/1425944/Fortuyn-killed-to-protect-Muslims.html

Ford, P. (2005, November 4). Deep roots of Paris riots. *Christian Science Monitor*.

Front National. (2010). *Immigration*. From Front National: http://www.frontnational.com/?page_id=1095

Geddes, A. (2003). *The Politics of Migration and Immigration in Europe.* London: Sage Publications.

Golder, M. (2003, May). Explaining Variation in the Success of Extreme Right Parties in Western Europe. *Comparative Political Studies, 36*(4), 432-466.

Hainmueller, J. M. (2007). Educated Preferences: Explaining Individual Attitudes toward Immigration in Europe. *International Organization, 61*(2), 399-442.

Hansen, R. (2003). Migration to Europe since 1945: Its History and its Lessons. *The Political Quarterly*, 25-38.

Kessler, A. E., & Freeman, G. P. (2005). Support for Extreme Right-Wing Parties in Western Europe: Individual Attributes, Political Attitudes, and National Context. *Comparative European Politics*(3), 261-288.

Knigge, P. (1998). The ecological correlates of right-wing extremism in Western Europe. *European Journal of Political Research*, 249-279.

Lubbers, M. (n.d.). *Expert Judgement Survey of Wester European Political Parties 2000.* NWO, Department of Sociology. Nijmegen, the Netherlands: University of Nijmegen.

Lubbers, M., Scheepers, P., & Gijsberts, M. (2002). Extreme right wing voting in Western Europe. *European Journal of Political Research*, 345-378.

Lucassen, L. (2005). *The Immigrant Threat.* Urbana: University of Illinois Press.

Luther, K. (2004). *Political Parties of the World in 2004: Austria.* Staffordshire: Keele University.

Massey, D., & Denton, N. (1989, August). Hypersegregation in US Metropolitan Areas. *Demographics, 26*(3), 373-392.

McLaren, L. (2003). Anti-Immigrant Prejudice in Europe. *Social Forces*, 909-936.

Moraes, C. (2003). The Politics of European Union Migration Policy. *Political Quarterly*, 116-131.

Norwegian Social Science Data Services. (2011). *European Election Database*. Retrieved from http://www.nsd.uib.no/european_election_database/

Pettigrew, T., Christ, O., Wagner, U., & Stellmacher, J. (2007). Direct and indirect intergroup contact effects on prejudice: A normative interpretation. *International Journal of Intercultural Relations, 31*, 411-425.

Rink, N., Phalet, K., & Swyngedouw, M. (2009). The Effects of Immigrant Population Size, Unemployment, and Individual Characteristics on Voting for the Vlaams Blok in Flanders 1991-1999. *European Sociological Review, 25*(4), 411-424.

Rossi, A. (2010, 10-June). *Far-Right Breakthrough Shocks Netherlands* . From Sky News: http://news.sky.com/skynews/Home/World-News/Netherlands-Elections-Far-Right-Breakthrough-Shock/Article/201006215646947?f=rss

Savelkoul, M., Scheepers, P., Tolsma, J., & Hagendoorn, L. (2010). Anti-Muslim Attitudes in The Netherlands: Tests of Contradictory Hypotheses Derived from Ethnic Competition Theory and Intergroup Contact Theory. *European Sociological Review*, 1-18.

Scheepers, P., Gijsberts, M., & Coenders, M. (2002). Ethnic Exclusionism in European Countries. *European Sociological Review, 18*(1), 17-34.

Schlueter, E., & Scheepers, P. (2010, March). The relationship between outgroup size and anti-outgroup attitudes: a theoretical synthesis and empirical test of group threat and intergroup contact theory. *Social Science Research, 39*(2), 285-295.

Schneider, S. (2007). Anti-immigrant Attitudes in Europe: Outgroup size and perceived ethnic threat. *European Sociological Review*, 1-15.

Sherif, M. (1967). *Group Conflict and Cooperation: Their Social Psychology.* London: Routledge and Kegan Paul.

Shore, Z. (2006). *Breeding Bin Ladens: America, Islam, and the Future of Europe.* Baltimore: Johns Hopkins University Press.

Stasi, B. (2003). *Rapport au President de la Republique.* La Commission de réflexion sur l'application du principe de laïcité dans la République. Paris: La Documentation Française.

Statham, P. (2003). Understanding Anti-Asylum Rhetoric: Restrictive Policies or Racist Publics? *The Political Quarterly*, 163-177.

Tafjel, H., & Turner, J. (1979). An Integrative Theory of Intergroup Conflict. In W. Austin, & S. Worchel, *The Social Psychology of Intergroup Conflict* (pp. 33-47). Monterey, CA: Brooks/Cole.

Topan, A. (2002). *The resignation of the Santer-Commission: the impact of 'trust' and 'reputation'.* European Integration Online Papers.

Wagner, U., Hewstone, M., & Machleit, U. (1989). Contact and Prejudice Between Germans and Turks: A Correlational Study. *Human Relations, 42*(7), 561-574.

Wilders, G. (2010, March 5). Speech to the House of Lords. London, UK.

Williams, R. M. (1947). *The Reduction of Intergroup Tensions.* New York City: Social Science Research Council.

Mentor Comments: Professor Jeffrey Ryan's enthusiasm and respect for Andrew's work is clear in the following mentor comments.

From my perspective, not only as an advisor but a scholar as well, Andrew Walchuk's thesis is an exemplar of how an undergraduate student can conduct first-rate scholarship when they commit themselves fully to the endeavor. I have supervised many, many honors theses in my 20-year career here and, quite simply, this is the very best of them all. I could, of course, go on for pages pointing out in detail how well conceived, constructed and presented Andrew's work is, but instead would like to address two facets of his experience that, to me, represent the drive and temerity that lies at his essence.

The first facet is the extraordinary degree to which Andrew attacked this very ambitious process. From the start, he never looked back, never retreated and never wilted in the face of daunting challenges. We determined early on (actually, in the spring of his junior year) that, in order to appropriately and rigorously test his hypotheses, fairly sophisticated quantitative skills would be needed. As he did not at the time have these skills and as I am generously described as being semi-literate in this area, what did he do? First, he enrolled in an advanced statistical analysis course during his fall senior semester. Then, as he ventured deeper into his analysis, he arranged personal meetings with a faculty specialist who, no doubt impressed by this young man's self-drive and ambition, quickly agreed to tutor Andrew. Later, as he was gathering data, he found gaps in the availability of critical measures for a single case, so what did he do? Rather than simply discard the case and pursue an 'easier' one, he directly called electoral authorities in the relevant country. They quite helpfully provided the necessary data and Andrew, as ever, kept moving forward. This is who he is; voracious for knowledge, relentless in the face of obstacles and possessed of an intellect that is one of the sharpest that I have seen in my professional life. As I tell anyone who will listen, Andrew was a colleague, not a student. I was only along for the ride and a fantastic one at that.

The second facet represents to me the most significant contribution of this work to academia most broadly conceived. To put it in very simple terms, Andrew did his research the way it should be done. This may sound puzzling, but the disturbing truth is that we in our disciplines all too often actually pervert the process of scientific inquiry. How? By 'creatively' selecting our cases, by 'torturing' the data and worst of all, by starting with our conclusions then working our way backwards. Why? Because our professional lives are driven by publication and our journals abet the corruption of research by generally refusing to publish negative results. Andrew, and especially this journal, deserve our highest accolades for having the courage to accept that his hypotheses were not supported by the evidence. This is genuine and pure scholarship and confronted by Andrew's example, we in academia, including me, should collectively hang our heads in shame.

34 INQUIRY Volume 12 2011

THE OPAQUENESS OF FAIR VALUE ASSETS AND SYSTEMATIC RISK IN THE BANKING INDUSTRY

By Jody Wayne Bland
Department of Economics

Faculty Mentor: Jeff Jones
Department of Finance

Abstract

Opacity has economy-wide implications. A lack of information, whether from non-disclosure or complexity of business, creates uncertainty that even the most sophisticated of investors must face. In this paper, I analyze the relationship between opacity and the systematic risk of bank holding companies. Specifically, I find that investments in opaque assets required to be reported at fair value significantly affect the levels of financial institutions' systematic risk. Furthermore, I provide evidence that firm investments in opaque assets contribute to systematic risk to an even greater degree during times of financial crisis.

I. Introduction

Accurately assessing the true economic value of any firm can be an arduous task. When attempting to assess the underlying value of a portfolio of assets, information becomes critical. A lack of information, whether as a result of non-disclosure or complexity of business, creates uncertainty that even the most sophisticated of investors must face. Furthermore, the inherent nature of the banking industry lends itself to even greater informational asymmetries that manifest themselves in the form of opacity (Morgan, 2002). The existence of opacity in banks has economy-wide implications due to the vital role that financial institutions play in general economic activity (Bernanke, 1983). In this paper, I examine the relationship between financial opacity and the systematic risk of bank holding companies. Specifically, I investigate the impact of investments in assets required to be reported at fair value on the systematic risk of financial institutions.

The consequences of opacity have justified special regulatory oversight within the financial industry, as investors are forced to use non-firm specific valuation parameters to assess firm specific assets (Flannery, Kwan, and Nimalendran, 2004). In opaque industries such as banking, contagion that arises as a consequence of industry-wide revaluation around firm-specific events engenders an environment conducive to the development of speculative bubbles and crashes. Arising from the inability of investors to distinguish between bank-specific and systematic events, contagion is a product of information asymmetry (Diamond and Dybvig, 1983). Disclosure standards attempt to mitigate risks associated with opacity and information asymmetry by reducing the information gap between bank-insiders and investors. However, even full disclosure may not adequately resolve the problems associated with opacity (Jones, Lee, and Yeager, 2011a).

Opacity also influences the composition of a firm's risk. Morck, Yeung, and Yu (2000) show how opaque markets tend to have greater systematic risk and lower idiosyncratic risk. The positive relationship between opacity and systematic risk occurs because, in the absence of reliable, firm-specific information, a firm's equity price tends to just "follow along" with the overall movement of the market. Jones, Lee, and Yeager (2011a) demonstrate how the increasing opacity of banks during the period 2000-2006 increased the systematic risk of banks while decreasing idiosyncratic risk. Moreover, the more opaque banks suffered the greatest price decline during the 2007 financial crisis.

In this paper, I use a recent change in U.S. accounting rules to examine the impact of opacity on the systematic risk of banks. In 2007, US accounting regulatory bodies introduced SFAS 157, *Fair Value Measurement*, to address the increasing investment by financial institutions in illiquid and opaque assets. SFAS 157 requires firms to report certain assets at fair value, classified into categories of Level 1, 2, and 3. Across Level 1, 2, and 3 classifications, investors face greater degrees of information risk – uncertainty regarding the valuation parameters for underlying assets. To investigate the contributions of opacity to systematic risk, I utilize such fair value measurements to capture increasing levels of illiquidity and opacity. Consistent with previous finance literature, my results show that opacity is positively related to the systematic risk of banks.

II. Hypothesis Development and Research Design

My hypotheses and analysis build upon the assertions in previous work that information risk of bank assets is non-diversifiable in an economy (Easley and O'Hara 2004; Lambert, Leuz, and Verrachia 2007; Jones, Lee, and Yeager 2011b). When one bank's assets are particularly hard to value due to their opaque nature, outside investors must turn to idiosyncratic valuation parameters of other opaque yet seemingly similar firms. Consequentially, the correlation between the entire industry is intensified. As the industry-wide asset composition of financial firms contains relatively greater degrees of opaque assets than the non-financial industry, investors face difficulty in discriminating across good banks and bad banks (Morgan 2002). Such a scenario creates return synchronicity, reduces idiosyncratic risk, and increases systematic risk (Jones, Lee, and Yeager, 2011b).

To evaluate the impact of opacity on systematic risk, I take advantage of recent accounting disclosure requirements that force financial institutions to report assets at Fair Value (SFAS, 157). Fair value is defined by SFAS 157 as "the price that would be received to sell an asset or paid to transfer a liability in an orderly

transaction between market participants at the measurement date." Furthermore, SFAS 157 requires firms to report assets at Fair Value Level 1, Level 2, or Level 3. Level 1 fair value inputs utilize quoted prices for identical items in active markets. Level 2 assets are valued using quoted prices in active markets for similar items or quoted prices in inactive markets for identical items. Market information helps to bring validity to such valuation models. Finally, Level 3 assets are valued with unobservable, firm-supplied estimates based on firm developed models. These models are left largely unaffected by market information. As one can certainly see, each fair value level indicates progressively more illiquid and opaque assets with Level 1 securities being relatively liquid and transparent and Level 3 being the most opaque. Therefore, by decomposing a firm's equity beta among various types of assets, I can begin to analyze the contribution of opacity to a firm's systematic risk.

As previously noted, finance theory implies that information risk – uncertainty regarding the valuation parameters for an underlying asset – increases the systematic risk of a firm. Consequently I expect that Level 2 and 3 assets will lead to greater systematic risk compared to other types of assets. Stated in hypothesis form:

> **H_1**: Level 2 and 3 assets should be positively related to a firm's equity beta.

I furthermore expect the magnitude of contribution to systematic risk to be monotonically increasing across Level 2 and 3 fair value assets, stated formally as:

> **H_2**: Level 3 assets should make a larger contribution to systematic risk compared to Level 2 assets.

Finally, I expect that the contribution of Level 2 and 3 assets to vary over time. During a financial crisis, opacity leads to increased synchronicity of returns. Consequently, my third hypothesis is stated as follows:

> **H_3**: Level 2 and 3 assets should make larger contributions to systematic risk during times of financial crisis.

III. Sample and Descriptive Statistics

My sample covers the period March 2007 through September 2010. Commencing the sample in March 2007 allowed me to take advantage of FAS 157, which provided financial institutions the option to report assets at fair value; however, only beginning in March 2008 did the standard become mandatory. I collected data to serve as proxies for opacity by identifying the entire sample of Bank or Financial Holding Companies (BHCs) that file the Federal Reserve's Consolidated Financial Statements for Bank Holding Companies (FR Y-9C) and that 1) reported at least one positive value at the Level 1, 2, or 3 designation, 2) have total assets in excess of $5 billion, and 3) are publicly traded. This led to a sample of 99 unique banks with 786 firm quarters of data collected. Market data for the sample was collected from the Center in Research and Security Prices (CRSP).

I computed the percent of assets reported as fair value Level 2 (*FV2*) and Level 3 (*FV3*) from the FR Y-9C. All other assets (*OA*) represent the percent of assets not classified as Level 2 or 3. I also computed the leverage (*Liab_to_Assets*) of the banks as total liabilities scaled by total assets. The market beta (*MktBeta*) was computed each quarter for each bank using weekly equity returns and the market model as follows:

$$r_{it} = \alpha_{it} + \beta_i (VW_t) \qquad (1)$$

where *VW* represents the CRSP value-weighted index.

On average, Level 2 (Level 3) assets represent 18.46% (1.19%) of total assets. The average equity beta is 1.58. Figure 1 plots the average asset composition of firms across the sampled time period. Of note, in January 2008, revisions to fair value accounting standards led firms to report more assets at Level 1 fair value designation rather than Level 2, thus a precipitous drop in Level 2 assets can be seen in the figure. Finally, the calculated leverage ratio (total liabilities to total assets) of sampled firms followed industry expectations with a mean of 89.12%.

IV. Empirical Results

In this section, I first analyze the impact of Level 2 and Level 3 assets on the systematic risk of the bank. I then examine the relative contribution each type of asset makes to overall systematic risk and the temporal differences of the impact on systematic risk during crisis and non-crisis periods.

IV.A. Opacity and Equity Risk

To ascertain the impact of Level 2 and 3 assets on the systematic risk of the bank, I estimate the following regression:

$$MktBeta_{ij} = \alpha_i + \beta_1 FV2_{ij} + \beta_2 FV3_{ij} + \beta_3 Liab\_to\_Assets_{ij} + \varepsilon_{ij} \qquad (2)$$

controlling for leverage. The intercept term represents the average market beta for other assets (*OA*), and the coefficients β_1 and β_2, the marginal contribution of Level 2 and Level 3 assets, respectively. Table 2 presents the results of estimations using both ordinary least squares (OLS) and weighted least squares[1] (WLS). Table 3 displays results with control variables for heterogeneity across time (fixed-effects model).

All models hold similar and significant degrees of validity. Coefficients for both Level 2 and Level 3 assets prove to be statistically significant at the 5% probability level within each model, with Level 3 assets carrying significance at the 1% probability level within each. The baseline regressions presented in Table 2 lack strong r-squared values. However, after controlling for time, the OLS Decomposition of Beta with fixed-effects provided the greatest goodness of fit measurement with an r-squared value of just over 16%. Each model's F-value proved statistically significant as well.

Interestingly, the results estimate a negative coefficient for FV2 assets. Such results suggest that, relative to the more opaque

[1] The weight in this regression is the inverse of the standard error from the model used to estimate the market beta, which controls for heteroskedasticity across the computed market betas.

Table 1: Summary statistics for each variable with number of quarterly observations collected and used.

Quarter	Observations
31-Mar-07	9
30-Jun-07	9
30-Sep-07	9
31-Dec-07	9
31-Mar-08	38
30-Jun-08	38
30-Sep-08	50
31-Dec-08	51
31-Mar-09	55
30-Jun-09	89
30-Sep-09	90
31-Dec-09	88
31-Mar-10	88
30-Jun-10	86
30-Sep-10	85
Total Observations Collected	794
Missing of Observations with Missing Values	8
Total Observations Used	786

Variable	Mean	Median	Std Dev
Dependent Variable			
MktBeta	1.5845809	1.4922536	0.7254663
Explanatory Variables			
OA/Intercept	80.24%	85.35%	24.49%
FV2	18.46%	13.64%	23.36%
FV3	1.19%	0.32%	1.83%
Liab_to_Assets	89.12%	89.85%	7.31%

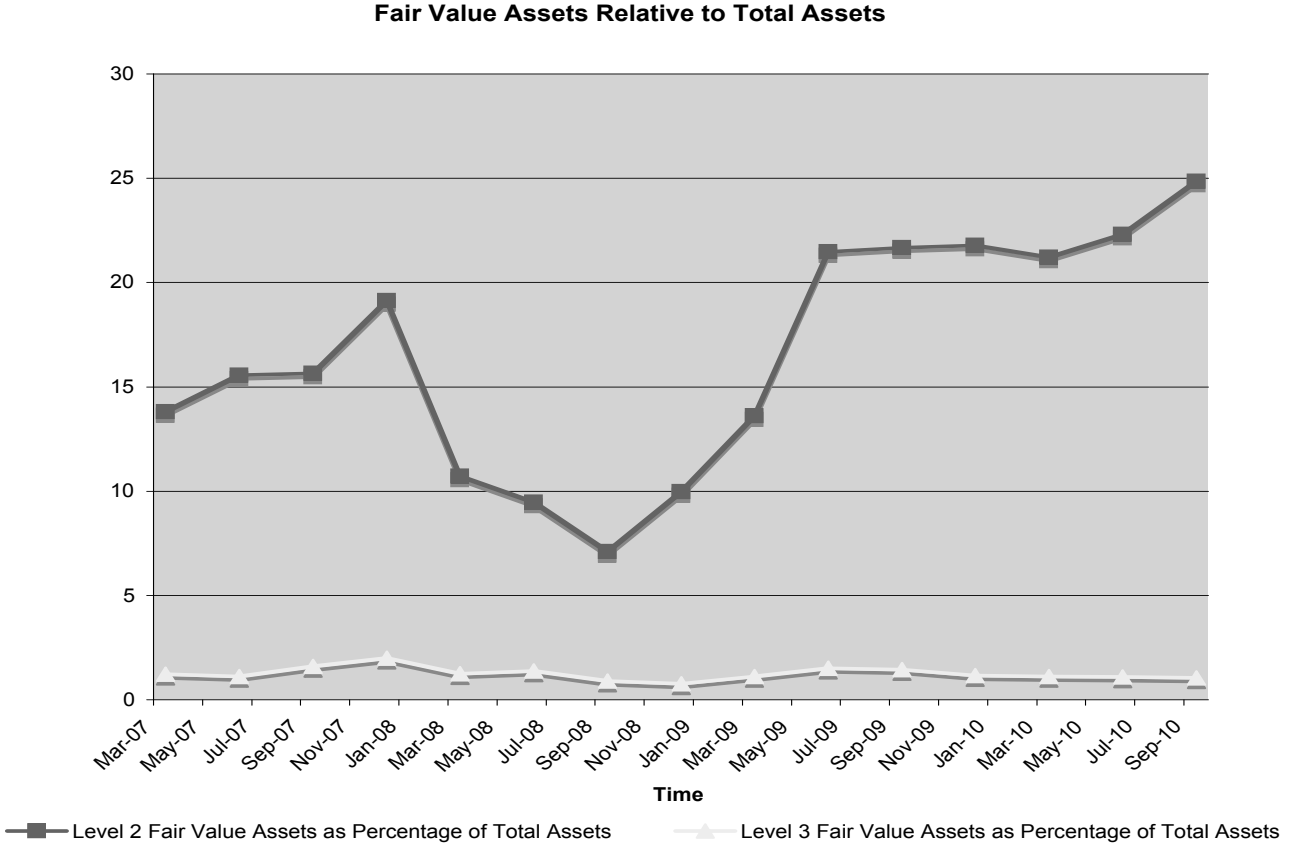

Figure 1: Fair Value Assets Relative to Total Assets

Table 2: Decomposition of equity beta: ordinary least squares and weighted least squares results of regression.

	Ordinary Least Squares Decomposition of Beta		Weighted Least Squares Decomposition of Beta	
Variable	Coefficient	t-statistic	Coefficient	t-statistic
Asset Portfolios				
Other Assets/Intercept	1.44931***	4.67	1.49342***	6.67
FV2	-0.5086***	-3.38	-0.26891**	-2.32
FV3	8.89846***	5.23	9.97159***	6.19
Liab_to_assets	0.13405	0.38	-0.20336	-0.8
Model Analysis				
R^2	0.0358		0.0503	
Adj R^2	0.0321		0.0467	
F-Value	9.68		13.81	
N	786		786	

*p< .10, ** p< .05, ***p< .01

This table reports the ordinary least squares and weighted least squares results of regressing market beta (scaled equity beta for firm I in quarter j) on the FV2 and FV3 components of the decomposed financial asset compositions of sampled firms. The basic model development follows that of Riedl and Serafeim (2009). For both the OLS and WLS models, market beta was used as the dependent variable with observations from March 2007 to September 2010. Coefficients and t-statistics for the explanatory variables of OA (all assets not measured at Level 2 or 3 Fair Value), FV2 (Level 2 Fair Value Assets), FV3 (Level 3 Fair Value Assets), and Liab_to_assets (a leverage component) can be found.

FV3 assets, FV2 assets carry with them much less information risk. In fact, it appears that investments in FV2 assets may actually reduce a firm's systematic risk. As noted earlier, FV2 assets are required to be valued "using quoted prices in active markets for similar items or quoted prices in inactive markets for identical items." The transparency of such valuation parameters appears to reduce investor uncertainty regarding FV2 assets compared to investment in FV3 assets. Without further asset decomposition within each level, however, I am unable to identify specific securities or asset types that contribute to increased transparency.

Most salient to the analysis, FV3 assets carry with them a strikingly positive coefficient. For example, in the OLS with fixed effects model, the coefficient of 7.613 provides strong evidence that investments in assets reported as Level 3 significantly contribute to systematic risk. The finding provides support for the first hypothesis that investments in opaque assets increase a firm's systematic risk. Additionally, the results provide support for the second hypothesis that FV3 assets should have a greater impact on systematic risk than FV2 assets.

IV.B. Robustness

While both the baseline regression and time-controlled models provide evidence that FV3 assets contribute to systematic risk, it is possible that illiquidity of the assets, and not opacity, may be driving the results. To remedy this problem and ensure the models predict the contributions of opacity rather than liquidity, I expanded the model to control for liquidity by inserting another measure into the regression analysis. A proxy for liquidity risk is computed according to the methodology of Pastor and Stambaugh (2003). Specifically, an OLS time-series regression for each bank *i* is estimated.

$$r^{e}_{i,d+1,q} = \theta_{i,q} + \phi_{i,q} * r_{i,d,q} + \gamma_{i,q} * sign(r^{e}_{i,d,q}) * v_{i,d,q} + \varepsilon_{i,d+1,q} \quad (3)$$

In (3), $r_{i,d,q}$ is the equity return for firm *i* on day *d* in quarter *q*; $r^{e}_{i,d,q}$, the excess equity return over the CRSP value-weighted for day *d* in quarter *q*; and $v_{i,d,q}$, the dollar trading volume on day *d* in quarter *q*. The equation is intended to capture return reversals related to lack of liquidity. The coefficient of reflects the liquidity risk of the stock and will be negative and larger in magnitude for a less liquid stock.

Table 4 presents the results that include the Pastor-Stambaugh liquidity factor as a control variable. Results are quantitatively similar to those presented in Table 3. The liquidity variable fails to achieve statistical significance; therefore my presumption regarding the opacity is of FV3 assets becomes stronger. Such results with an included liquidity factor add an important degree of qualitative robustness to the study in that I am able to differentiate between the contributions of liquidity and opacity toward equity risk of financial institutions. Furthering the work of Riedl and Serafeim (2009), I conclude that information risk for Level 3 assets appears to be primarily attributed to opacity.

IV.C. Temporal Analysis

Flannery, Kwan, and Nimalendran (2010) suggest that bank opacity varies across time. Though my study does not attempt to validate this claim, I am able to provide evidence about the impact of opacity on a systematic risk during times of crisis and non-crisis. My third hypothesis predicts that during times of financial crisis, FV2 and FV3 assets should make greater contributions to systematic risk.

In order to test the third hypothesis, I performed a Fama-Macbeth (1973) regression procedure and plotted the quarterly coefficients in Figure 2, which also highlights key events throughout the financial crisis.. Notice the spike in the coefficient for FV3 assets during the period January 2008 to January 2009. In fact, the coefficients for Level 3 assets during the third and fourth quarters of 2008 are nearly twice as great in magnitude as from the same quarters in the previous year. As markets suddenly revise expectations and valuations for such assets, the crisis is further exacerbated.

Table 3: Decomposition of equity beta with fixed effects, regressing on Level 2 and Level 3 Fair Value Assets.

	OLS Decomposition of Beta with Fixed Effects for Time		WLS Decomposition of Beta with Fixed Effects for Time		Decomposition of Beta with Fixed Effects for Time (Clustered at Firm Level)	
Variable	Coefficient	t-statistic	Coefficient	t-statistic	Coefficient	t-statistic
Asset Portfolios						
Other Assets/Intercept	1.01857***	3.23	1.08249***	4.62	1.0824908***	7.34
FV2	-0.40829***	-3.18	-0.35571***	-3.12	-0.3557121**	-2.31
FV3	7.61304***	4.73	9.86821***	6.4	9.868206***	4.36
Liab_to_assets	0.14341	0.44	-0.03119	0.8974	-0.0311871	-0.25
Time Dummy Variables						
Year 08	0.45543***	3.73	0.11575	1.19	0.1157532	0.51
Year 09	0.68782***	5.86	0.56902***	6.01	0.5690224***	6.27
Year 10	0.1224	1.03	0.17774	1.89	0.1777365**	2.07
Model Analysis						
N	786		786		786	
R^2	0.1622		0.1494		0.1494	
Adj R^2	0.1558		0.1428			
F-Value	25.14		22.8			

*** p<.01, ** p< .05, and * p< .10

This table presents the results of regressing market beta on the Level 2 and Level 3 Fair Value Assets of firm i in quarter j while controlling for heterogeneity across time using fixed effects. The addition of dummy variables for time (Year08, Year09, Year10) in the OLS and WLS models adds robustness to the study. By adding time dummy variables the goodness of fit for the regression (Adj R^2) shows a relatively large jump from between 3% and 5% in the non-time controlled models to between 14% and 16% in the time controlled models. ***, **, and * represent statistical significance of all relevant variables at the 1%, 5%, and 10% levels respectively.

To further validate my claim, I performed a seemingly unrelated regression (SUR) to compare fair value asset coefficients during crisis and non-crisis periods. Though economic significance appears obvious in Figure 2, a SUR is required to substantiate the statistical significance. Results of the SUR models with variables for both crisis and non-crisis periods are presented in Table 5. As expected, F-values that test the difference in coefficients reveal that coefficients for both FV2 and FV3 assets are statistically higher during the crisis period compared to the coefficients during the non-crisis period, thereby confirming the presumption that investments in opaque assets carry varying degrees of systematic risk across time.

V. Conclusion

To summarize, I find that opacity contributes to financial instability by exposing firms with heavy investments in Level 3 fair value assets to a marked degree of systematic risk during times of crisis. The lack of transparency associated with these assets noticeably alters investors' risk perceptions, as they face uncertainty regarding the valuation parameters used to report Level 3 fair value assets. Hence, firms holding large portfolios of opaque assets may be among the first to feel the effects of an oncoming financial firestorm.

An examination of investments in informationally opaque fair value assets by bank holding companies yields significant evidence that opacity contributes to the systematic risk of a bank. Results signify that the market valuation of financial institutions is a product of those institutions' investments in Level 2 and 3 fair value assets. Additionally, the results imply that contributions of opacity to systematic risk are not consistent over time. During periods of turmoil, investments in opaque assets create a greater degree of systematic risk than in non-crisis periods.

The results suggest that the recent conversation about disclosure standards and mark-to-market accounting during times of crisis are legitimate. Recent implementation of fair value standards has allowed us to better understand how investors value different types of assets during varying market conditions. Fluctuations in the contributions of assets to systematic risk over time, particularly during crisis periods, indicated that current disclosure requirements still may not be sufficient to completely assuage investor uncertainty concerning such assets. Further regulation in the banking industry to bring greater degrees of transparency to highly opaque assets may increase market efficiency and alleviate the intensity of financial downturns. In short, enhanced disclosure standards for illiquid and opaque assets appear warranted.

References

Bernanke, Ben (1983). "Nonmonetary effects of the financial crisis in the propagation of the great depression." *American Economic Review* 73, 257-276.

Diamond, D. and P Dybvig (1983). "Bank runs, deposit insurance, and liquidity." *Journal of Political Economy* 91, 401-419.

Easley, D. and M O'Hara (2004). "Information and the cost of capital." *Journal of Finance* 59, 1553-1583.

Fama, E., and J. Macbeth, 1973. Risk, return, and equilibrium: Empirical tests. *Journal of Political Economy* 81, 607-636.

Table 4: Decomposition of equity beta adding Pastor-Stambaugh liquidity factor.

	OLS Decomposition of Beta with Pastor-Stambaugh Liquidity Factor		WLS Decomposition of Beta with Pastor-Stambaugh Liquidity Factor		OLS Decomposition of Beta with Pastor-Stambaugh Liquidity Factor (Clusterd at Firm-Level)	
Variable	Coefficient	t-statistic	Coefficient	t-statistic	Coefficient	t-statistic
Asset Portfolios						
Other Assets/Intercept	1.01711**	3.23	1.07625***	4.6	1.0762493***	7.18
FV2	-.40660**	-3.16	-.35467***	-3.11	-.3546663**	-2.31
FV3	7.58947***	4.72	9.81575***	6.37	9.8157497***	4.42
Liquidity	-0.72987	-0.67	-1.38156	-1.31	-1.3815591	-0.76
Liab_to_assets	0.14316	0.44	-0.02785	-0.12	-0.0278478	-0.22
Time Dummy Variables						
Year 08	0.45904***	3.75	0.12366	1.27	0.1236617	0.56
Year 09	0.68945***	5.87	.57367***	6.05	.5736719***	6.11
Year 10	0.12471	1.04	.18319*	1.94	.1831876**	2.04
Model Analysis						
N	786		786		786	
R^2	0.1627		0.1513		0.1513	
Adj R^2	0.1552		0.1436			

*** p<.01, ** p< .05, and * p< .10

This table presents the results of regressing market beta on the Level 2 and Level 3 Fair Value Assets of firm i in quarter j with a proxy for liquidity risk. The proxy for liquidity risk is computed according to the methodology of Pastor and Stambaugh (2003). Qualitative analysis of the results remains similar to results of fixed-effects OLS models in Table 3. . ***, **, and * represent statistical significance of all relevant variables at the 1%, 5%, and 10% levels respectively.

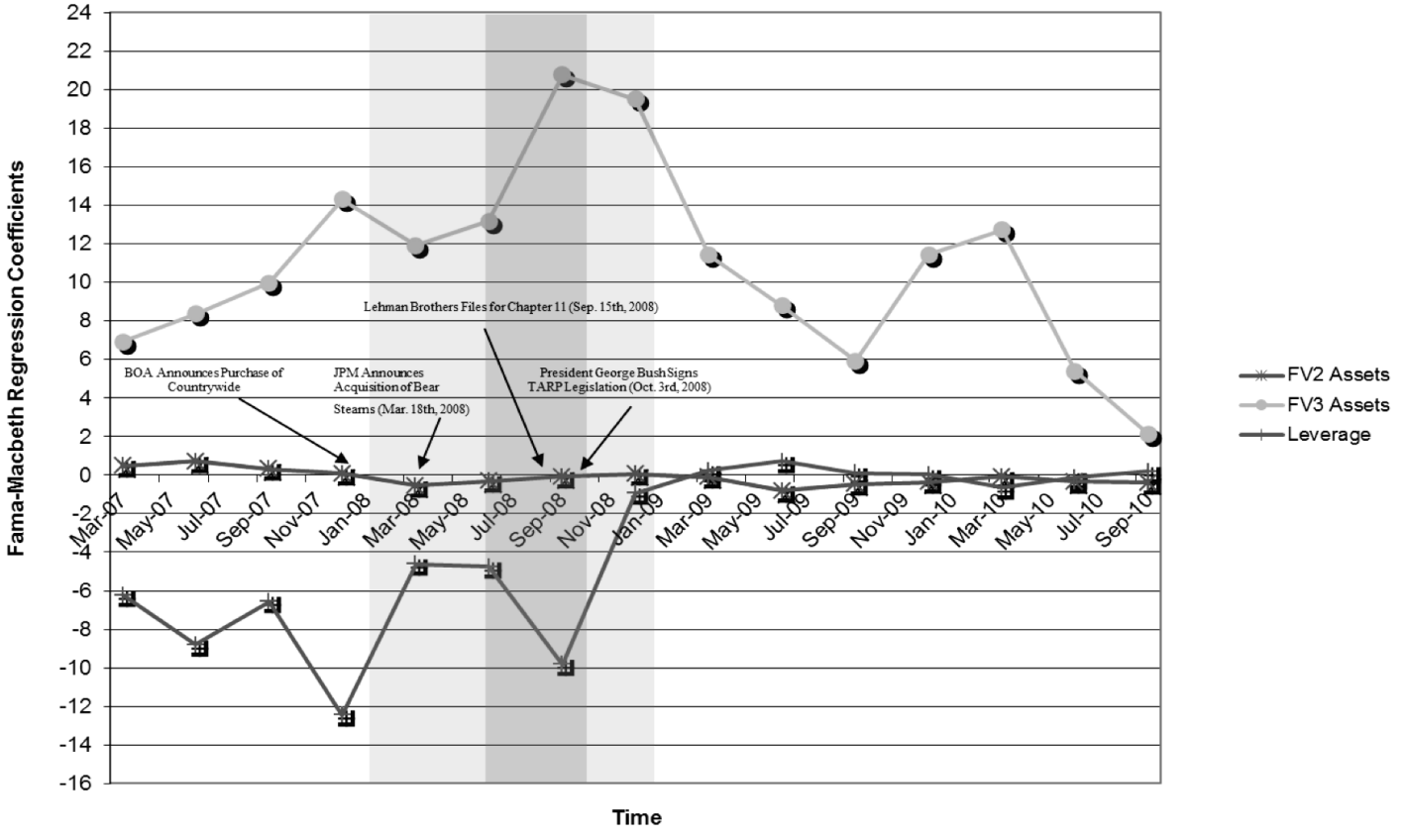

Figure 2: Fair Value Coefficients Across Time

Table 5: Fama-Macbeth procedure results/tests for differences between crisis and non-crisis periods.

	OLS Test for Differences Between Crisis and Non-Crisis Periods		WLS Test for Differences Between Crisis and Non-Crisis Periods	
Variable	Coefficient	t-statistic	Coefficient	t-statistic
Intercept	1.1153***	3.61	1.15516***	5.05
FV2_Crisis	0.02599	0.13	-0.04792	-0.26
FV2_NonCrisis	-.65430***	-4.13	-.47593***	-3.53
FV3_Crisis	10.66145***	4.63	15.12463***	6.38
FV3_NonCrisis	3.43554	1.61	5.26646***	2.72
Liab_to_assets	0.14929	0.47	-0.01392	-0.06
Year 08	0.28095**	2.29	-0.04111	-0.42
Year 09	0.5916***	5.11	.48130***	5.16
Year 10	0.12186	1.04	0.09226	1.86
Model Analysis	F-Value	Pr > F	F-Value	Pr > F
FV2	7.81	0.0053	3.63	0.0571
FV3	5.36	0.0209	10.47	0.0013

Fama-Macbeth Implied Betas		
Quarter	FV2 Coefficient	FV3 Coefficient
31-Mar-07	0.47889	6.9137
30-Jun-07	0.7145	8.3525
30-Sep-07	0.32244	9.9758
31-Dec-07	0.07578	14.291
31-Mar-08	-0.53859	11.9109
30-Jun-08	-0.31685	13.1637
30-Sep-08	-0.075	20.7681
31-Dec-08	0.06075	19.4953
31-Mar-09	-0.10543	11.4045
30-Jun-09	-0.81894	8.7906
30-Sep-09	-0.46253	5.9243
31-Dec-09	-0.36429	11.4266
31-Mar-10	-0.08238	12.7273
30-Jun-10	-0.33475	5.4026
30-Sep-10	-0.40045	2.1241

*** p<.01, ** p< .05, and * p< .10

This table presents the quarterly implied equity betas of FV2 and FV3 assets from March '07 through September '10. It also presents results of seemingly unrelated regressions to test for significance of coefficients in crisis and non-crisis periods. F-value's reveal that the coefficients are statistically higher in crisis periods (defined as March '08 to January '09). . ***, **, and * represent statistical significance of all relevant variables at the 1%, 5%, and 10% levels respectively.

Flannery, Kwan, and Nimalendran M (2004). "Market evidence on the opaqueness of banking firms' assets*." Journal of Financial Economics,* 71, 419-460

Flannery, Kwan, and Nimalendran M (2010). "The 2007-2009 financial crisis and bank Opaqueness." *Federal Reserve Bank of San Francisco Working Paper.*

Lambert, R., Leuz, C., and Verrachia, R (2007). "Accounting information, disclosure, and the cost of capital." *Journal of Accounting Research* 45, 385-420.

Morck, R., Yeung, B., Yu, W., 2000. The information content of stock markets: Why do emerging markets have synchronous stock price movements? *Journal of Financial Economics* 58, 215-160.

Morgan, Donald P. (2002). "Rating banks: risk and uncertainty in an opaque industry." *American Economic Review* 92, 874-888.

Jones, Jeffrey S., Lee, Wayne Y. and Timothy Yeager (2011a). Opaque banks, price discovery, and financial instability. *Working Paper*, University of Arkansas.

Jones, Jeffrey S., Lee, Wayne Y. and Timothy Yeager (2011b). Valuation and systemic risk consequences of bank opacity. *Working Paper*, University of Arkansas.

Pastor, L., and R. Stambaugh, 2003. Liquidity risk and expected stock returns. *Journal of Political Economy* 111, 642-685.

Riedl, Edward and George Serafeim (2009), "Information risk and fair value: An examination of equity betas and bid-ask spreads," Working Paper, Harvard Business School.

Mentor Comments: Professor Jeff Jones describes the manner in which Jody took advantage of a recent change in accounting disclosure requirements to explore the relationship between opacity of assets and bank risk, noting the independence and sophistication of his work.

As an important supplier of credit to the economy, a healthy banking industry is essential for economic prosperity. The opacity of the banking industry, however, can jeopardize the health of the industry (and the overall economy) since opacity fosters price contagion that exacerbates the cycle of speculative bubbles and crashes that create financial instability. Price contagion that arises in opaque markets can manifest itself in a number of ways, one of which is a change in the composition of risk. Since opacity makes it difficult for investors to "see inside" individual firms, it tends to decrease idiosyncratic (firm-specific) risk and increase systematic risk. When the systematic risk of all firms in an industry becomes elevated, it creates a high degree of return synchronicity. In such an environment, negative information about a single firm tends to drive down the stock prices of all firms in the industry, creating the potential for a systemic crisis. Consequently, understanding how the activities and assets of banks impact this process is of critical importance to abating the negative consequences of opacity.

I became acquainted with Jody in 2010 while he was a student in two of my courses. During this time, we had a number of out of class discussions regarding the causes and consequences of the recent financial crisis. I shared with him some of the research projects I had been working on related to the opacity of the banking industry as a contributing factor to the financial crisis. Soon after, he approached me with an idea that he wished to explore for his Senior Honors Thesis. His work on this project has consistently exceeded

my expectations of an undergraduate student, and in fact is of a quality that would rival that of many PhD students. I am extremely impressed by how well Jody was able to independently process the literature and recognize how to make a significant contribution.

In this project, Jody uses a novel approach, made possible by a recent accounting change, to investigate how investments in opaque assets impact the systematic risk of a bank. The recently adopted SFAS 157 requires banks to classify certain assets into 3 levels and report them at fair value. Level 1 assets are considered relatively transparent, and Level 2 and Level 3 assets are considered increasingly opaque, respectively. Jody finds that investing in greater quantities of Level 3 assets significantly increases the systematic risk of a bank. Moreover, the contribution to systematic risk for both Level 2 and Level 3 assets was much higher during the height of the 2007-2008 financial crisis compared to periods of relative tranquility. Thus, Jody effectively demonstrates how the opaqueness of banks can exacerbate a financial crisis, providing useful information for policymakers and regulators.

PARALLELIZING SCALE INVARIANT FEATURE TRANSFORM ON A DISTRIBUTED MEMORY CLUSTER

By Stanislav Bobovych
Department of Computer Science and Computer Engineering

Faculty Mentor: Amy Apon
Department of Computer Science and Computer Engineering

Abstract

Scale Invariant Feature Transform (SIFT) is a computer vision algorithm that is widely-used to extract features from images. We explored accelerating an existing implementation of this algorithm with message passing in order to analyze large data sets. We successfully tested two approaches to data decomposition in order to parallelize SIFT on a distributed memory cluster.

Introduction

In certain domains, it is very useful to extract information about objects in images. A specific domain, geospatial sciences, is facing the problem of ever increasing high resolution data. Streams of data from satellites, unmanned aerial vehicles, airplanes, and people need to be accurately georeferenced and registered. Using conventional methods, including desktop computers that run serial programs, to analyze this data takes too long or requires more resources than a single desktop contains. Parallel cluster computing provides more resources than a desktop and allows processing of different parts of the problem at the same time. Using parallel processing, it is possible to solve the problem of analyzing large sets of geospatial data.

Manual time-consuming tasks like image mosaicking, stitching, alignment, and matching of geospatial data collected by multiple sensors can be made autonomous by the use of computer vision algorithms such as Scale Invariant Feature Transform (SIFT). These techniques are extensively used in geospatial sciences. Specifically, there exists a need to take an input image from a user, analyze and describe it, and finally match the image to a known location that has been georeferenced. The work presented here is part of a larger project that is building a system that uses computer vision techniques, databases, and algorithms to quickly and autonomously solve certain geospatial science problems like georeferencing and registering new and existing Geospatial Information Systems (GIS) data. The GIS data sets that motivate this parallel implementation are terabytes in size. A single image may be larger than the memory of a single node, hence the need to extract features and descriptors from an image in parallel. Also, as output of data from different sensors increases, the amount of data that needs to be processed in a timely manner will increase.

This article describes ways to implement a distributed memory parallel version of a popular computer vision algorithm Scale Invariant Feature Transform (SIFT) using the Message Passing Interface (MPI) library in order to solve the problem of timely analysis of large GIS data sets for which the original implementation of SIFT was not designed. There have been successful prior parallel implementations of SIFT, but they are geared toward real-time processing of small data whereas this implementation emphasizes scalability and capacity computing.

Background

A number of basic concepts in image processing and in geospatial science are essential to understanding this research project. SIFT is an example of a feature detection and description algorithm. SIFT++ and VLFeat are examples of SIFT implementations. Clusters are a type of parallel architecture used for executing parallel applications, and InfiniBand is a fast interconnect network technology that is typically used in clusters. Message Passing Interface is a programming model. Each of these topics is covered in more detail in the following sections.

SIFT

There are a multitude of feature detection algorithms. [16] The computer vision algorithm SIFT was chosen as the keypoint detection algorithm for this research because it is well known in the scientific community and it provides the best results compared to the computation effort. [6] [10] [3] This algorithm automatically detects and describes interesting features (blobs/regions in high contrast areas) in images. These descriptions are unique, stable with respect to scale, rotation, and translation, and are used in computer vision applications. [9] SIFT is designed to take an input image and output descriptors of unique points, called keypoints, in the image.

The following are the steps in the SIFT algorithm:

1. Scale-space extrema detection: A scale space pyramid is built. Extrema are detected over all scales and image locations. Difference-of-Gaussian function is used to identify potential interest points that are invariant to scale and orientation.

2. Keypoint localization: Once a potential keypoint is found, location and scale are determined. Keypoints are filtered based on their stability. Keypoints in low contrast areas or ones that are poorly localized along an edge are thrown out.

3. Orientation assignment: Keypoints are assigned one or more orientations based on local image gradients. These orientations are used for all future operations. This step allows the generation of descriptions that are invariant to orientation, scale and position.

4. Keypoint descriptor: The local image gradients are measured at the selected scale in the region around each keypoint. These are transformed into a transformation invariant representation. [8] [7]

At the time of the writing of this paper, there are two major serial implementations of the SIFT algorithm, SIFT++ [18] and VLFeat [19]. The first implementation is a C++ implementation of the SIFT algorithm and was designed to be as close as possible to David Lowe's original implementation. VLFeat is a set of computer vision libraries written in C. SIFT++. It was chosen as the base code for this research because it was faster, used less memory and was already used by researchers at University of Arkansas.

There have been previous attempts to parallelize SIFT. Examples include a Graphical Processing Unit (GPU) implementation [13], a Field Programmable Field Array (FPGA) implementation [1], and a multi-threaded implementation [20]. The GPU implementation cited here achieves 10x speedup over the optimized CPU implementation. The multi-threaded implementation yields a speedup of 2x when using eight processors. Also, [20] explores GPU acceleration of SIFT with offloading the Gaussian convolution to the GPU. The particular part of the code was accelerated by a factor of 13, but the total execution time of the application was accelerated by a factor of 1.9. Another highly optimized multi-threaded implementation [21] was able to achieve an average of 6.4x speedup.

Most of the effort in accelerating SIFT has been in the real-time computer vision domain. This subject area deals with small images, for example 640x480 images streamed at 30 frames per second. This kind of processing does not stress the memory architecture since the data is so small. However, once the scale space generated of an image can no longer be held in a cache, memory bandwidth and memory size become the limiting factors in performance of an application. These solutions cannot be used to solve the geospatial domain problems.

Technology

The Star of Arkansas at the Arkansas High Performance Computing Center and Ranger at the Texas Advanced Computing Center were used in this research. Each system is described briefly.

The system used for development and testing was the Star of Arkansas. This cluster consists of 157 Symmetric Multi-Processing (SMP) compute nodes. Each node contains dual quad-core Xeon E5430 processors, 2x6MB cache, running at 2.66GHz with 1333 MHz FSB. Each core has 2 GB of main memory. The theoretical peak performance of Star is 13.36 teraflops (13.36 × 1012 floating point operations per second).

The network interconnect on the Star of Arkansas is InfiniBand and runs at 10 Gbps. The cluster is interconnected with an additional Gigabit Ethernet network for NFS access, and another Gigabit Ethernet network for management.

The Star of Arkansas has NFS and Lustre file systems. The NFS file system is used for permanent storage and is 4 TB. The Lustre file system resides on Data Direct Networks storage, is used for fast temporary storage, and is 21 TB. Lustre is an open source distributed parallel file system for high performance cluster computing. [11] A Lustre system is composed of file system clients which access the file system, object storage servers (OSS) which provide file I/O service and metadata servers (MDS), which manage the names and directories in the file system. All of this is transparent to applications which access the file system using normal POSIX semantics. [2]

After initial development and testing, TACC's Ranger system was used to conduct large-scale tests. This cluster consists of 3,936 SMP compute nodes. Each node contains four AMD Opteron Quad-Core 64-bit processors (16 total), running at 2.3GHz with 1.0 GHz HyperTransport system Bus, and 2 channels with 667 MHz DDR2 DIMMS. Each processor has 64 KB of L1 cache, 4x512 KB L2 Cache, and 2 MB of on-die (shared) L3 Cache. Each node has 32 GB of main memory. The theoretical peak performance of Ranger is 579.4 teraflops (579:41012 floating point operations per second). The interconnect topology is a 7-stage, full-CLOS fat tree with two large Sun InfiniBand Datacenter switches at the core of the fabric (each switch can support up to a maximum of 3,456 SDR InfiniBand ports). [12]

InfiniBand is a switched communications link with high throughput, low latency, quality of service and failover, and scalability. Applications use InfiniBand as a messaging service. It is used for storage, Inter Process Communication (IPC) or any other communication between the application and its environment. This is different from the byte-stream oriented TCP/IP/Ethernet, which works on transporting bytes of information between application sockets and requires the operating system to move bytes from the program's virtual buffer space, to the kernel's network stack and finally onto the wire. InfiniBand does not request the operating system for access to communication resources. Applications access the InfiniBand messaging service directly. [5]

Message Passing Interface (MPI) is an Application Programming Interface (API) that allows communication between processes using a message passing paradigm. [14] It is used to create scalable high performance parallel applications. Processes can reside on the same machine or on multiple machines in a cluster, and communicate through explicit messages. This is unlike the shared-memory paradigm, where threads communicate using shared buffers and have symmetric memory access to memory. [15]

Methodology

We have discussed the need for a fast and scalable implementation of SIFT that can be used in geospatial science. In order to avoid duplicating work, an existing implementation, SIFT++ by Andrea Vedaldi of University of British Columbia, was used as base code. [17] In the computer vision community, this is a well known open source implementation. [20] This implementation, compiled into a binary called sift, was analyzed for hot spots and memory usage; different parallelization implementations using this base code were tested. The goal was to reduce the overall runtime of the application while generating the same results as the serial implementation.

Performance Metrics

There are many ways to measure performance. One can measure the wall time or the system/user time of an application, latency, response time, rate of integer or floating point operations, or the efficiency of an application. [4] The chosen metrics have to be relevant and meaningful within the application's domain and have to be accepted by the users in that domain.

In the domain of geospatial science and the problems this specific application is trying to solve, three metrics are of most concern. The first is the wall time of the application. Scientists in the field are willing to tolerate the delays between asking a question and getting an answer anywhere from a few seconds to a few hours, so reducing the wall time of an application is important. There is a distinction between wall time and run time. Wall time incorporates the I/O, operating system jitter, and the actual work done by the application. In this paper, wall time and run time are used synonymously. The second metric closely tied to the first is the speedup over the serial implementation. Speed up is the serial run time divided by the parallelized run time. This is the way to measure if the effort and resources spent to make the application run faster were worth it. The final metric is the accuracy of the results because bad answers that are generated quickly are not useful to domain users. The output of the parallelized application has to match the serial version's output.

Single Node Performance

SIFT++ is both memory intensive and computationally expensive. Scale space generation's computation time is deterministic. This process uses a great deal of memory since the scale space is generated once and all of it is stored in memory throughout the life of the application. Analyzing the code, the memory usage by the scale space pyramid is:

$$Memory\ usage = 4\ bytes * l \sum_{i=s}^{m} \frac{w * h}{2^{2i}} a$$

The parameters in this equation are: final octave *m*, first octave *s*, current octave *i*, number of levels per octave *l*. Using a 800x640 image with standard parameters as an example, generation of scale space is 25% of computation and takes up 62.5 MB of memory.

During testing, the serial implementation of SIFT failed to analyze a 9600 x 7200 image, on a Star of Arkansas node, a system with 16 GB of RAM. The domain space uses images of this size and greater. Besides the serial implementation failing to process large images, given the right parameters this implementation would fail to process relatively small images. The problem of single node memory exhaustion had to be overcome.

As shown in Figure 1, the computation time is highly dependent on the number of keypoints found in an image. The number of keypoints is dependent on the objects in the image and the size of the image. Once all of the keypoints are found, the majority of the computation is spent calculating descriptors for these keypoints.

Parallelization Strategy

In this application, time and memory are the constraining factors when processing data on single nodes. Previous attempts at parallelizing SIFT involved speeding up specific parts of the algorithm using fine grained parallelism. [20] In this implementation, the whole application is being made to run faster using high level data parallelism. Instead of focusing on making a particular part of the algorithm fast, the data used by the application is divided between multiple instances of the application. One approach is to simply partition the image into horizontal slices and distribute pieces of the image among nodes. Each node uses SIFT to process the data and outputs a description of the image slice. The output from the nodes is aggregated to form a final description of the whole image. The second approach partitions the image into blocks. The number and the size of the blocks depends on the dimensions of the image and the number of nodes used to process the image. Each block is processed by different nodes in parallel and the descriptions are aggregated. The parallelization strategy is outlined in the following steps:

1. Partition (decompose) the image into smaller pieces.
2. Either send each piece to a different node, or have each node read a different piece of the image directly from the file system.
3. Compute SIFT descriptors on each piece of the image.
4. Aggregate the descriptors.

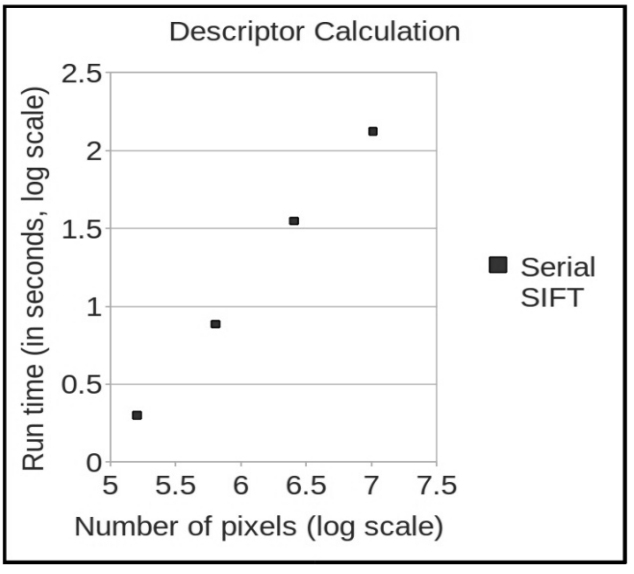

Figure 1. Keypoint descriptor calculation run times.

Implementation

Due to memory limitation of single nodes, the solution was to reduce the memory footprint of the data on each node. This was done by partitioning the image into smaller pieces and sending each piece to a different compute node in the cluster. Each node then ran SIFT on its piece, computed the descriptors, adjusted the coordinates of the descriptors, and output the descriptors. Finally, the descriptors were aggregated into a single descriptor file that is useful to other applications and scientists.

Row-Wise Decomposition

The first attempt at splitting the image was to slice the image horizontally. The image was divided between the nodes; each node

received a small slice of the original image. The root node loaded the entire image into memory, then scattered different pieces to different nodes. Each node was responsible for adjusting the x,y coordinates of the keypoints based on its rank. At first, the MPI code was directly integrated with the original SIFT++ code to accomplish this. This approach was simple and generated results in which data loss due to boundary effects was between 1% and 3%. However, this approach was not the most efficient, since certain images can be partitioned in a better way. Before moving on to the next approach, the code was rewritten. Most of the MPI code was transferred to a decomposition driver and the SIFT driver was made into a library function that was called from the MPI driver. The SIFT driver accepted command line arguments with which the program was started, an image buffer, process rank, x and y offsets. This generic SIFT driver allowed easy decomposition driver swapping.

Figure 2. Row-wise decomposition.

Block-wise Decomposition

The second attempt at partitioning the image was to use block decomposition. The image was divided into equally sized blocks, and each block was sent to a node for processing. Each node adjusted the x,y coordinates of keypoints and output the data to a file. This approach was particularly challenging because of how the data is organized. The data was stored in an image format called Netpbm. After the image was loaded into memory, it is stored as a one dimensional array of floats. To properly stride through the data, various MPI mechanisms were used.

Block decomposition was achieved in a first implementation in the following way. First, the original image was loaded into memory by the master process. The height and width of the image were broadcast to all nodes. The master process then calculated the proper dimensions of an individual partition of the original image. The partition dimensions were broadcast to all processes.

A two dimensional Cartesian Communicator was created. The sizes of the dimensions were determined by the ratios between the original width and height, and the partition width and height. The MPI communicator was non periodic and reordering was not allowed. Every process allocated a buffer that contained a partition of the original image.

Figure 3. Block-wise decomposition.

A new MPI data type was created so that the original image could be easily split between different processes. The rows of a partition of the original image can be thought of as blocks, the pixels in each row as block elements, and the spacing between pixel rows as the block spacing. A vector that contained the number of blocks, the number of elements in a block and the block spacing was created. A struct was created to hold the vector. Offsets for each image partition were calculated. The original image was then scattered to the Cartesian communicator using the calculated offsets and the new data type as the type. Each process then worked on its portion of the image and output descriptors. The x,y coordinates were adjusted based on the Cartesian coordinates of the process. Later, block-wise decomposition was reimplemented using the driver paradigm described in the row-wise decomposition section.

Decomposition Using Parallel I/O

It was also possible to exploit parallelism in data access and storage. In the first two implementations, the master node read the image and distributed different pieces to different processes using MPI communication. In the third implementation, each process read different portions of the image in parallel using MPI I/O.

The first attempt at using MPI I/O was to implement row-wise decomposition. Each process read the header of the image file, calculated appropriate file offsets, set the file view and read a portion of the image into a buffer. Then each process used the SIFT driver on the buffer. In a later implementation of the row-wise I/O partitioning, only the master process read the header of the image file and determined the header offset. Once that was known, the master thread broadcast the width of the partition, height of the partition, and an offset to all the processes. Each process then created an appropriately sized buffer, set its file view, read its portion of the image using MPI I/O, and executed the SIFT algorithm on its portion of the data.

Block-wise decomposition was accomplished in a similar fashion to the row-wise decomposition. The master process read the image, extracted height and width, and broadcast the information. Each process in turn calculated the block dimensions and created a distributed array. The distributed array was used to create an MPI filetype, which in turn was used to set the file view

for each process. Each process then read its portion of the file, stored the data in a buffer, and executed the SIFT algorithm on that buffer.

Experiments and Analysis

Three experiments were set up to test the parallel implementations. The first experiment involved analyzing a sequence of images with SIFT. The sequence consisted of differently sized random pieces of the same geospatial image. The reason for using random pieces is that SIFT's computation time is dependent on the number of keypoints found in an image. Using the same image and upscaling it to create larger images would be an unrealistic test since in the geospatial domain larger images should contain a larger number of interesting features than smaller images.

The second experiment analyzed the correctness of the output of the parallel implementations by comparing their output with the serial version's output. The first and second experiments used the serial, row-wise in-memory decomposition, block-wise in-memory decomposition, row-wise I/O decomposition and block-wise I/O decomposition. The final experiment was SIFTing an actual geospatial image on a TeraGrid resource, Ranger.

Experiment 1 – Run time

Data parallelization successfully reduced the runtime of SIFT. The comparison of serial and parallel implementations can be seen in Table 1. The runtime of the serial implementation increases as the number of pixels in the images increases. In comparison, the runtime of the parallel implementations increases at a slower rate compared to the runtime of the serial implementation. Both decomposition methods achieved significant performance improvements over the serial version.

The average speed-up was 19.5x, with row-wise parallel IO decomposition achieving a speed-up of 20.18. The superlinear speed-up was attributed to the fact that the parallel implementations were able to utilize memory bandwidth better than the serial version by keeping a larger portion of the data in cache. Row-wise decomposition in memory and parallel I/O were slightly better than the block-wise decomposition. This may be due to the fact that C stores arrays in memory in row-major format. Rows of data were accessed more efficiently than columns, since access by rows of data accesses contiguous memory regions. The block-wise decomposition, as with column-major access, requires a number of accesses to memory that were not contiguous. Contiguous accesses to memory have high Central Processing Unit (CPU) cache hit rate, allowing the CPU to fetch data from the cache. Non-contiguous access to memory generates CPU cache misses, requiring the CPU to access main memory, which is slow compared to accessing cache.

Experiment 2 – Correctness

The results of the second experiment are shown in Figure 4. The parallel implementations had data loss due to boundary effects between the partitions of the original data. The figure shows that the block decomposition had less loss on all of the images tested, by more than a factor of two for all images tested.

The data loss may not be a problem, since domain images generate millions of keypoints. With increasing image size, the ratio of keypoints to lost keypoints decreases. Block decomposition created partitions that have smaller perimeters as a function of the partition area than row decomposition.

The loss of keypoints was due to how SIFT finds and filters keypoints. Keypoints found on borders of an image tend to be rejected. Also, the descriptions of a keypoint in the original image and in the fragment were different since different neighborhoods were used for the description. The loss of keypoints and differences in descriptors on image partitions are collectively called edge effects.

Experiment 3 – Scalability

The last experiment was SIFTing an actual geospatial image. A 116987x11005, 1.2 GB image, was SIFTed on Ranger, a TeraGrid resource, using in-memory block decomposition. Data are shown in Table 2.

Row-wise decomposition was attempted, but failed due to lack of sufficient memory on the nodes. MPI I/O was not used because it is not supported on Ranger. In all the trials, a single process ran on a single node. This was to maximize memory availability for each process. This particular implementation scaled well when the number of cores/nodes increased. Increasing the node count reduced the memory usage per node, yielding even better speed-up.

Conclusion and Future Work

Data parallelization of SIFT on a distributed memory cluster is a viable way to find interesting features in geospatial images. Block-wise partitioning scheme is shown to scale well. MPI constructs and advanced communication functions are well suited to accomplish this task. MPI I/O makes the implementation of block-wise and row-wise decomposition methods easier than in-memory block decomposition; it is also faster than in-memory decomposition. Edge effects in large images are almost negligible.

The results from this research suggest several directions for future work. Specific lines of inquiry include memory exhaustion, edge effects, and descriptor aggregation.

If the image is of sufficient size, partitioning the image into pieces and sending the pieces to nodes will fail if during processing of partitions, node memory is exhausted. To solve this problem, the maximum partition size has to be determined before image partitioning. The image then needs to be partitioned in such a way that the maximum partition size is not exceeded. If the

Table 1. Experiment 1 run times (in seconds).

Pixels	Serial time	Row-wise run time	Row-wise IO time	Block-wise run time	Block-wise IO time
160000	1	0.66	0.66	0.66	0.66
640000	6	0.33	0.33	0.33	0.33
2560000	23.3	2	2	2	2
10240000	114	6.33	6	7.33	7
40960000	622	26.66	26.66	28.33	27.66
69120000	848	45.33	44.33	47.66	47
Avg. speedup	1	19.85	20.18	18.7	19.07

number of partitions in this scheme is larger than the number of processing nodes, partitions should be added to a work queue and submitted to be processed in batches or on demand basis.

Keypoints that lie along the edge of an image tend to be filtered out and do not appear in the final solution. Since all of the mentioned partition schemes generate image edges, keypoints are lost. Overlaps between partitions will fix this problem. The

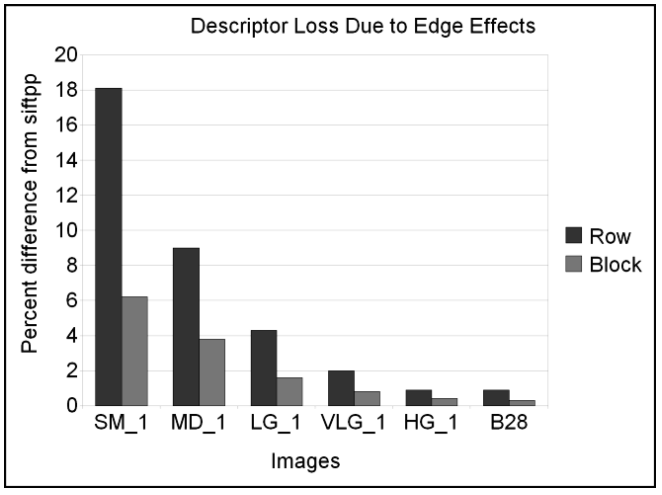

Figure 4. Experiment 2: Image size increases from left to right.

overlaps would generate redundant keypoints that will have to be filtered out.

Currently each process writes its descriptors to its own file, and at the end the files are concatenated to generate the final descriptor file. It may be possible to have all the processes write their results to a single file. Both of these additions would utilize a fast file system and take load off the master node.

References

[1] Cristina Cabani and W. James MacLean. 2006. A Proposed Pipelined-Architecture for FPGA-Based Affine-Invariant Feature Detectors. In *Proceedings of the 2006 Conference on Computer Vision and Pattern Recognition Workshop* (CVPRW '06). IEEE Computer Society, Washington, DC, USA, 121-. DOI=10.1109/CVPRW.2006.19 http://dx.doi.org/10.1109/CVPRW.2006.19

[2] High-performance storage architecture and scalable cluster file system. White paper, Sun Microsystems, 2007. Available online (20 pages).

[3] Herbert Bay, Tinne Tuytelaars, and Luc Van Gool. Surf: Speeded up robust features. In In ECCV, pages 404–417, 2006.

[4] Jeffrey J. Evans, Cynthia S. Hood, and William D. Gropp. Exploring the relationship between parallel application run-time variability and network performance in clusters. Local Computer Networks, Annual IEEE Conference on, 0:538, 2003.

[5] Paul Grun. Introduction to infiniband for end users. White paper, InfiniBand Trade Association, 2010. Available online (54 pages).

[6] Asaad Hakeem, Roberto Vezzani, Mubarak Shah, and Rita Cucchiara. 2006. Estimating Geospatial Trajectory of a Moving Camera. In *Proceedings of the 18th International Conference on Pattern Recognition - Volume 02* (ICPR '06), Vol. 2. IEEE Computer Society, Washington, DC, USA, 82-87. DOI=10.1109/ICPR.2006.499 http://dx.doi.org/10.1109/ICPR.2006.499

[7] David G. Lowe. Method and apparatus for identifying scale invariant features in an image and use of same for locating an object in an image. U.S. Patent #6711293 issued

03/23/2004, March.

[8] David G. Lowe. Distinctive image features from scale-invariant keypoints. Int. J. Comput. Vision, 60:91–110, November 2004.

[9] D.G. Lowe. Object recognition from local scale-invariant features. In Computer Vision, 1999. The Proceedings of the Seventh IEEE International Conference on, volume 2, pages 1150 –1157 vol.2, 1999. 31

[10] Krystian Mikolajczyk and Cordelia Schmid. A performance evaluation of local descriptors. IEEE Transactions on Pattern Analysis & Machine Intelligence, 27(10):1615–1630, 2005.

[11] The University of Arkansas. Hardware. http://hpc.uark.edu/hpc/about/hardware.html

[12] The University of Texas at Austin. Ranger user guide. http://services.tacc.utexas.edu/ index.php/ranger-user-guide.

[13] Sudipta N. Sinha, Jan michael Frahm, Marc Pollefeys, and Yakup Genc. Gpu-based video feature tracking and matching. Technical report, In Workshop on Edge Computing Using New Commodity Architectures, 2006.

[14] M. Snir, S. W. Otto, S. Huss-Lederman, D. W. Walker, and J Dongarra. MPI: The complete reference. MIT Press, Cambridge, MA, 1996.

[15] Sayantan Sur, Matthew J. Koop, and Dhabaleswar K. Panda. High-performance and scalable MPI over infiniband with reduced memory usage: an in-depth performance analysis. In Proceedings of the 2006 ACM/IEEE conference on Supercomputing, SC '06, New York, NY, USA, 2006. ACM.

[16] Tinne Tuytelaars and Krystian Mikolajczyk. Local Invariant Feature Detectors: A

Survey. Now Publishers Inc., Hanover, MA, USA, 2008.

[17] A. Vedaldi. An open implementation of the SIFT detector and descriptor. Technical Report 070012, UCLA CSD, 2007.

Table 2. Experiment 3 run times and memory usage.

Core count	Run time (in seconds)	Scale space memory usage per core (in gigabytes)
32	444	11048.16
64	233	5523.32
128	159	2761
256	90	1380.45
512	67	689.96

[18] A. Vedaldi. Sift++ source code and documentation, 2009. Available online.

[19] A. Vedaldi and B. Fulkerson. Vlfeat: An open and portable library of computer vision algorithms, 2008. Available online.

[20] Seth Warn, Wesley Emeneker, Jackson Cothren, and Amy W. Apon. Accelerating sift on parallel architectures. In CLUSTER, pages 1–4. IEEE, 2009. 32

[21] Qi Zhang, Yurong Chen, Yimin Zhang, and Yinlong Xu. Sift implementation and optimization for multi-core systems. Parallel and Distributed Processing Symposium, International, 0:1–8, 2008. 33

Mentor Comments: Professor Amy Apon highlights the importance of Stan's work in numerous current and future applications and notes that it is unusual to see such difficult research taken on by an undergraduate.

Image registration takes two or more images and aligns them so that they form a single, larger image. Image registration is an important problem in many areas of research that utilize image analysis, including medical applications, computer vision, and geospatial processing. In the area of geospatial processing there is a need to align and overlay images from a wide variety of sources, including satellite and aerial images. Registration is difficult to do for many of the very large images that are available since the memory required to execute the registration algorithm is very large, and writing partial results to disk storage during execution can increase the runtime of the application by two orders of magnitude. While there are a few very large memory computers that can perform registration on very large images, these computers are still very expensive and uncommon.

The goal of this project is to parallelize the Scale Invariant Feature Transform (SIFT) application, the most commonly used algorithm that is used to do image registration, in order to make possible the alignment of very large images, such as those that come from satellites. The approach uses distributed memory computing on a commodity supercomputing cluster. The developed code uses open source software libraries to divide the images into smaller pieces, distribute them across the memories of the different computers, perform the registration, and then recombine the result. There have been other recent examples of the parallelization of SIFT and this is one of the most effective seen in the literature for this type of problem. Two variations of the developed parallel SIFT application were tested on the Star of Arkansas supercomputer and on a national TeraGrid supercomputer. The techniques are very efficient and result in less than 2% data loss. In addition, the application was shown to scale very well to very large images and to a large number of processors.

Parallelizing applications to run on a supercomputer is very complex and difficult to do well. This development of the scalable parallel SIFT application is a great accomplishment for an undergraduate. An earlier version of this work was presented as a poster at the annual Supercomputing conference, SC10, in November, 2010, a mark of accomplishment of this research.

SEQUENCE ANALYSIS OF THE ANGIOTENSIN II TYPE 1 RECEPTOR (AGTR1) GENE FOR MUTATIONS CONTRIBUTING TO PULMONARY HYPERTENSION IN THE CHICKEN (*GALLUS GALLUS)*

By John Russell Burks
Department of Biological Sciences

Faculty Mentor: Douglas Rhoads
Department of Biological Sciences

Abstract

Our multidisciplinary group at the University of Arkansas has been investigating the suitability of the chicken as a medical model for pulmonary arterial hypertension (PAH) in humans. There are several forms of PAH in humans arising from elevated pulmonary arterial pressure and pulmonary vascular resistance. Spontaneous cases of PAH are known as idiopathic PAH (IPAH), where the exact physiological causes are not known. IPAH patients that do not respond to standard treatments have a prognosis of only a few years. Currently, there is no acceptable animal model for IPAH. As part of our effort to pursue the chicken as model for IPAH, we have mapped chromosomal regions associated with susceptibility to ascites, an industry term for PAH in chickens. One region identified contains the angiotensin II type 1 receptor gene (AGTR1), a gene known to be associated with particular forms of PAH in humans. My project was to sequence the exonic regions of AGTR1 from chickens selected for susceptibility and resistance to ascites. I identified a total of 15 single nucleotide polymorphisms (SNPs) in intronic regions and 9 affecting exonic sequences that distinguish resistant and susceptible birds. One of the SNPs alters the encoded protein, but more sequencing data is needed to confirm the presence of this SNP. The 24 SNPs have become the basis for further genotypic efforts using quantitative polymerase chain reaction high-resolution melt (qPCR-HRM) assays to determine the association of alternative alleles of AGTR1 with PAH in the chicken. This knowledge will help the poultry industry in genetic selection to reduce incidence of ascites. Characterization of the genetic determinants of ascites in the chicken will also identify specific gene networks and further our understanding of PAH in humans.

Introduction

Pulmonary arterial hypertension (PAH) is currently accepted as being classified into three main types: 1) idiopathic pulmonary arterial hypertension (IPAH), 2) familial pulmonary arterial hypertension (FPAH), and 3) pulmonary arterial hypertension related to associated conditions or risk factors (APAH) (Simmonneau et al., 2004). IPAH and FPAH have also been classified as types of primary pulmonary hypertension, meaning they have no known cause. APAH has been classified as secondary pulmonary hypertension because the hypertension is believed to be due to an underlying cause.

IPAH results in increases in pulmonary arterial pressure and in pulmonary vascular resistance, which ultimately causes right ventricular failure and death if untreated or unresponsive to treatment (Widlitz and Barst, 2003). The increased vascular resistance in patients with pulmonary hypertension is due to vasoconstriction, thrombosis in situ, and vascular remodeling (Rubin, 1997). Primary pulmonary hypertension, including IPAH, is defined as having a mean pulmonary artery pressure of 25 mmHg or greater at rest or 30 mmHg or greater during exercise, with no related underlying condition (Widlitz and Barst, 2003). IPAH is diagnosed in one to two new patients per million each year, with an average survival of 2.5 years after initial diagnosis (Rubin, 1997).

Adults with primary pulmonary hypertension generally develop plexiform lesions and seemingly irreversible pulmonary vascular changes (Widlitz & Barst, 2003). These vascular changes are phenotypic changes in the endothelial and smooth muscle cells in pulmonary arteries and are influenced by cell proliferation, apoptosis, matrix proteins, and matrix turnover. Upregulation of the transcription factor Oct-4 has been shown to be involved in the irregular vasculature of the pulmonary arterial smooth muscle cells in IPAH (Firth et al., 2010). Hemodynamic influences are also important in the etiology of PAH. Additionally, gene expression in pulmonary vascular cells is related to environmental factors, receptors, growth factors, signaling pathways, and genetic influences, all of which can interact with each other in the disease process.

Serotonin metabolism has been shown to be central to the etiology of PAH (MacLean, 2007). Serotonin (5-hydroxytryptamine, 5HT) can be synthesized in the pulmonary endothelium and released to either interact with serotonin cell surface receptors or enter the smooth muscle cells via the serotonin transporter (SERT). Serotonin can act to induce proliferation and contraction of pulmonary smooth muscle cells through 5HT receptors on the vascular epithelium. The actions of 5HT receptors have been shown to be involved in PAH in humans (Humbert et al., 2004).

The Renin-Angiotensin Aldosterone System (RAAS) is a hormonal cascade that is important in the pathogenesis of cardiovascular disorders (Atlas, 2007). The RAAS functions in maintaining the homeostasis of arterial pressure, tissue perfusion, and extracellular volume. The cascade begins with the secretion of renin by the juxtaglomerular cells of the kidneys. In the extracellular space, renin functions to cleave ten amino acids from the N-terminus of angiotensinogen, which is constitutively

secreted by the liver. The cleaved angiotensinogen is an inactive ten amino acid peptide known as angiotensin I. Two amino acids from the C-terminus of angiotensin I are cleaved by membrane-bound angiotensin-converting enzyme (ACE), creating the octapeptide, angiotensin II. Angiotensin II is the primary biologically active product of the RAAS and acts as a potent vasoconstrictor.

At least four types of angiotensin receptors have been identified, but the type 1 receptor (angiotensin II type 1 receptor, or AGTR1) is involved in most of the known physiology of angiotensin II (Atlas, 2007). Cardiovascular effects of angiotensin II and AGTR1 include vasoconstriction, increased blood pressure, increased cardiac contractility, and vascular and cardiac hypertrophy. Angiotensin II and AGTR1 have also been shown to stimulate aldosterone synthesis by the adrenal cortex, inhibit renin release, increase sodium reabsorption in the kidneys, and affect the sympathetic nervous system. Angiotensin II and AGTR1 also mediate effects on cell growth and proliferation, inflammatory responses, and oxidative stress. AGTR1 contains the seven transmembrane domains characteristic of the G protein-coupled receptor superfamily and is found on many cell types in angiotensin II target organs.

The RAAS has been shown to be genetically involved in human PAH (Chung et al., 2009). A specific polymorphism in the angiotensin-converting enzyme (ACE) gene has been shown to be associated with primary pulmonary hypertension (IPAH) and right ventricular function (Abraham et al., 2003). Increased expression of ACE has also been seen in the plexiform lesions of PAH (Orte et al., 2000). Recent research has shown that certain variants of AGTR1 are significantly related to PAH. Specifically, an adenine (A)/cytosine (C) substitution at position 1166 in the 3' untranslated region of AGTR1 is significantly associated with early onset IPAH in humans (Chung et al., 2009). This SNP occurs within a potential target site for the miRNA-155, a microRNA (miRNA) binding site (Ceolotto et al., 2011). They theorized that miRNA-155 can target the 1166A allele, but not the 1166C allele. A study of hypertensive subjects found that AGTR1 protein expression was negatively correlated with miRNA-155 expression and that AGTR1 protein expression was significantly greater in subjects homozygous for the C allele than in heterozygous (CA) or homozygous A subjects. This would be consistent with miRNA-155 repression of the 1166A alleles and lack of repression of the 1166C SNP. Overexpression of AGTR1 protein would then lead to higher blood pressure.

Ascites, the industry term for PAH in chickens, results from a fast growth rate and causes significant mortality in chickens (Pavlidis et al., 2007). Ascites is among the most common and most deadly cardiovascular conditions in modern lines of broiler chickens (Olkowski, 2007). Increased genetic selection for fast growth rate and the creation of diets that stimulate fast growth contribute to the development of ascites in the broiler chicken (Julian, 1993). Pulmonary hypertension in poultry causes right ventricular hypertrophy, valvular insufficiency, increased venous pressure, and ascites. Because the chicken heart has a thin-walled right ventricle and a muscular right atrioventricular valve, pulmonary hypertension causes heart failure and death quickly in the chicken. Also, the broiler chicken is relatively small, but has very large breasts, causing increased pressure on the air sacs of the relatively small lungs.

The etiology of ascites in the broiler chicken begins with the high basal metabolic rate required for fast growth (Government of Alberta, 2008). Broilers are susceptible to ascites when their pulmonary vascular capacity cannot tolerate the cardiac output necessary for meeting the metabolic requirements of rapid growth, which could be due to anatomical or functional restrictions (Wideman et al., 2007). This inadequate capacity causes a deficit in oxygen, which in turn causes the right ventricle to increase the amount of blood pumped to the lungs to be oxygenated (Government of Alberta, 2008). Because the right ventricle is thin in the chicken, it often expands due to the increase in blood flow. The increased blood flow causes increased pulmonary arterial pressure and right ventricular hypertrophy. More red blood cells are produced by the chicken to increase the oxygen carrying capacity of the blood, but more red blood cells also cause the blood to thicken and further increase vascular resistance. Valvular insufficiency causes right ventricular failure and the associated backflow causes liver edema, which leads to leakage of plasma into the body cavity. This leads to an accumulation of fluid in the abdomen (ascites). In the poultry industry the term is also "water belly" and leads to either mortality or condemnation at the plant. Ascites can be treated in the chicken with beta agonists and dietary arginine, both of which increase ventilation and pulmonary blood flow (Currie, 1999). Also, feed restriction is used to cause a tachycardia that may protect birds from the brachycardia associated with hypoxia-induced ascites.

There are several currently used animal models for human pulmonary hypertension, with the most common being derived from exposing the animal to chronic hypoxia or to monocrotaline injury (Stenmark et al., 2009). Animals used include rats, mice, piglets, calves, and macaques. Fawn-hooded rats are commonly used because pulmonary hypertension manifests most severely in these animals. However, none of these develops the plexogenic arteriopathies found in humans and chickens. Our collaborative group at the University of Arkansas is examining whether ascites in the chicken (*Gallus gallus*) is a medical model for PAH/IPAH. Ascites is easily induced in the chicken and lines of PAH resistant and susceptible chickens have been developed. There are genetic and pathophysiological similarities between ascites in the chicken and PAH in the human. Chickens with ascites form plexogenic arteriopathies that are indistinguishable from plexiform lesions found in the lungs of humans with advanced PAH (Wideman et al., 2011). Genetic evidence for the chicken being an appropriate medical model for PAH can be found in our group's identification of chromosomal regions associated with ascites in the chicken that contain genes that have been found to be involved in PAH in humans (Chung et al., 2009; MacLean, 2007; Orte et al., 2000; Smith, 2009).

A number of methods have been employed to induce PAH in the chicken, including injection of bacterial lipopolysaccharide (LPS), injection of micro-particles of cellulose, and exposure to hypoxia to simulate high altitudes, such as growth in a hypobaric chamber (Chapman et al., 2005; Currie, 1999; Pavlidis, 2007).

Dr. Nicholas Anthony (University of Arkansas) has developed divergently selected lines of broiler chickens that are resistant (RES) or susceptible (SUS) to ascites using a hypobaric chamber to induce the disease (Pavlidis, 2007). The chamber simulated high altitude conditions via a partial vacuum to lower the partial pressure of oxygen in the chamber. The RES and SUS lines were created based on sib-selection over successive generations in the hypobaric chamber.

Our group then used a cross of the RES and SUS lines to map several chromosomal segments contributing to PAH in the chicken (Smith, 2009). One of those regions contains a serotonin receptor-transporter (5HT receptor), which has been associated with some forms of human PAH (MacLean, 2007). Another region contained the ACE gene. Those genes are under investigation by other students in the laboratory. A third region contains the gene AGTR1, which is located on chromosome 9 and codes for the angiotensin II type 1 receptor. As already mentioned, this gene and the RAAS have been shown to be involved in PAH in humans (Atlas, 2007; Chung et al., 2009). The implications of our preliminary data is that mis-regulation of angiotensin II production by ACE and the subsequent response by AGTR1 may be a contributing factor for development of ascites.

Understanding the genetics of PAH in the chicken model will identify specific gene networks and will advance understanding of the underlying processes leading to PAH in humans. This knowledge may also lead to genetic selection in the poultry industry to lessen the economic losses associated with ascites.

The region containing the AGTR1 gene on chromosome 9 (Gga9) was previously associated with ascites in the chicken through a whole genome association study and then confirmed using variable number tandem repeat (VNTR) genotyping (Smith, 2009). Further research in our laboratory has associated this region with ascites in our lines and in three commercial lines (Sriram Krishnamoorthy, personal communication). Therefore, this region appears to contain a major determinant of ascites susceptibility in chickens. A region in the human genome that contains the AGTR1 gene has been associated with some forms of PAH, thus it is likely that mutations affecting the AGTR1 gene could contribute to ascites in chickens.

My research project was to sequence the AGTR1 gene from the resistant and susceptible lines to determine whether mutations could be found that represent alternative alleles of AGTR1. I then developed qPCR-HRM assays for the alternative alleles of AGTR1 for use in genotyping a larger collection of DNAs. Additional genotype data will determine whether these particular mutations are associated with susceptibility to PAH. As depicted in Figure 1, the chicken AGTR1 gene's three exons are distributed across 20,979 bases (Gga 9: 13,475,625 – 13,496,603), with the entire coding sequence located in exon 3 (International Chicken Genome Sequencing Consortium, 2004). The three exons produce a final mRNA transcript of 1427 bases. The first two exons are non-coding while the final exon encodes a predicted 359 amino acid protein that is the receptor.

Materials and Methods

DNA Isolation

DNAs were previously isolated by Sriram Krishnamooorthy, Ph.D. candidate University of Arkansas, from chickens that were then phenotyped in a hypobaric chamber. These DNAs have been previously validated by others in our laboratory for PCR amplification of numerous regions.

Primer Design for Polymerase Chain Reaction (PCR)

The genomic region representing AGTR1 was downloaded from the UCSC genome browser. Primer3 (http://frodo.wi.mit.edu/primer3/) was used to design oligonucleotide primers covering all of the exonic regions. Primers were synthesized by Eurofins-Operon. PCR conditions were then optimized for primer pairs.

Polymerase Chain Reaction (PCR)

PCR mixtures were assembled incorporating H_2O, PCR Buffer, deoxyribonucleotide triphosphate (dNTPs), Taq polymerase, primers, and target DNA. Twenty µl PCR mixtures contained 1X PCR Buffer (50 mM TrisCl, 1 mM $MgCl_2$, 3 mg/ml BSA), 0.2 mM dNTPs, 3 units Taq polymerase, 2 µl target DNA, and 1 µM forward and reverse primer mixture. Reactions for sequencing consisted of 200 µl of the same concentrations of 1X PCR Buffer, 0.2 mM dNTPs, 1 µM forward and reverse primer mixture, but differed by using 10 units Taq polymerase, and 5 µl target DNA. Reactions were cycled in one of four PCR machines in our laboratory to obtain amplicons of the three exons of AGTR1 in the resistant and susceptible birds.

Gel Electrophoresis for Quality of PCR Product

A portion of the PCR product was resolved on a 1.5% agarose gel to evaluate the quality of the product. Five µl of PCR product was mixed with 5 µl of loading dye prior to loading into gel. The loading dye used was 10 µg/ml ethidium bromide (EthBr), 15% Ficoll, 20mM EDTA, 0.1% Bromophenol Blue 0.1% Xylene Cyanol. Molecular weight ladder was pGEM5 digested with Sau3A. Gels were submerged in 0.5X TBE with 0.5 µg/ml EthBr and electrophoresed for approximately 5-10 minutes at 40 Volts

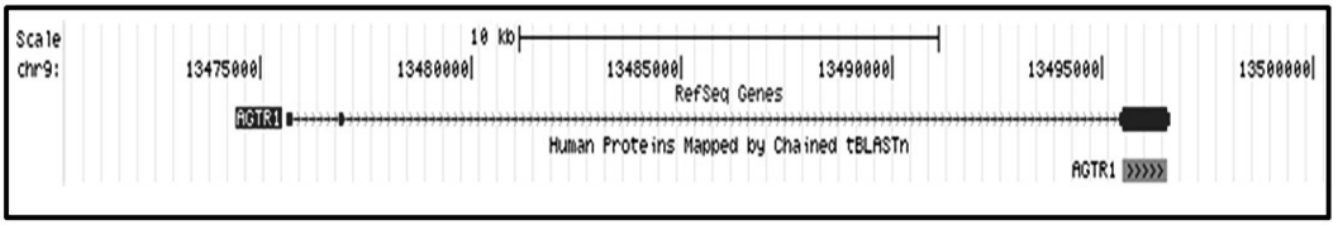

Figure 1: UCSC genome browser view of the chicken AGTR1 gene on chromosome 9 (International Chicken Genome Sequencing Consortium, 2004). http://genome.ucsc.edu.

(V) and then for approximately 90 minutes at 70 V.

Gel Imaging

Gels were imaged either using an Ultraviolet Transilluminator captured with a CCD camera and FlashPoint FPG software, or the gels were scanned at 600nm using a Model 9600 Typhoon Imager (GE HealthCare) and analyzed with ImageQuant Software.

Purification and Quantification of PCR product

To purify DNA samples for sequencing, reactions were diluted 1x with TE (10 mM TrisCl, 1 mM EDTA, pH 7.5) and extracted with phenol:chloroform:isoamyl alcohol (50:48:2) and then with chloroform:isoamyl alcohol (24:1). The solution was brought to 0.3 M with sodium acetate and DNA precipitated by addition of 3 volumes of 95% ethanol. The mixture was incubated at -20°C for 1-2 hours and then DNAs were collected by centrifugation (10 min at 10,000 rpm). The pellet was rinsed with cold 70% ethanol, dried under vacuum and redissolved in 10 mM TrisCl, 0.1 mM EDTA. DNA was quantified using a Model TKO 100 Hoefer Scientific Instruments DNA Fluorometer according to the manufacturer's instructions.

DNA Sequencing and Analysis

Purified PCR products (5-20 ng) were mixed with 3.4 pM of individual primers, and submitted to the UA DNA Resource Center for capillary sequencing. The sequence files were aligned using Seqman software from DNAStar.

Quantitative PCR – High Resolution Melt (qPCR-HRM) Assays for SNPlotyping

Primers were designed that flank single nucleotide polymorphisms (SNPs) to generate a short amplicon (generally less than 60 base pairs). The oligonucleotide primers were designed using Primer3 (http://frodo.wi.mit.edu/primer3/) and were synthesized by Eurofins-Operon.

Twenty µl PCR reactions each contained 1X PCR Buffer (50 mM TrisCl, 1 mM $MgCl_2$, 3 mg/ml BSA), 0.2 mM dNTPs, 3 units Taq polymerase, 1 µl target DNA, 1 µM forward and reverse primer mixture, H_2O, and an intercalating dye (SYBR Green, LCGreen, or EvaGreen). The qPCR-HRM assay was performed on a BioRad CFX96 Real-Time System. The protocol used included the following steps: 1) 95°C for 30 seconds, 2) 95°C for 15 seconds, 3) 50°C for 15 seconds, 4) 72°C for 30 seconds and plate read, 5) Repeat steps 2-4 39 times, 6) 72°C for 3 minutes, 7) 95°C for 3 minutes, 8) 65°C for 3 minutes, and 9) Gradient from 65°C-90°C at 0.1°C increments for 10 seconds with plate read at each increment.

Results

I designed four pairs of oligonucleotide primers that amplify the three exonic regions of the AGTR1 gene. The size of exon 3 required the use of two pairs of primers, while exons 1 and 2 required one pair each. Two additional pairs of primers were designed to flank exon 3 because the original pair flanking one portion of exon 3 produced no PCR product. All primers were optimized for annealing temperatures and cycling conditions using chicken genomic DNA. The primer pair names, sequences, and optimized PCR conditions are shown in Tables 1 and 2.

The primer pair for exon 1 (AGTR1 X1 F1/R1) was optimized for 20 µl PCRs but no product was obtained when a 200 µl PCR was performed for sequencing. The AGTR1 X3-2 F1/R1 primer pair did not produce a PCR product.

Quality amplicons of exons 2 and 3 were obtained from 200 µl PCR reactions, purified, and sequenced. Sequences were obtained from two of the three AGTR1 exonic regions from several resistant and susceptible birds (usually 3 of each). The sequences were aligned with the AGTR1 gene from the 2006 genome assembly of the Red Jungle Fowl (*Gallus gallus*) sequence. The alignments for exon 2 and exon 3 are presented in Figures 2 and 3, respectively.

Comparisons between Jungle Fowl, resistant, and susceptible sequences identified 24 single nucleotide polymorphisms (SNPs), four of which affected the AGTR1 coding sequence. All identified SNPs are listed in Table 3. Fourteen SNPs were found in the intronic sequence 5' of exon 2 and three SNPs were found within exon 2. One SNP was found in the intronic sequence 5' of exon 3. Six SNPs were identified in exon 3 including one SNP in the 3' untranslated region (UTR).

Five pairs of primers were designed to amplify specific SNPs in exons 2 and 3 for high resolution melt analyses. Two primers designed to amplify regions containing SNPs were optimized using genomic chicken DNA and are ready to be used in a SNPlotyping application. Three of the five primer pairs designed to amplify the SNP regions were not optimized.

A LCGreen qPCR-HRM assay to SNPlotype multiple resistant and susceptible chickens was completed for the SNP located at base 2513. The AGTR1_2513F/R primer pair was used and the melt curve is shown in Figure 4.

Discussion

Several polymorphisms were identified that establish that there are at least two forms of the AGTR1 gene in our RES and SUS lines (Pavlidis, 2007). The 14 SNPs found in the intronic region 5' of exon 2 and the three SNPs in exon 2 do not affect the coding region for the AGTR1 protein, as these SNPs are in non-coding regions. Two SNPs, one in the intronic region 5' of exon 3 and one in exon 3, need more sequence from additional chickens for confirmation. Sequence data was only obtained from two individuals, both resistant, for each of these two SNPs. The intronic SNP would have no effect on the protein sequence, but the SNP in exon 3 is in the first position of a proline codon at position 82 of the protein (Pro82) and would change the encoded amino acid to serine. Proline residues are normally considered as disrupters of secondary structure. This proline is located within the extracellular portion of the alpha helical transmembrane II domain (G Protein-Coupled Receptor Database, 2011). Because of its location outside of the hydrophobic membrane, replacement of the proline with a hydrophilic serine would not alter the hydrophilicity of the region but certainly could alter a secondary structure. Pro82 is highly conserved in human, cow, mouse, rat, opossum, lizard, frog, and zebrafish (See Figure 5). Four other SNPs found in exon 3 are located in the third codon position (i.e., the wobble position) and would be silent with respect to the encoded protein. The specific codon changes are shown in Table 3.

Table 1: Primer information. Sequence in capital letters indicate exonic sequences, with lowercase for intronic sequences. Numbers in SNP primer pair names correspond to the base pair location of the SNP in the mRNA for exonic SNPs and relative to the transcription start site in the gene for intronic SNPs.

Amplified Region	Primer Pair Name	Fragment Length (bp)	Forward Sequence (5' - 3')	Reverse Sequence (5' - 3')
Exon 1	AGTR1 X1 F1/R1	808	gtcacgcacactcccttagcaa	ggtccttcctctgccaacttca
Exon 2	AGTR1 X2 F1/R1	844	tcaaaaatcaccgaaggcagtg	caacaagcaaaagggactgacg
Exon 3-1	AGTR1 X3-1 F1/R1	785	gcagattaattgccgactattcca	AAAGCCACAGACCGTCATGTTC
Exon 3-2	AGTR1 X3-2 F1/R1	760	TCACGAATCCGACGTACCATGT	gatgtctgggactgcagatgga
Exon 3-1	AGTR1 X3-1 F2/R2	836	gtgcccacaatccagttttc	CCACAGACCGTCATGTTCAA
Exon 3-2	AGTR1 X3-2 F2/R2	697	CTTGCTGGTGTGGCCAGT	ctgggactgcagatggattt
Intron Indel/SNP	AGTR1_2228_2235 F/R	50	gtattcttccaagcaaatcc	agtgcttgtccataccatga
Exon 2 SNP	AGTR1_2513 F/R	50	aaaaggacttttgtctatttgga	AGTCCCCTCTTCTCCTGCTC
Exon 3 SNP	AGTR1_21618 F/R	50	GCCCGTCATCATTCATCG	TCATGTTCAAGTTCTCTGCAAAA
Exon 3 SNP	AGTR1_21945 F/R	52	CATGTAATAACAGACTGCAAAAT	AGGGCATAGCTGTATCCACAA
Exon 3 SNP	AGTR1_22050 F/R	59	TTTTTATGTTTTCTTTGGAA	TGTATTTTATTAGCTGAAGGAAG

Table 2: Optimized PCR conditions for primer pairs.

Primer Name	Step 1: Initial Denaturation	Step 2: Denaturation	Step 3: Annealing	Step 4: Extension	Number of Cycles (repeat steps 2-4)	Step 5: Final Extension
AGTR1 X1 F1/R1	90°C, 60s	90°C, 20s	55°C, 20s	72°C, 2min	40	72°C, 3min
AGTR1 X2 F1/R1	90°C, 60s	90°C, 20s	53°C, 20s	72°C, 2min	40	72°C, 3min
AGTR1 X3-1 F1/R1	90°C, 60s	90°C, 20s	50°C, 20s	72°C, 2min	40	72°C, 3min
AGTR1 X3-2 F1/R1	90°C, 60s	90°C, 20s	50°C, 20s	72°C, 2min	40	72°C, 3min
AGTR1 X3-1 F2/R2	Not Optimized					
AGTR1 X3-2 F2/R2	Not Optimized					
AGTR1_2228_2235 F/R	90°C, 30s	90°C, 15s	50°C, 15s	72°C, 30s	44	72°C, 3min
AGTR1_2513 F/R	90°C, 30s	90°C, 15s	50°C, 15s	72°C, 30s	44	72°C, 3min
AGTR1_21618 F/R	Not Optimized					
AGTR1_21945 F/R	Not Optimized					
AGTR1_22050 F/R	Not Optimized					

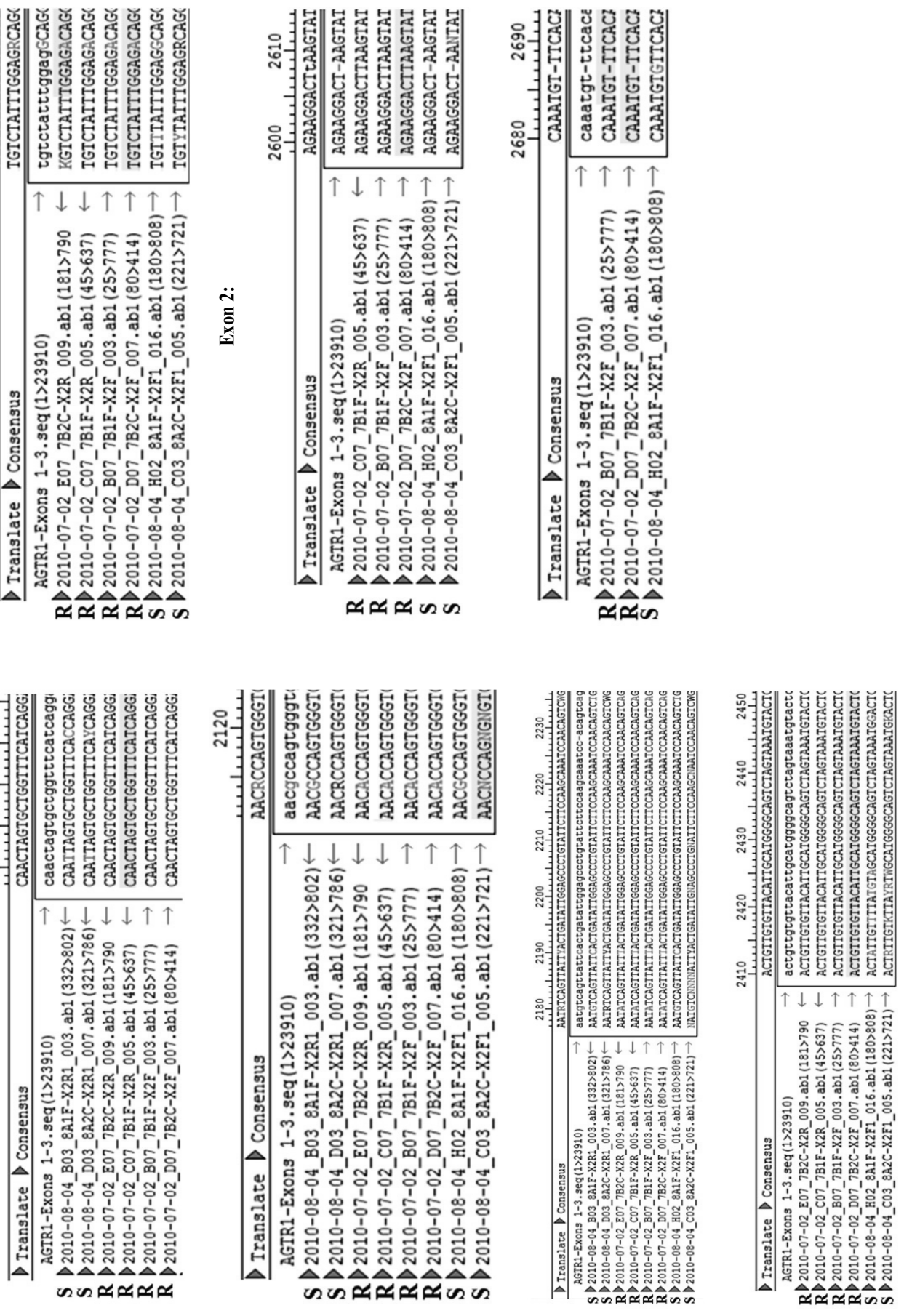

Figure 2: AGTR1 SNPs in the intronic region 5' of exon 2 and in exon 2. (**R**) denotes PAH-resistant birds and (**S**) denotes PAH-susceptible birds. Sequences are aligned with the 2006 Red Jungle Fowl sequence assembly (International Chicken Genome Sequencing Consortium, 2004).

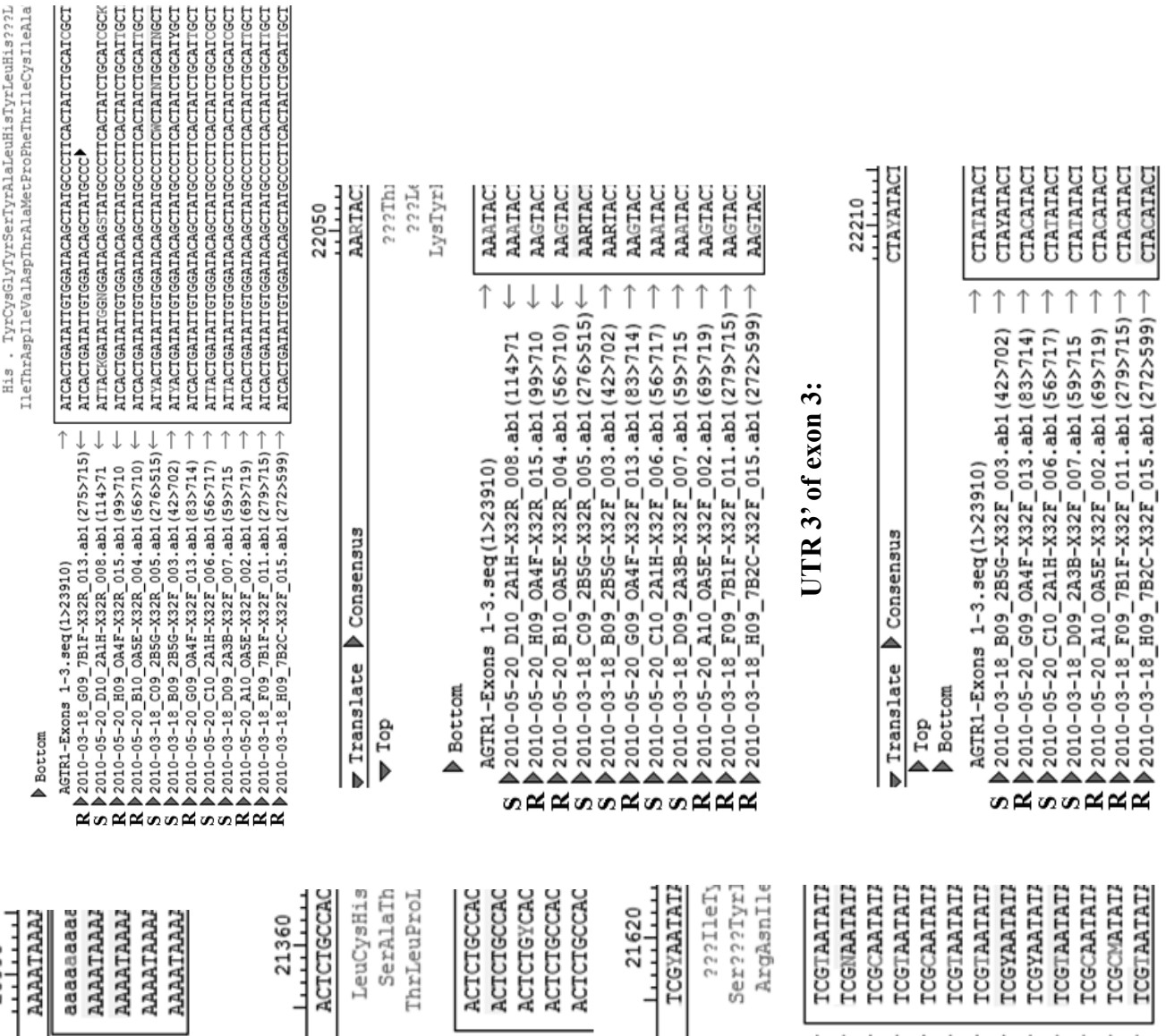

Figure 3: AGTR1 SNPs in the intronic region 5' of exon 3, in exon 3, and in the UTR 3' of exon 3. **(R)** denotes PAH-resistant birds and **(S)** denotes PAH-susceptible birds. Sequences are aligned with the 2006 Red Jungle Fowl sequence assembly (International Chicken Genome Sequencing Consortium, 2004). Sequence within the coding region of exon 3 is shown with the associated protein sequence (bottom reading frame).

Table 3: SNP Information. Jungle Fowl genotype was obtained from the 2006 assembly of Red Jungle Fowl (*Gallus gallus*) (International Chicken Genome Sequencing Consortium, 2004). Codon Change is relative to the Jungle Fowl sequence. *More sequence data is needed to confirm.

SNP Region	Locus (bp)	Jungle Fowl Genotype	Resistant Genotype(s)	Susceptible Genotype(s)	Codon Change
Intronic region 5' of exon 2	1996	CC	CC	TT	N/A
Intronic region 5' of exon 2	2011	TT	TT	CC, C/T	N/A
Intronic region 5' of exon 2	2114	GG	AA	GG, G/A	N/A
Intronic region 5' of exon 2	2180	GG	AA	GG, G/A	N/A
Intronic region 5' of exon 2	2190	CC	TT	CC, C/T	N/A
Intronic region 5' of exon 2	2228	No Base	AA	AA	N/A
Intronic region 5' of exon 2	2235	AA	AA	TT, A/T	N/A
Intronic region 5' of exon 2	2413	GG	GG	AA, A/G	N/A
Intronic region 5' of exon 2	2418	GG	GG	TT, G/T	N/A
Intronic region 5' of exon 2	2422	CC	CC	TT, C/T	N/A
Intronic region 5' of exon 2	2423	AA	AA	GG, G/A	N/A
Intronic region 5' of exon 2	2425	TT	TT	AA, A/T	N/A
Intronic region 5' of exon 2	2448	TT	TT	GG, G/T	N/A
Intronic region 5' of exon 2	2503	CC	CC	TT, C/T	N/A
First base of exon 2	2513	GG	AA	GG, G/A	N/A
Exon 2	2608	No Base	TT	No Base	N/A
Exon 2	2687	No Base	No Base	GG	N/A
*Intronic region 5' of exon 3	20991	AA	TT	No Data	N/A
*Exon 3	21361	CC	C/T	No Data	CCA (Pro) to TCA (Ser)
Exon 3	21618	TT	TT	CC, C/T	CGT (Arg) to CGC (Arg)
Exon 3	21945	CC	CC	TT, C/T	ATC (Ile) to ATT (Ile)
Exon 3	21987	CC	TT	CC, C/T	ATT (Ile) to ATC (Ile)
Exon 3	22050	AA	GG	AA, A/G	AAA (Lys) to AAG (Lys)
UTR 3' of exon 3	22210	TT	CC	TT, C/T	N/A

The SNP found in the 3' UTR of exon 3 was not found to be analogous to the 3' UTR SNP found to be associated with PAH by Chung et al (2009). The SNP in the human AGTR1 gene was 86 bases 3' to the terminator codon, but the SNP found in the chicken was 13 bases 3' to the stop codon. However, this SNP may still be of importance in terms of its potential effects on miRNA binding sites. There are several miRNA binding sites located in the 3' UTRs of the human AGTR1 mRNA, so SNPs located in one of these binding sites could have an effect on miRNA function and gene expression (Elton et al., 2010). Perhaps the SNP found in the 3' UTR of the chicken is localized in a miRNA binding site or creates a novel miRNA binding site, both of which could affect miRNA function and gene expression.

New primers may need to be designed to amplify exon 3 and three of the SNP regions, while a different strategy or primer redesign may be necessary to obtain sequence for exon 1. Sequence data needs to be obtained for exon 1 and additional sequence data is needed for the first portion of exon 3. Also, more work can be done to determine whether any particular AGTR1 allele is associated with PAH susceptibility. One approach used in our laboratory is the development of qPCR-HRM (quantitative PCR High-Resolution Melt) assays for SNPlotyping a collection of DNAs representing different susceptible and resistant lines. Two of the five SNP primers I designed are ready for this analysis, whereas three others need further optimization or need to be redesigned. Statistical analysis of the frequency of each SNPlotype can be performed to determine whether there is an association of any of these SNPs with ascites phenotype. In addition, based on frequencies and concordance, it can be determined which SNPs are in linkage and define different particular haplotypes (alleles) for AGTR1.

The melt curve obtained from a qPCR-HRM assay for the SNP located at base 2513 showed insufficient allelic discrimination (data not shown). That is, the melting temperatures were not significantly different between the resistant and susceptible chickens so as to determine that there are or are not two alleles. Additional analysis using qPCR-HRM assays are being pursued to examine additional SNPs identified in AGTR1.

A Ph.D. candidate in the lab is currently using qPCR on cDNA to study expression levels of AGTR1 in different tissues from resistant and susceptible chickens. He has detected significant differences in expression of AGTR1 in RNA from whole blood. With qPCR-HRM assays we should be able to correlate expression levels with particular alleles to determine whether the allelic effect is associated with differences in expression or the protein product.

Further genetic analysis of the different forms of the AGTR1 gene from both susceptible and resistant birds will lead to insight into how particular mutations in the gene may contribute to the development of ascites in the chicken. It is this knowledge of the genetics of ascites in chickens that will lead to genetic selection to reduce ascites in chickens, and further develop the chicken as a medical model for PAH in humans. Availability of an animal medical model will provide the means to develop and evaluate new treatments for PAH in humans.

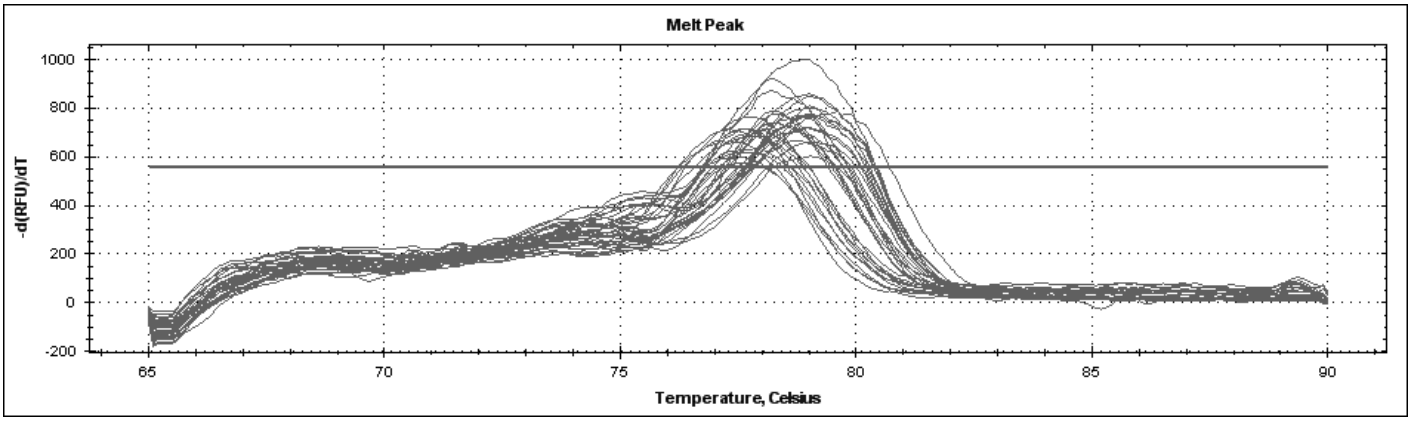

Figure 4. Melt Curve for SNP at base 2513. The peaks represent melting temperatures of each sample. There is insufficient discrimination between RES and SUS chickens to determine if two alleles are or are not present.

Human	FLLNLALADLCFLLTLPLWAVYTAMEYRWPFGNYLCKIASASVSFNLYAS
Chimpanzee	FLLNLALADLCFLLTLPLWAVYTAMEYRWPFGNYLCKIASASVSFNLYAS
Cow	FLLNLALADLCFLLTLPLWAVYTAMEYRWPFGNYLCKIASASVSFNLYAS
Mouse	FLLNLALADLCFLLTLPLWAVYTAMEYRWPFGNHLCKIASASVSFNLYAS
Rat	FLLNLALADLCFLLTLPLWAVYTAMEYRWPFGNHLCKIASASVSFNLYAS
Opossum	FLLNLALADLCFLMTLPLWAAYTAMEYRWPFGNCLCKIASAGISFNLYAS
Lizard	FLFNLALADLCFIVTLPLWAATTAMEYRWPFGNCLCKLTSAAASFNLYAS
Frog	FLMNLALSDLCFVITLPLWAVYTAMHYHWPFGDLLCKIASTAITLNLYTT
Zebrafish	YIGNLALADLTFVITLPLWAVYTALGYHWPFGVALCKISSYVVLVNMYAS
G.gallus	FLLNLALADLCFLITL**P**LWAAYTAMEYQWPFGNCLCKLASAGISFNLYAS

Figure 5. Alignment of AGTR1 proteins from selected vertebrates. The region of AGTR1 from residue 66 to 115 (based on *G. gallus*) are shown for the indicated organisms. Protein sequences were extracted from GenBank and aligned at http://www.ncbi.nlm.nih.gov/tools/cobalt/cobalt.cgi. The proline residue affected by the SNP is underlined and bold (see text).

References

Abraham, W. T., Raynolds, M. V., Badesch, D. B., Wynne, K. M., Groves, B. M., Roden, R. L.,Robertson, A. D., Lowes, B. D., Zisman, L. S., Voelkel, N. F., Bristow, M. R., and Perryman, M. B. (2003). Angiotensin-converting enzyme DD genotype in patients with primary pulmonary hypertension: increased frequency and association with preserved haemodynamics. Journal of Renin-Angiotensin-Aldosterone System 4:27-30.

Atlas, S. A. (2007). The renin-angiotensin aldosterone system: pathophysiological role and pharmacologic inhibition. Journal of Managed Care Pharmacy 13:S9-S20.

Bailes, S. M., Devers, J. J., Kirby, J. D., and Rhoads, D. D. (2007). An inexpensive, simple protocol for DNA isolation from blood for high-throughput genotyping by polymerase chain reaction or restriction endonuclease digestion. Journal of Poultry Science 86:102-106.

Ceolotto, G., Papparella, I., Bortoluzzi, A., Strapazzon, G., Ragazzo, F., Bratti, P., Fabrico, A. S., Squarcina, E., Gion, M., Palatini, P., and Semplicini, A. (2011). Interplay between miR-155, AT1R A1166C polymorphism, and AT1R expression in young untreated hypertensives. American Journal of Hypertension 24:241-246.

Chapman, M. E., Wang, W., Erf, G. F., and Wideman, R. F. (2005) Pulmonary hypertensiveresponses of broilers to bacterial lipopolysaccharide (LPS): Evaluation of LPS source anddose, and impact of pre-existing pulmonary hypertension and cellulose micro-particleselection. Poultry Science 84:432-441.

Chung, W., Deng, L., Carrol, J., Mallory, N., Diamond, B., Rosenzweig, E., Barst, R., and Morse, J. (2009). Polymorphism in the angiotensin II type 1 receptor (AGTR1) is associated with age at diagnosis in pulmonary arterial hypertension. Journal of Heart and Lung Transplant 28:373-379.

Currie, R. J. (1999). Ascites in poultry: recent investigations. Avian Pathology 28(4):313-326.

Elton, T. S., Sansom, S. E., and Martin, M. M. (2010). Cardiovascular disease, single nucleotide polymorphisms; and the rennin angiotensin system: is there a microRNA connection? International Journal of Hypertension 2010:1-13.

Firth, A. L., Yao, W., Remillard, C. V., Ogawa, A., and Yuan, J. X. (2010). Upregulation of Oct- 4 isoforms in pulmonary smooth muscle cells from patients with pulmonary hypertension. American Journal of Physiology 298:L548-557.

G Protein-Coupled Receptor Database. (2011). AGTR1_Chick. Retrieved April 7, 2011, from <http://www.gpcr.org/7tm/proteins/agtr1_chick>.

Government of Alberta, Agriculture and Research Development. (2008). Ascites. Retrieved March 24, 2011, from <http://www1.agric.gov.ab.ca/$department/deptdocs.nsf/all/pou3546>.

Humbert, M., Morrell, N. W., Archer, S. L., Stenmark, K. R., MacLean, M. R., Lang, I. M., Christman, B. W., Weir, E. K., Eickelberg, O., Voelkel, N. F., and Rabinovitch, M. (2004). Cellular and molecular pathobiology of pulmonary arterial hypertension. Journal of the American College of Cardiology 43(12):S13-S24.

International Chicken Genome Sequencing Consortium. (2004). Sequence and comparative analysis of the chicken genome provide unique perspectives on vertebrate evolution. Nature 432:695-716.

Julian, R. J. (1993). Ascites in poultry. Avian Pathology 22:419-454.

MacLean, M. R. (2007). Pulmonary hypertension and the serotonin hypothesis: where are we now? International Journal of Clinical Practice 61:27-31.

Mousseau, T. A., Ritland, K., and Heath, D. D. (1998). A novel method for estimating heritability using molecular markers. Heredity 80:218-224.

Olkowski, A. A. (2007). Pathophysiology of heart failure in broiler chickens: structural, biochemical, and molecular characteristics. Poultry Science 86:995-1005.

Orte, C., Polak, J. M., Haworth, S. G., Yacoub, M. H., and Morrell, N. W. (2000). Expression of pulmonary vascular angiotensin-converting enzyme in primary and secondary plexiform pulmonary hypertension. Journal of Pathology 192:379-384.

Pavlidis, H. O., Balog, J. M., Stamps, L. K., Hughes, Jr., J. D., Huff, W. E., and Anthony, N. B. (2007). Divergent selection for ascites incidence in chickens. Poultry Science 86:2517- 2529.

Rubin, L. J. (1997). Primary pulmonary hypertension. New England Journal of Medicine 336: 111-117.

Simmoneau, G., Galie, N., Rubin, L. J., Langleben, D., Seeger, W., Domenighetti, G., Gibbs, S., Lebrec, D., Speich, R., Beghetti, M., Rich, S., and Fishman, A. (2004). Clinical classification of pulmonary hypertension. Journal of the American College of Cardiology 43:5S-12S.

Smith, C. (2009). Applications of variable number tandem repeat genotyping in the validation of an animal model and gene flow studies in threatened populations of reptiles. Doctoral Dissertaion. Department of Biological Sciences, University of Arkansas.

Stenmark, K. R., Meyrick, B., Galie, N., Mooi, W. J., and McMurty, I. F. (2009). Animal models of pulmonary arterial hypertension: the hope for etiological discovery and pharmacological cure. American Journal of Physiology 297(6):L1013-L1032.

Wideman, R. F., Chapman, M. E., Hamal, K. R., Bowen, O. T., Lorenzoni, A. G., Erf, G. F., and Anthony, N. B. (2007), An inadequate pulmonary vascular capacity and susceptibility to pulmonary arterial hypertension in broilers. Poultry Science 86:984-998.

Wideman, R.F., Hamal, K. R., Bayona, M. T., Lorenzoni, A.G.,Cross, D., Khajali, F., Rhoads, D. D., Erf, G. F., and Anthony, N. B.. (2011), Plexiform Lesions in the Lungs of Domestic Fowl Selected for Susceptibility to Pulmonary Arterial Hypertension: Incidence and Histology. The Anatomical Record 294:739-755

Widlitz A., and Barst R. J. (2003). Pulmonary arterial hypertension in children. European Respiratory Journal 21:155-176.

Mentor Comments: Dr. Rhoads' comments place Russell's work into the larger context of a major interdisciplinary research initiative that showcases some of the most exciting work taking place on the University of Arkansas campus.

Russell Burks' sequence analyses of the AGTR1 gene is part of a collaborative project between several research groups on the University of Arkansas campus investigating Pulmonary Arteriole Hypertension (PAH) in the chicken. PAH results in a disease known as Ascites in the poultry industry with annual costs estimated at over $100,000,000. During the past 15 years, Dr. Nicholas Anthony in Poultry Science developed ascites susceptible and ascites resistant lines of chickens. We then collaborated on mapping the gene regions contributing to ascites phenotype. One gene region contained the AGTR1 gene which, in humans, has been implicated in some forms of PAH. Sriram Krishnamoorthy (Ph.D. student in Dr. Anthony's group) has confirmed that the region of AGTR1 is associated with Ascites phenotype in the experimental lines and in commercial lines.

Therefore, Russell took on the task of sequencing the AGTR1 gene from the resistant and susceptible lines. He used PCR to amplify the exonic regions from multiple chickens. Sequences of those regions revealed a number of single nucleotide polymorphisms (SNPs). Some of these SNPs are not in exons, while a few affect exonic sequences including one that would alter the AGTR1 protein. Although none of these SNPs may be the actual mutation that contributes to ascites susceptibility/ resistance, they are excellent markers for investigating this region further. AGTR1 is part of the angiontensin pathway which regulates vasoconstriction and kidney function. Dr. Robert Wideman (Poultry Science) and Dr. Heidi Kluess (Health Science, Kinesiology, Recreation and Dance) have been investigating the pharmacology of vasoconstriction in lung arterioles of the chicken. Adnan Al-Rubaye (Ph.D. student in my laboratory) is investigating the expression levels of AGTR1 in different tissues from resistant and susceptible chickens. Therefore, Russell's contribution is a set of molecular tools that will allow us to correlate particular AGTR1 alleles with gene expression levels, physiological responses, and prediction of ascites phenotype.

What is truly exciting about this is that the research at the University of Arkansas has been demonstrating that the chicken may very well be one of the best medical models for PAH in humans. The AGTR1 work is part of that and demonstrates that the chicken has many of the same underlying physiological and genetic bases for PAH as found

in humans. Thus, we are not only going to understand the disease to minimize the impact on the poultry industry, but may also develop an excellent model for understanding and developing new treatments for the disease in humans.

This work has been funded by grants to Drs. Anthony and Rhoads from the Arkansas Biosciences Institute, and to Dr. Wideman from the National Institutes of Health.

CLEAN ENERGY WATER DISINFECTION FOR SMALL, REMOTE RURUAL COMMUNITIES (WERC Environmental Design Contest)

By Ryan M. Lee*
Department of Chemical Engineering

Faculty Mentor: W. Roy Penney
Ralph E. Martin Department of Chemical Engineering

Abstract

Access to drinking water is essential to all life, yet in many developing and remote communities, it is often contaminated with disease causing pathogens. This project was created in response to the annual WERC Environmental Design Competition. This year's specific challenge was to develop human powered, stand-alone, effective, easily implemented, and economical water disinfection systems. Many technologies were evaluated; however, bleach and ultraviolet (UV) light treatments were determined to be most applicable to remote and impoverished communities. The Razorback Microcide WERC Crew designed and demonstrated two systems independently featuring bleach and UV disinfection technology. Both systems include a high capacity, human powered treadle pump which sustainably operates at 15 gpm. The bleach system, which operates using only human power, treats 3,000 gallons of water in five hours. The UV system treats 3,000 gallons of water in 9 hours using solar power. Both systems can be assembled in remote locations, can be operable in five days, and are portable via light truck. The first cost of the UV system is $1,485 and the operating cost is $0.002 per gallon. The first cost of the bleach system is $550 and the operating cost is $0.001 per gallon. The bleach system is advantageous because it has lower costs, uses only human energy, and requires fewer specialized parts, while still delivering an EPA recommended disinfection. The UV technology is a feasible alternative that does not add chemicals to the water. The Razorback Crew made arrangements to implement the project in Haiti, but were prevented from doing so because of government travel restrictions.

Introduction

Water-borne illness continues to trouble developing countries as well as disaster-stricken areas. The United Nations estimates that water-borne diseases account for nearly 80 percent of all deaths in the developing world and that one in six people do not have access to clean water.[1] This project proposed methods to treat 3,000 gallons of water per day to World Health Organization (WHO) drinking standards for a small community of around 500 people using only clean energy.

Many technologies are used for water disinfection. Chlorine, iodine, and ozone are some chemical methods of water disinfection. Filtration, including microfiltration, ultrafiltration, and reverse osmosis, is used to remove bacteria. In addition to chemical and filtration technologies, one can disinfect water using UV irradiation, ultrasonic treatment, electrolysis, solar disinfection, and slow sand filtration.

Currently, there are few clean energy water solutions being employed in third world settings for communities. Existing solutions are either for one household or are part of an existing infrastructure and therefore are not portable. Slow sand filtration is used successfully to provide potable water for individual households.[2] Tablet chlorine systems have been implemented to disinfect municipal water supplies.[3] General Electric has implemented an ultrafiltration unit in several locations in Haiti which can produce 5,000 gallons of clean water per day, although the system costs roughly $25,000.[4] Many third world water solutions have been implemented through the support of philanthropic sponsors and various organizations. However, there are still not enough sustainable drinking water systems in these countries. This article describes the design premises and processes used by the University of Arkansas WERC Crew to respond to the 2011 WERC Environmental Design Contest Task # 7: Develop and demonstrate a stand alone, non-fossil based energy source for a water disinfection/treatment system to be used for a small, remote community.

Design premises

The clean energy disinfection systems developed in this project had to be compliant with specific design premises. Each must:

1. utilize clean energy (i.e. solar, wind, human)
2. disinfect water to World Health Organization (WHO) drinking water standards for bacterial contamination
3. provide 3,000 gallon per day of disinfected drinking water
4. be designed so it is:
   a) easy to implement
   b) easy to maintain and operate
   c) portable
   d) cost effective
   e) applicable to rural and third-world settings

Technology Considered

While many different technologies were considered, not all fit the requirements. The advantages and disadvantages of various systems are discussed, along with the primary reason for rejecting each approach.

* *The Razorback MicrocideWERC Design Team included: Nathan L. Bearden, Allen A. Busick, Howard R. Heffington Jr., Jennifer E. Herrera, James T. Hudson, Ryan M. Lee, and Timothy R. Meyer. Ryan Lee was team leader and hence primary author.*

Slow sand filtration is most often implemented in a single family setting. Slow sand filtration is essentially a multimedia filter with different layers of sand and gravel. Over a period of 1-2 months, a biological layer called a schmutzdecke develops on the surface, which digests disease causing parasites and viruses. After passing through the schmutzdecke, the water enters the filter bed where screening and sedimentation take place. The operation yields potable water, but the limited capacity and slow startup of the system were severe disadvantages for satisfying the stated requirements of 2011 WERC Competition Task # 7.

Ultrafiltration (UF) is an excellent defense against bacteria, viruses, protozoa, and cysts, provided membrane integrity is conserved. The small pore size (0.001-0.02 μm)[6] of UF units rejects all harmful microbes including *Giardia lamblia* and *Cryptosporidium,* which are resistant to chlorine treatments. Ultrafiltration can be implemented with only a sediment filter before the unit to produce potable water; it represents a very complete solution itself. The primary disadvantage of UF is the relatively high pressure drop. Seader and Henley report that UF membranes require a pressure drop from 10-100 psi.[6] A disadvantage of a UF system is the power requirements are greater than can be provided by human power. Another disadvantage is the need for backwashing to mitigate fouling.

As with ultrafiltration, microfiltration provides ample removal of bacteria. According to WHO[8], microfiltration removes 99.9% of bacteria and 90% of viruses. Microfiltration, like UF, also requires a preceding sediment filter. Microfilters pose the same problems as ultrafiltration to an extent. Microfilters require only 1-10 psi[6], but the increased pore size (0.02-10 μm)[6] leads to the need for more frequent backwashing and unrecoverable fouling due to pore pluggage. Like all membrane systems, membrane integrity is an issue because of possible rupture. Another disadvantage of microfiltration compared to UF is shorter membrane life. The smaller pores of UF completely reject particles which can lodge in a microfilter, making the microfilter more susceptible to fouling.[5] These disadvantages combined with the high capital cost make both micro and ultrafiltration unacceptable for Task # 7.

The third membrane separation process considered was reverse osmosis (RO). RO removes nearly all contaminants. The high pressure drop (40-60 psi), high cost of membrane units in parallel, and membrane integrity make RO very uneconomical.

Both solar distillation and radiation were considered as methods of disinfection. While both provide ample bacteria removal, both also require large heat transfer areas, thus portability is a key issue. Most ultrasonic disinfection systems are used in conjunction with UV systems to help inactivate *Giardia lamblia* and *Cryptosporidium*. Ultrasonic systems are effective, but the amount of energy input required outweighs the potential benefits.

Ozone is widely used in water treatment. It causes fewer dangerous byproducts than other chemical treatments and disinfects 3000 times faster than chlorine.[17] Treating water with ozone kills 99.9% of bacteria and also kills viruses. Ozone was eliminated because its equipment is very expensive and it requires large amounts of energy.

Iodine is mainly used as a field water disinfectant. It is added in tablet or crystallized form. It works best when the water is over 68°F. Iodine is available in kits and is more effective than chlorine in removing *Giardia lamblia* cysts. Disadvantages of iodine, however, outweigh the benefits for this application. Iodine kills many pathogens, but not all. It was eliminated because it also leaves a bad taste, is sensitive to light, and causes allergic reactions in some people.

Hydrogen peroxide (H_2O_2) acts in a similar manner as ozone. Free radicals decompose pollutants. It reacts very fast and decomposes into oxygen and water. H_2O_2 is easy to use and prevents formation of colors and byproducts. Yet H_2O_2 is phytotoxic in high dosages, decreases pH, requires high concentrations to be effective, and is expensive.

In addition to alternative disinfection techniques, the team evaluated several technologies for the pumping of water. The bicycle pump is a proven, effective means of pumping water. The biggest drawbacks of bicycle pumps are (1) the limited sustainable flow rate and (2) the required energy input from humans. Harvest H_2O[7] estimates a sustainable flow rate for a healthy male is about three gallons per minute. A treadle pump is more efficient than a bicycle pump because the treadle pump is operated with a natural stepping motion rather than a rotary motion. The piston pump has a higher pumping efficiency than a centrifugal or tubing pump, which are the pumps normally powered by bicycle.

Electric pumps provide a steady stream of water at a constant pressure, and given sufficient electrical power, are ideal pumps. For this competition, power is the biggest issue associated with electrical pumps. Battery systems charged by solar panels or other renewable energy sources are necessary. The pumps and their power systems are also expensive compared to human powered pumps. Electric pumping systems are complicated thus skilled labor is required should repairs become necessary. In small sizes, the pump and motor are inefficient, so electricity becomes uneconomical. Thus electric pumps are unacceptable for the designated challenge.

If available, hydroelectric power (HEP) is another reliable source of alternative energy. But HEP comes with some major disadvantages. The availability severely hinders the applicable sites. Also, small HEP systems are not economical. Wind power is potentially one of the cheapest sources of alternative energy but, like hydroelectric, is reliable only in certain locales.

All of the technologies discussed were eliminated because they did not meet the requirements for Task # 7. The chosen technologies of bleach and ultraviolet light (UV), and other system elements that meet Task # 7 are discussed in the following sections.

Experimentation

Experimentation was divided into three major categories: pre-filtration, pumping, and disinfection. System designs and operations were varied in order to determine the optimum effectiveness of each category. Objectives included reducing turbidity, removing sedimentation and bacteria, and decreasing time required to pump 3,000 gallons of water.

Pre-filtration

Both bleach and UV systems require turbidity reduction in order to provide the greatest effectiveness. Effectiveness of the pre-filtration system was determined based on turbidity reduction of the filtered water. Turbidity was tested using a nephelometer. A gravity fed five gallon sand filter was initially used. This design fed water through the bottom of a sand filter, then rose and flowed into a bag filter. The pressure drop of this system was too high and there was insufficient turbidity reduction. The final design for the pre-filter was an 18 gallon submersible sand filter, which is described below. Turbidity tests were conducted using two sources of water. Turbidity within creek water was reduced from an average of 5.1 nephelometric turbidity units (NTU) to 2.2 NTU. Water from a standing pond had a turbidity reduction from an average of 22 NTU to 10 NTU. Both cases showed a 55% reduction in turbidity. The sand filter effectively removed all sediment from the water.

The water from both sources still had a mild green tint, caused by organic molecules, after flowing through the sand filter. A second filter containing activated carbon was found to remove all color and further reduce turbidity because of activated carbon's adsorptive abilities. In the case of creek water, carbon reduced turbidity from 2.2 NTU to 1.5 NTU. With pond water, carbon reduced the turbidity from 10 NTU to 4 NTU.

A one micron bag filter was also tested for reducing turbidity. It removed sand, carbon, and residual sediment; however, it had little effect on reducing turbidity. The one micron bag filter is also capable of removing larger bacteria and protozoa such as *Cryptosporidium* and *Giardia lamblia* not removed by the sand filter. According to the Washington State Department of Health[10], *Cryptosporidium* cysts range from four to seven microns and can effectively be removed by filters of pore size one micron or less.

Pumping

To eliminate the need for energy outside the local community, a human powered pumping system was designed and constructed. The treadle pump uses a natural stepping motion to create suction of water into the pump and pressure to discharge the water. A two piston prototype treadle pump 4' x 4' footprint was built and successfully tested. This pump produced a flow rate of 5-7 gpm with a sand filter on the suction side. After its use, stability and efficiency issues were addressed, such as heavy frictional losses within the pulley system. To improve pumping performance, a two person, four piston treadle pump was designed and constructed. This two person design eliminated the need for a pulley system. The improved pump increased the flow rate to 15 to 20 gpm, thus shortening the time required to pump 3,000 gallons to less than four hours.

UV Disinfection

According to WHO[8] the minimum energy flux required to kill 99% of bacteria and 99% of viruses is 7 mJ/cm^2 and 59 mJ/cm^2, respectively.[8] However, the EPA's strict requirement of zero coliform bacteria in the water was chosen to be the goal of this project.[18] While the task does not require addressing virus inactivation, the UV system kills a significant fraction of viruses. The UV system operates at five gallons per minute with a flux of 54 mJ/cm^2. The system is gravity fed, and the flow is achieved by adjusting the height of the exit tube from the UV chamber (see Figure 6). Efficiency of disinfection was tested using water from three different locations within the city of Fayetteville, AR: Mulline Creek, Goose Creek, and Paul R. Noland Waste Water Treatment Facility. Bacteria counts were determined using an agar test strip before and after the treatment system. The UV system completely deactivated all coliform bacteria from Mulline Creek and Goose Creek. As a worst case scenario, clarified water from a waste water facility, containing roughly 100,000 colony forming units per milliliter (CFU/mL), was run through a one micron bag filter and tested. After treatment, the water was found to have 52 CFU/mL total coliform, a 99.96% reduction, and 2 CFU/mL E. coli, 99.94% reduction. These test results were obtained by the Arkansas Water Resources Center at the University of Arkansas, Fayetteville. These tests show that, except for severely contaminated sewage water, the UV system meets EPA and WHO guidelines.

Bleach Disinfection

Bleach systems have been used to provide potable water for remote communities and in the third world. According to EPA guidelines[9] for drinking water, bleach can be used to disinfect water by adding 1/8 teaspoon of 6wt% solution of sodium hypochlorite (NaOCl) per gallon of contaminated water and allowing a 30 minute residence time. That corresponds to about half a gallon of bleach per 3,000 gallons of drinking water. Experiments using source water from two water sources, Goose Creek and Mulline Creek, confirmed this recommendation with complete disinfection of coliform and E. coli bacteria. The test results for the current study found that 15 minutes is the minimum residence time required for complete disinfection. This finding confirms EPA's[9] recommendation, "*Mix the treated water thoroughly and allow it to stand, preferably covered, for 30 minutes."* The Crew design incorporated a residence time of 30 minutes as a safety factor to insure all pathogens are killed.

Experiments were conducted for the removal of chlorine. WHO[16] states "*….the guideline value is 5 mg/litre (rounded figure). It should be noted, however, that this value is conservative, as no adverse effect level was identified in this study.*" It was found that chlorinated water flowing through activated carbon reduced the chlorine concentration from 5 ppm to less than 0.5 pp. However, adding a carbon filter to improve taste is not normally justified because water containing the recommended level of NaOCl is quite palatable. Consequently, the Razorback Microcide WERC Crew did not recommend removing the residual chlorine.

Full Scale Design

After the experimental stage, the final design consists of two separate systems: bleach and UV disinfection. Both contain the same pre-disinfection components, which include a sand filter, a treadle pump, and a one micron bag filter containing activated carbon. After these common steps, both systems then follow their respective disinfection processes.

Pre-disinfection (both systems)

The sand filter removes debris and turbidity from the source water. The suction of the pump connects to a one inch PVC

pipe which terminates at the bottom of an 18 gallon bucket in an inlet flow distributor. The flow distributor consists of cloth-covered perforated (1/8" holes) pipes as shown in Figure 1. The distributor is positioned at the bottom of the bucket. Above the distributor is placed 4" of gravel covered with 14" of sand. A cloth is secured by bungee cords over the bucket top for protection of the sand filter against mud and debris and to prevent the loss of sand. The distributer, bucket, sand, and cloth are all shown in Figure 1. The filter is immersed in the source water. The pressure drop through the sand filter is about 2" water column while operating at 7.5 gpm, which is minimal for the treadle pump.

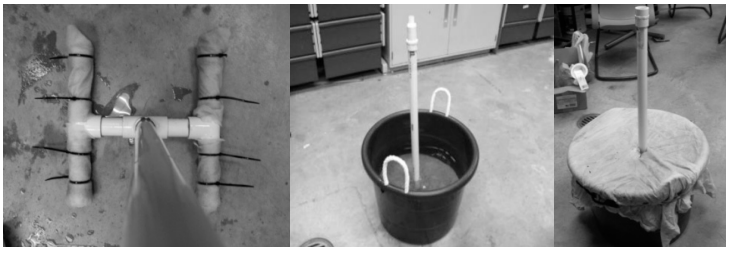

Figure 1. Sand filter.

The source water is pumped from the sand filter by a human powered treadle pump (see Figure 2). The pump, which is used in both processes, was constructed by unskilled labor in a laboratory room at the University of Arkansas without the use of machined parts. Each pumping stroke delivers four liters of water. Two people can operate this treadle pump with a sustainable output of 15 gpm. The pumping operation may be compared to slowly walking up stairs and does not require the exhaustive effort required to operate a bicycle pump. While lumber for the pump can be bought, cut, drilled, and then shipped with instructions, the pump can also be constructed with local materials or may be improvised depending on the materials and tools available. Weighing about 150 pounds it can be carried short distances or transported long distances via light truck. A detailed set of plans for constructing the treadle pump is available on the University of Arkansas Department of Chemical Engineering website.

Bleach Process

The bleach system, as shown schematically in Figure 3, consists of the following sections: (1) sand filter, (2) treadle pump, (3) one micron bag filter filled with activated carbon, and (4) disinfection and storage. An advantage of the bleach system is it only takes thirty minutes to disinfect the water in a well-mixed tank using a small amount of bleach. The power requirement is limited to two humans pumping less than four hours a day. At a pumping rate of 15 gpm, treated water is available in the first 1,500 gallon storage tank two and a half hours from the start of pumping.

After the sand filter, water is pumped through a one micron bag containing nine ounces of activated carbon into a 1,500 gallon holding tank. The one micron filter is held in place by a casing on the side, inside the 1,500 gallon tank, and is effective at removing cysts and larger bacteria. Four cups of household bleach (6% sodium hypochlorite) are added and blended with a paddle which is positioned in the tank through an oarlock. Five minutes is required to blend the bleach into the tank contents. Once the tank is well mixed, the bleach treatment stands for a minimum of 30 minutes. According to the EPA[9], the disinfected water "*should have a slight chlorine odor*."[9] The slight odor of bleach gives an affirmation that the water has been disinfected. Bacteria test strips are another possible option for verification, but the daily cost is about $4. At 15 gallons per minute, the pump will fill one 1,500 gallon tank in less than two hours and fill the second 1,500 gallon tank in another two hours. The first tank is ready for consumption within two and a half hours of the beginning of each day and the second is ready within five hours. Thus, consumers can draw water for 21 hours every day.

Figure 2. Two person treadle pump.

The storage tanks will be constructed locally using a flexible design. A sturdy option for storage uses 4' X 8' plywood sheets, 2"x4"x8' supports, plastic (polyethylene) lining, and a tarp covering as shown in Figure 4. A square of four 4' X 8' plywood sheets, placed in a two foot deep 8'x8' hole in the ground, provides the sides for a 1,900 gallon (1,500 gallons working volume) storage tank. The tank will be placed in a two foot deep hole to provide support. Other possibilities include digging a similar sized hole and lining with sand, clay, plastic or some combination. The choice of construction of the storage tanks is dependent upon the availability of materials and tools. The plastic lining has the potential to incur growth of bacteria and algae and should therefore be cleaned or replaced as required.

With four barrel pumps total (two on opposite sides of each tank) giving a draw capability of 20 gpm, the minimum time to dispense 3,000 gallons is about three hours. Consequently, on average, water needs to be drawn only 14% of the time. With two 1,500 gallon tanks and four barrel pumps there will be virtually no waiting for water draw.

As mentioned earlier, WHO gives a guideline of 5 mg/liter or 5 ppm for the safe concentration of chlorine in water.[8] This study verifies that 5 mg/liter is safe to drink; however, to implement a conservative treatment, eight cups per 3,000 gallons, which is 10 mg/liter and is the EPA recommended treatment level, is recommended. This level of bleach is safe in drinking water; consequently, there is no need for chlorine

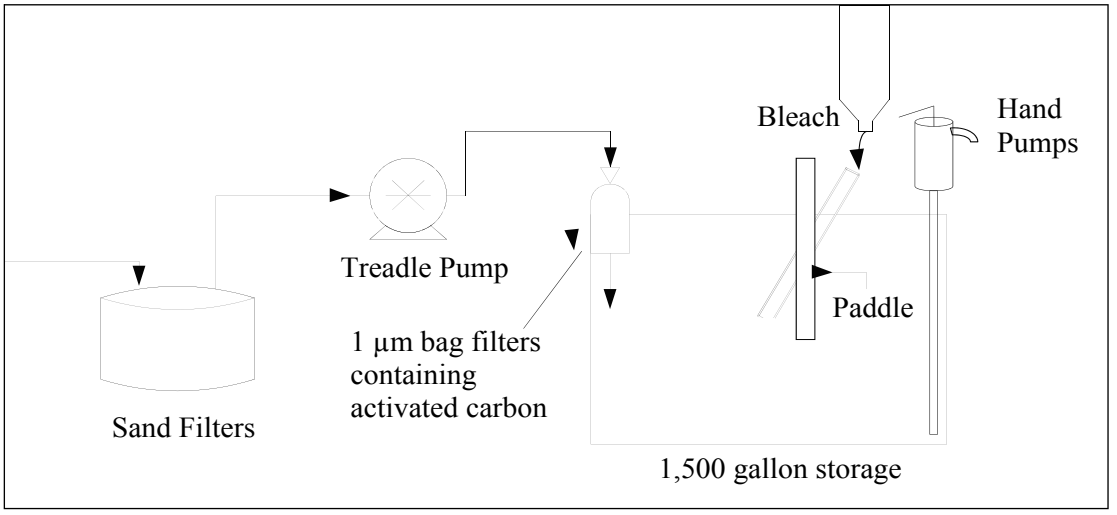

Figure 3. Process flow diagram of bleach process.

removal. If chlorine removal is still desired, for whatever reason, a simple carbon filter may be added at the suction of the barrel pumps. The optional post carbon filter can be constructed easily using a bucket, lid, cloth, and four inch PVC pipe as shown in Figure 5. Holes must be drilled in the bucket and in the pipe. Both the inside pipe and the outside of the bucket are wrapped with cloth. Carbon is poured into the annulus between the pipe and the inside of the bucket. The delivered water will be drawn by the consumer using a hand operated barrel pump also shown in Figure 5. The barrel pump will be installed above the post carbon filter, if a post carbon filter is utilized. The post carbon filter will be submerged in the storage tank. The piping between the carbon filter and the barrel pump will be the proper length to place the barrel pump at a height for operating ease. The extra cost of replacement carbon for the post carbon filter is very high compared to the recommended system, strictly to make the water a bit more palatable.

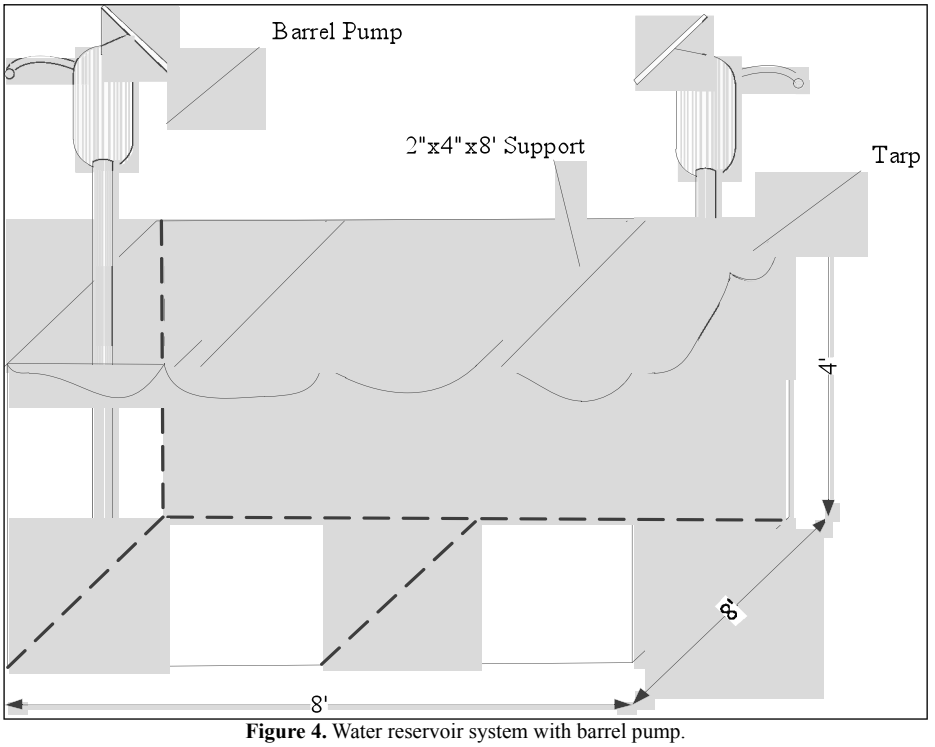

Figure 4. Water reservoir system with barrel pump.

UV Process

The components of the UV system include the following: (1) a sand filter, (2) a treadle pump, (3) a carbon filter plus surge tank, (4) a level controlled reservoir, (5) a UV lamp, and (6) two storage tanks, as shown schematically in Figure 6. The UV system can sanitize 3,000 gallons of contaminated water in 8-10 hours with a demonstrated 3-log reduction in *E.coli* and total coliform bacteria.

Water is pumped from the sand filter through a one micron bag filter containing nine ounces of granular activated carbon into a 300 gallon tote. The activated carbon removes any free organics, color, and some turbidity. The one micron bag filter eliminates large protozoa and large bacteria. The rate at which the activated carbon must be replaced is dependent on the source water but it typically needs replacement weekly. The 300 gallon tote is a surge tank that allows the pump to be operated at a variable pace without affecting the flow rate through the UV chamber.

An 18 gallon storage bin equipped with a float valve allows a flow rate up to 6 gpm through the UV chamber. The level in the controlled UV feed reservoir will be maintained approximately 40” above the overflow outlet of the UV unit. This constant level will ensure that the flow rate through the UV unit remains constant, even though the pumping rate into the surge tank is variable. This also prevents the treadle pump from being required to operate continuously. If the 40” is exceeded, the flow rate through the UV chamber may be too great and will therefore become less effective at bacterial disinfection due to a decreased residence time.

The UV bulb requires 50 Watts which is powered from a 12V battery through a DC-AC power inverter. One 12V, 16 Amp-hour battery will provide power to the UV lamp while the two 45 Watt solar panels recharge another 12V battery in order to provide continuous operation of the UV bulb. The UV chamber has a residence time of 8.5 seconds and provides an energy flux of 54 mJ/cm^2, which is capable of greater than 99.9% inactivation of all bacterial and protozoan contamination. After exiting the UV unit, the treated water is then pumped to one of two 1,500 gallon reservoirs as described above. The water contained in the storage tanks

Figure 5. Optional post carbon filter housing.

will need to be tested daily for the presence of residual coliform bacteria before consumption. The bacteria test is an antibody-based kit that detects bacterial presence within twenty minutes. The kit includes a sterilized pipette, vial, and test strip with basic, easy to follow instructions.

The UV system is susceptible to short circuiting due to adverse weather and is therefore fitted with a waterproof housing to protect the ballast and all electrical connections. Over time,

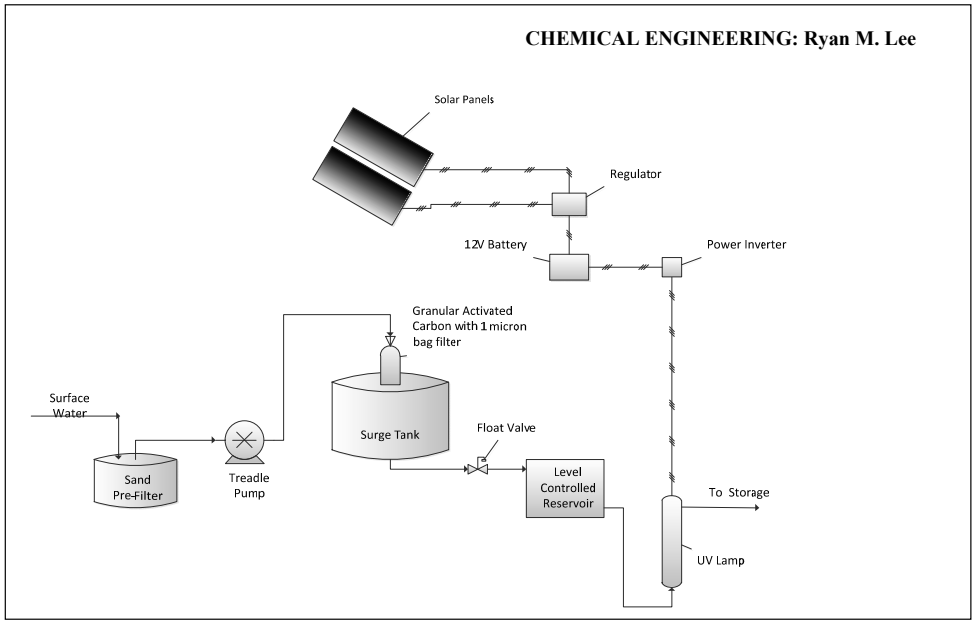

Figure 6. UV process flow schematic.

minerals in the water can form a coating over the protective quartz sleeve, which decreases the energy flux of the UV lamp to the water. To insure the full energy flux is provided, the quartz tube must be removed and wiped with a dilute bleach solution on a weekly basis. The UV system is dependent on full solar flux to provide sufficient power to recharge the 12V batteries. If adequate sunlight is not available, the system is limited to the power stored in the batteries. A fully charged 16 Amp-hour battery will operate the UV bulb for two and a half hours. UV bulbs should be replaced yearly. An alarm will sound if the bulb prematurely goes out or breaks.

UV vs. Bleach Systems

In virtually every community in the US, sufficient technical talent is available to operate and maintain a UV system. Because it produces potable water with characteristics similar to most city water, it may be the logical choice in the US even though the system is more expensive. However, in less developed countries, the needed technical talent may not always be available. Thus, the bleach system is much preferred outside the US.

Economic Analysis

The itemized materials and price list for the components of the bleach system are presented in Table 1. The first cost (initial cost of construction of system) is $550. The operating cost is $20 per week or $944 per year. The operating cost includes buying bleach, replacing the activated carbon, and replacing the one micron filter bag every other week. The price of the disinfected water after the first week of operation is $0.027 per gallon, including first costs. After a month, the price of water is $0.0074 per gallon. After a year, the price of water is only $0.0013 per gallon. The operating cost is only $0.001 per gallon, if first costs are not included.

The itemized materials and price list for the components of the UV system are presented in Table 1 and Table 2. The price of the sand filter, treadle pump, and miscellaneous costs common to both bleach and UV systems are in Table 1, while the UV and storage costs are in Table 2. The first cost of the system was $1,485. The operating costs for a week and a year are $41 and $2,016, respectively. The operating costs include buying bacteria test strips, replacing the activated carbon every week, and replacing the one micron filter bag every other week. After a week, month, and year, the price of disinfected water is $0.5, $0.02, and $0.0032, respectively. Removing first costs lowers the operating costs to $0.002 per gallon. If bacterial testing is removed from the UV system, the operating cost would be $12 per week and $491 per year.

Safety and Environmental Considerations

The bleach and UV water filtration systems described in this paper were designed to ensure safety for both the persons constructing the systems and the end users of the filtered water. Safety relating to the handling of bleach and elimination of UV radiation exposure was of the most importance. In addition, designers recognized the need to create a filtration process with byproducts that pose little to no environmental risks. The following sections describe safety and environmental issues addressed in this design project.

Chemical Considerations

Common household bleach contains the following hazardous ingredients: 6% sodium hypochlorite (active ingredient) and 1% sodium hydroxide. According to the MSDS's, none of these

Table 1. Itemized materials and price list for the bleach system.

Pre-Filter				**Storage**			
Item	Unit Price	Quantity	Price	Item	Unit Price	Quantity	Price
18 Gallon Tub	$5.97	2	$11.94	Carbon	$1.35/9oz	1	$2.70
Play Sand	$3.66	4	$14.64	1 Micron Bag Filter	$4.49	2	$8.98
All Purpose Gravel	$3.28	2	$6.56	Polyethylene 10' by 100'	$18.00	1	$18.00
1" Sch 40 Tee	$0.64	6	$3.84	Tarp 12' by 16'	$21.99	2	$43.98
1" PVC Endcap	$0.51	8	$4.08	Wood 2"x4"x8'	$1.59	12	$19.08
1" Sch 40 10' Pipe	$2.48	2	$4.96	Plywood 1/4"x4'x8'	$11.77	8	$94.16
Nylon Barb 3/4"	$2.24	2	$4.48	Paddle	$10.00	2	$20.00
Bushing threaded 1" x 3/4"	$0.47	2	$0.94	**Total**			**$206.90**
1" Adapter (slipxthread)	$0.66	2	$1.32				
Cloth 2 yards	$3.00	2	$6.00	**Miscellaneous**			
Total			**$58.76**	Item	Unit Price	Quantity	Price
				Purple Primer	$3.78	1	$3.78
Treadle Pump				All Purpose Cement	$4.58	1	$4.58
Item	Unit Price	Quantity	Price	Sealant	$5.00	1	$5.00
Wood 2"x4"x8'	$1.59	16	$25.44	1" Hose Clamp (Box of 10)	$4.50	2	$9.00
Scrap Leather	$5.99	1	$5.99	4" Hose Clamp	$1.29	8	$10.32
3/4" PVC Check Valve	$7.19	8	$57.52	Bleach	$1.87/3 quarts	0.67	$1.25
3/8" All Thread 6'	$5.37	1	$5.37	Screws	$3.98	1	$3.98
3/8" All Thread 3'	$2.68	1	$2.68	3/4" Washers	$0.10	16	$1.60
1" Dowel Rod 3'	$4.69	1	$4.69	3/4" Nuts	$0.15	24	$3.60
1/2" Metal Rod 3'	$4.82	1	$4.82	Thread Tape	$3.20	1	$3.20
1/2" Weld Steel Tube	$5.23	2	$10.46	Barrel Pump	$25.99	2	$51.98
4" Sch 40 Pipe 10'	$10.14	1	$10.14	Zip Ties	$1.25	1	$1.25
4" Cap	$0.92	4	$3.68	**Total**			**$99.54**
3/4" Sch 40 PVC 10'	$1.99	1	$1.99				
3/4" Braided Tube per ft	$1.47	20	$29.40				
1" Braided Tube per ft	$2.24	6	$13.44				
3/4" Barb Tee	$0.71	5	$3.55				
Nylon Barb 3/4"	$2.24	4	$8.96				
3/4" x 1" Reducer	$1.12	1	$1.12				
Miscellaneous PVC parts	$8.47	1	$8.47				
Total			**$197.72**				

Table 2. Itemized materials and price list for the UV system.

UV				**Miscellaneous**			
Item	Unit Price	Quantity	Price	Item	Unit Price	Quantity	Price
Battery	$19.00	2	$38.00	Purple Primer	$3.78	1	$3.78
350W Inverter	$69.99	1	$69.99	All Purpose Cement	$4.58	1	$4.58
Model C4	$399.00	1	$399.00	Sealant	$5.00	1	$5.00
Solar Panels	$179.99	2	$359.98	1" Hose Clamp (Box of 10)	$4.50	2	$9.00
3/4" Barb	$0.79	2	$1.58	4" Hose Clamp	$1.29	8	$10.32
Total			**$868.55**	Bleach	$1.87/3 quarts	1	$1.87
				Screws	$3.98	1	$3.98
Storage				3/4" Washers	$0.10	16	$1.60
Item	Unit Price	Quantity	Price	3/4" Nuts	$0.15	24	$3.60
1 Micron Bag Filter	$4.49	2	$8.98	Thread Tape	$3.20	1	$3.20
Carbon	$1.35/9oz	2	$2.70	Barrel Pump	$25.99	2	$51.98
300 gallon tote	$50.00	1	$50.00	Test Strips	$20.95	1	$20.95
18 Gallon Tub	$5.97	1	$5.97	Zip Ties	$1.25	1	$1.25
Float Valve	$16.00	1	$16.00	**Total**			**$121.11**
Ball Float	$1.00	1	$1.00				
Polyethylene 10' by 100'	$18.00	1	$18.00				
Tarp 12' by 16'	$21.99	2	$43.98				
Wood 2"x4"x8'	$1.59	12	$19.08				
Plywood 1/4"x4'x8'	$11.77	8	$94.16				
Paddle	$10.00	2	$20.00				
Total			**$279.87**				

ingredients are on the IARC, NTP, or OSHA carcinogen lists. Rubber or nitrile gloves, safety glasses, closed toe shoes, and long pants should be worn while handling bleach. Bleach irritates the skin and can cause eye damage and even blindness. Complete safety and environmental information is found on the MSDS[11], which will be provided to all users. Based on experiments conducted by WHO[16], "*the guideline value for free chlorine in drinking-water is derived from a NOAEL* [No Observable Adverse Effect Level] *of 15 mg/kg of body weight per day.*" This gives a conservative total daily intake (TDI) value of 5mg/L, which is well above the chlorine concentration in the bleach process. Activated carbon is a stable, non-toxic substance.[15]

Environmental Considerations

Guidelines state that sodium hypochlorite is not a threat to the environment according to EPA 40 CFR Parts 9, 156, and 165 because of its rapid decomposition. Waste is created only from activated carbon and the bag filters. The weekly replacement of nine ounces of carbon and the three ounce bag filter will generate 39 pounds of non-hazardous waste yearly. This will create a minimal impact on the environment.

User Safety

To ensure safety, users will be trained on how to appropriately handle bleach and the equipment, as well as on troubleshooting procedures. A detailed operation manual will be provided to the users and can also be obtained from the Ralph E. Martin Department of Chemical Engineering at the University of Arkansas. The OSHA regulation 29 CFR 1926.501(b) (1) Subpart M states, "each employee on a walking/working surface (horizontal and vertical surface) with an unprotected side or edge which is 6 feet (1.8m) or more above a lower level shall be protected from falling by the use of guardrail systems, safety net systems, or personal fall arrest systems." The treadle pump does not require an operator to be six feet off the ground. However, guardrails will be used for the operation of the treadle pump.

UV System Regulations

There are no OSHA-mandated employee exposure limits to ultraviolet radiation except laser-generated ultraviolet light.[14] For UV water disinfecting systems in the United States, the EPA UV Guidance Manual is typically used. The EPA's UV Guidance Manual requires that all UV reactors that disinfect water be tested to determine the disinfecting performance with either MS2 or T1 bacteriophages at various flow rates.[13] The manufacturer affirms that the UV unit used by the team meets all legal standards. The lamp used in the UV disinfection unit contains mercury. The following OSHA regulations for mercury include the following: the ceiling permissible exposure limit (cPEL) is 0.1 mg-Hg/m^3 and the NIOSH immediately dangerous to life or health (IDLH) is 10 mg-Hg/m^3. The lamp is well protected and is not likely to present a mercury hazard. If, however, the lamp does burst, the power box will alert the operators of the loss of current. The water contaminated by the mercury must not be ingested. The mercury present, however, is in small enough concentrations to be released to the environment for safe dilution.

Other Recommendations Related to Safety

Chlorine reacts with organic substances such as leaves, bark, sediment, urine, sweat, hair, and skin particles, to make disinfection by-products (DPB) such as trihalomethanes which include chloroform, bromoform, bromodichloromethane, and dibromochloromethane. In the United States, the EPA limits the maximum contaminant level (MCL) of total trihalomethanes (TTHMs) and total haloacetic acid in treated water to 80 parts per billion and 60 parts per billion, respectively.[12] TTHMs have been associated with an increased risk of certain types of cancer and other health effects as stated in the *EPA Guidance Manual: Alternative Disinfectants and Oxidants*.[12] According to the EPA, granular activated carbon is the best available technology to remove organic matter, chlorine, and chlorine DPB from water. People operating the water purification device should be cautious when taking samples in order to not contaminate the water. According to WHO, "Where local circumstances require that a choice must be made between meeting either microbiological guidelines or guidelines for disinfectants or disinfectant by-products, the microbiological quality must always take precedence."[19]

Conclusions and Recommendations

The Razorback Microcide WERC Crew investigated a variety of alternatives for producing safe clean water using only human power. Study outcomes determined that the bleach and UV systems satisfied the requirements of WERC Environmental Design Competition Task # 7 significantly better than any of the other evaluated alternatives. The following summarizes outcomes:

1. The bleach system is ideal for third-world, developing countries because it lends itself to construction and operation using unskilled labor, has moderate first costs and minimal operating costs, and requires low maintenance.
2. The UV system provides clean, safe water which tastes as chemical free as tap water. For communities, especially in the US, where taste may be a primary consideration and costs a secondary consideration, the UV system may be preferred.
3. Both assembled systems are easily portable by light truck or, alternatively, can be easily assembled on site.
4. The bleach system is the overall more appropriate design choice as it has the smallest first cost of $550 and smallest operating cost of $944 per year.
5. One key difference between the operating cost of the bleach system and the UV system is the $1,485/year costs for conducting two bacteria tests per day.

Intel® recognized the Razorback Crew as designing the most innovative process at the IEE/WERC Environmental Design Contest. The team is currently investigating the possibilities for implementing a bleach system in Honduras in December 2011.

REFERENCES

1. Annan, Kofi. United Nations Press Release SG/SM/8707 OBV/348. <http://www.un.org/News/Press/docs/2003/sgsm8707.doc.htm>.
2. "Biosand Filter." *Clean Water for Haiti*. <http://www.cleanwaterforhaiti.org/_what_biosand.html >.
3. *Bringing Clean Water to Haiti-International Action*. <http://www.haitiwater.org/ >.
4. Barker, Jack. *Alternative Energy Microbiological Water Purifier.* IWT, 2008. <http://sustainablebusinessforum.com/marcgunther/50032/how-ge-learned-think-small-and-serve-poor>.
5. "Alternative Separation Processes". *Perry's Chemical Engineers' Handbook.* 7th Edition. 1997. *Knovel*. Web.
6. Seader, J.D. , Henley, E.J. "Separation Process Principles." John Wiley & Sons, Inc. Hoboken, NJ. 2006.
7. Gilg, Larry. *Bicycle Powered Water Pump*. HarvestH_2O.com, 2006. <http://www.harvesth2o.com/Pedaling_Bicycle_pump_disclosure.pdf>.
8. "Microbial Aspects". *Water forHealth: WHO Guidelines for Drinking-Water Quality*, Chapter 7. World Health Organization, 2010. <http://www.who.int/water_sanitation_health/dwq/7microbial.pdf>.
9. "Emergency Disinfection of Drinking Water." Environmental Protection Agency, 2010. <http://water.epa.gov/drink/emerprep/emergencydisinfection.cfm>.
10. "Cryptosporidium Fact Sheet." Washington Department of Health, 2009. <http://www.doh.wa.gov/ehsphl/factsheet/crypto.htm >.
11. "Chlorine Material Safety Data Sheet." KIK International, 2007. <http://yourfirstdue.com/manager/data/1213037401/File/great_value_bleach.pdf>.
12. "Disinfectant Use in Water Treatment." *EPA Guidance Manual Alternative Disinfectants and Oxidants*. Environmental Protection Agency, 1999. Chapter 2. <http://www.epa.gov/safewater/mdbp/pdf/alter/chapt_2.pdf>.
13. "Ultraviolet Dininfection Guidance Manual For the Final Long Term 2 Enhanced Surface Water Treatment Rule." Environmental Protection Agency, 2006. <http://www.epa.gov/safewater/disinfection/lt2/pdfs/guide_lt2_uvguidance.pdf>.
14. "Laser Hazards" *Osha Technical Manual*, TED 1-0.15A. Section III-Chapter6. United States Department of Labor, 1999. <http://www.osha.gov/dts/osta/otm/otm_iii/otm_iii_6.html>.
15. "Activated Carbon Material Safety Data Sheet." Envirotrol Inc, 2003. <http://www.water.siemens.com/SiteCollectionDocuments/Product_Lines/Environmental_Services/Brochures/MSDS%20ActivatedCarbon.pdf>.
16. "Chlorine in Drinking Water." *Guidelines for Drinking Water* Quality, Second Edition, v. 2. World Health Organization, Genivia, 1996. <http://www.who.int/water_sanitation_health/dwq/chlorine.pdf>.
17. "Ozone Enriched Water for Disinfection." Normex Ozone and Water Technologies, 2007. <http://www.hm-dis.com/OzoneEnrichedWater.pdf>.
18. "National Primary Drinking Water Regulations." Environmental Protection Agency, 2011. <http://water.epa.gov/drink/contaminants/index.cfm#Microorganisms>.
19. "Disinfectants and Disinfection By-Products." Guidelines for Drinking Water Quality, v. 2, ch. 16. World Health Organization, Genivia, 1996.

Mentor Comments: Professor Penney's student teams have enjoyed considerable success over the years in the WERC competitions. In the following, he describes the challenges confronting this year's team of seniors.

I served as mentor for a team of 7 Chemical Engineering Seniors - Bearden, Busick, Myers, Herrera, Heffington, Hudson and Lee - who competed in the 2011 WERC competition (http://www.werc.net). We have participated in this competition since the mid 90's and we have won 1st place several times. In fact, two (2005 and 2010) of our winning teams previously published articles in Inquiry in Vol. 6, p. 73-85, 2005 and Vol. 11. p 79-87. The WERC team competed in Task 7 of the 2011 competition. It was titled, "Clean Energy Water Disinfection for Small, Remote Rural Communities" and its objective was "Develop and demonstrate a stand alone, non-fossil based energy source for a water disinfection/treatment system to be used for a small, remote community. The community will need 3,000 gpd of disinfected drinking water. The proposed solution does not need to address water hardness or quality issues; however, it must address bacterial disinfection". The WERC team started work on January 1, 2011 and finished the competition at New Mexico State University on April 3-7, 2011. All team members received 3 credit hours for CHEG 4443, Senior Chemical Engineering Design II. This task was sponsored by the WERC Consortium which includes the Bureau of Water Reclamation. A simple, easily operated system was desired to provide potable water in rural communities and disaster areas where there is no electricity and no hydrocarbon fuels available.

The WERC team designed and demonstrated two systems - bleach and UV disinfection technology. In both designs, the pretreatment system consisted of a sand filter, a treadle pump, a granular carbon and a one micron bag filter. 3,000 gallon of storage is provided by inexpensive plastic sheet interliner, plywood sided and topped pits. The bleach system, which operates using only human power, treats 3,000 gallons of water in five hours. The UV system treats 3,000 gallons of water in 9 hours and operates using solar power. Both systems are portable via light truck. They both can be operable within two to five days and be built on-site in remote communities

and in third world settings, such as Haiti. Both systems have low operating costs.

Of the 10 teams competing in Task 7, the WERC crew won 2nd place and they scored within 12 points (out of 1000 total points) of the winning University of Idaho Team. The WERC team was awarded the Intel Environmental Innovation Award, which is awarded to the team which has the best project based on technical merit without any other consideration such as report and oral presentation quality. Essentially, it is awarded for "best of show". The team secured Honors College funds to implement the project in Haiti but were prevented from implementation because of travel restrictions. We have received inquiries from all over the world including Australia, Slovenia, Africa, India, US and others.

DESIGN, FABRICATION, AND TESTING OF AN ELECTROSPINNING APPARATUS FOR THE DEPOSITION OF PMMA POLYMER FOR FUTURE BIOMEDICAL APPLICATIONS

By Harsha Malshe
Department of Industrial Engineering

Faculty Mentor: Ajay P. Malshe
Department of Mechanical Engineering

Industry Mentor: Wenping Jiang
NanoMech, Inc.

Abstract

This paper describes the successful design and fabrication of a deposition system for synthesis and assembly of nanoscale and submicron sized fibers of poly(methylmethacrylate) (PMMA) polymer. To optimize the electrospinning deposition process, the distance between the needle and the electrically grounded substrate, the applied voltage, and the concentration of PMMA polymer in the solution were varied. PMMA fibers as small as 500 nanometers were observed using scanning electron microscopy (SEM). The chemical signature of PMMA was confirmed for best quality and retention of chemistry using Fourier Transformed Infrared spectroscopy (FT-IR). PMMA is a biocompatible polymer, and nanofibers of PMMA are key building blocks for scaffolds and other biomanufacturing applications, such as bioprinting for regenerative medicine and tissue engineering of synthetic organs (Mo, 2004).

1. Introduction

Nanomanufacturing is the science and engineering of advanced materials, their synthesis and manufacturing at submicron scales (National Nanotechnology Initiative, 2011). Metals, ceramics, polymers, semiconductors, and composites are the basic building blocks of bio-nanotechnology that are used in biomanufacturing. These materials vary not only in size but also in shape, such as fibers, rods, dots/particles, flakes, and other form factors. They are used to interface with biological and biomedical materials and components, including as organs, tissues, cells and macromolecules (e.g. DNA) (Schiffman, 2008). Thus there is a significant interest in synthesizing biocompatible materials, such as polymers, capable of interacting at submicron biointerfaces.

In the field of biomedicine today, biocompatibility in the research and development of advanced implants is a major problem (Balazsi, 2009). A challenge in engineering these implants is the ability to find materials and processing technology to create scaffolds that can mimic extracellular matrices, which promote implant-to-tissue compatibility (Balazsi, 2009). The substance ideally suited for scaffold creation is synthetic biomaterial, such as natural polymer, which can mimic the mechanical and biological properties of extracellular matrices. Thus biocompatible materials could be used to manufacture various biomedical constructs in order to realize advanced healthcare in the domain of nano-bio medicine and prosthetics.

Towards that goal, synthesizing uniform biocompatible materials with controlled dimension and chemistry is critical. Therefore an important research area is the design and development of an efficient and economically viable manufacturing process that will enable synthesis and deposit these materials at submicron scales and in a scaffold structure (Li, 2004). For example, in bio-printing, scaffolds are created from materials with various designs and chemistries that are then used as substrates, sometimes sacrificially, to allow the deposition of cells as basic building blocks for constructing the foundations of basic human tissues and organs. Nanofibers have the necessary morphological and dimensional requirements needed for scaffolds (Li, 2004), and they could also be used to embed and deliver other vital nanomaterials such as quantum dots for diagnostics and drugs for therapeutic applications (Li, 2004; Schiffman, 2008).

Based on this need, the research in this study had two objectives. The first was to design and fabricate an apparatus for reproducible synthesis of nanofibers manufactured from polymers deposited on a planar substrate using the electrospinning technique. Electrospinning, although not a new concept, has only been recently discovered as a new processing technique for fiber fabrication from organic polymers, especially on the micro to nano scale (Li, 2004). PMMA was selected as the polymer of choice from a wide range of biocompatible polymers, since PMMA can be used in biomedical applications, such as tissue engineering and wound dressing, and as supports or carriers for drug delivery (Mo, 2004; Wang 2010). In order to understand the deposition process, three critical parameters related to the deposition process were varied. The second objective was to validate the designed deposition apparatus by studying the size and chemistry of the deposited polymer for uniformity.

The research presented in this paper lays the foundation for the ultimate goal of scaffold creation for advanced biomedical manufacturing of implants, prosthetics, and functionalized delivery devices. The following text describes the deposition apparatus details, experimental process techniques, and analytical tools along with the deposition process mechanism. Results and discussion of conclusions are presented, along with suggestions for future research directions.

2. Materials and Methods

2.1 Design Criteria

Electrospinning is a drawing process that applies an external electric field to the charged jet of polymer molecules in a solution in order to segregate and deposit polymer fibers in solid form. Figure 1 shows the basic configuration of the electrospinning apparatus, which includes a polymer-injecting anode (syringe and needle), an injection pump, a solid fiber collection substrate cathode, a high voltage power supply (in the 0-30 kV range), and a polymer solution (polysol).

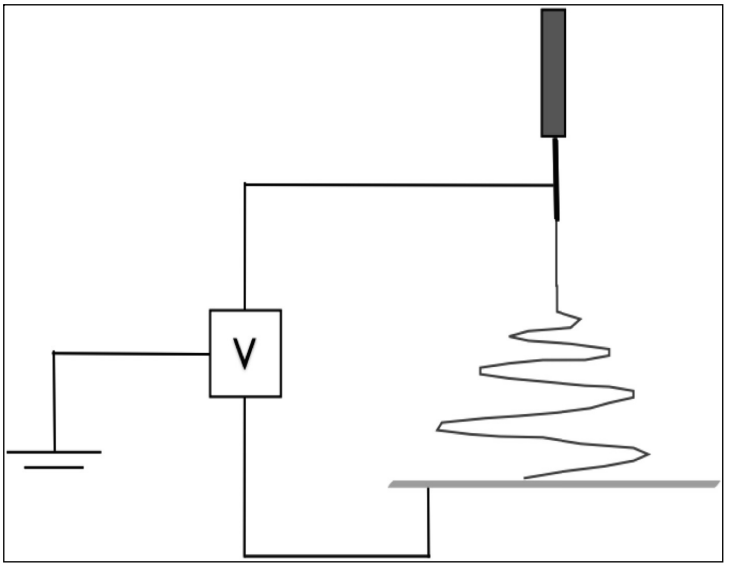

Figure 1. Illustration depicting basic equipment and design characteristics of an electrospinning deposition system.

The electrospinning process can be categorized into three stages: (A) formation of a stable jet of polymer molecules, (B) formation of a "whipping" unstable jet, and (C) formation of nanofibers through elongation, evaporation, and finally deposition (Figure 2) (Electrospinning: Map, 2011). During stage (A), both syringe pump and power supply are started and voltage is increased to around 5 kV (below the threshold voltage for polysol ejection). The voltage charges the drop forming at the tip of the needle, and the induced charges are evenly distributed. Electrostatic forces distort the drop into a specialized cone on the tip of the needle, called a Taylor Cone (Taylor, 1964). The geometry of the cone is governed by the ratio of solution surface tension to the forces of electrostatic repulsion and **E** field strength (Ramakrishna, 2005; Taylor, 1964). Also during stage (A), as the voltage is increased beyond the threshold voltage (~6kV), the strength of **E** field and electrostatic repulsions in the polysol increase and overcome the opposing force and the solution's surface tension, finally resulting in the forced ejection of a stable liquid jet from the needle (Ramakrishna, 2005). During stage (B), as the voltage is increased beyond the threshold voltage (>6kV) to near 11 kV, the stable jet destabilizes (Ramakrishna, 2005). This region is known as 'the region of jet instability,' and the bending instability results in formation of a "whipping jet." As shown in Figure 2, stage (B) is the boundary between the stable and whipping jet (Rutledge, 2001).

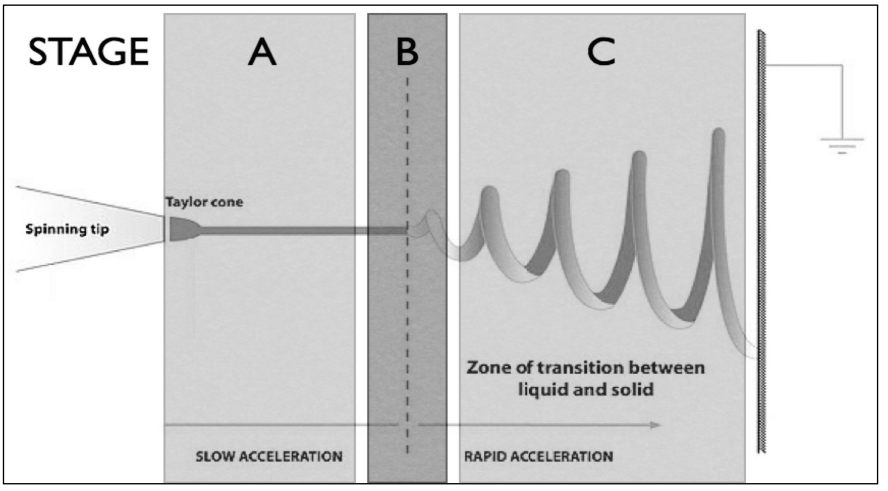

Figure 2. Illustration depicting the movement of the polymer solution fluid jet as a stage-by-stage process during electrospinning (Electrospinning: Map, 2011).

During stage (C), nanofibers are formed through the elongation, evaporation, and deposition of the whipping jet. Finally, the fibers are attracted toward the grounded substrate due to the attraction of opposite charges and are deposited onto the substrate (Ramakrishna, 2005). Although much of the solvent will evaporate as the jet whips through the air, some will evaporate upon deposition.

2.2 Fabrication of Apparatus

Using these process design criteria, the following apparatus was designed, fabricated, assembled, and tested. Figure 3 shows the final set up, which evolved over three generations during the process of designing and testing over one year. The apparatus included:

(1) a syringe pump (CHEMYX Fusion 100 Classic Syringe Pump; two syringe capacity – 0.5 µl to 60 ml) that was used to inject the polysol at a prescribed feed rate (Ramakrishna, 2005);

(2) a syringe (McMaster-Carr – 5cc) with a highly electrically charged metal needle (McMaster-Carr – 0.5 mm orifice diameter), which was used to contain and inject the polysol and was mounted on the described syringe pump;

(3) an electrically conducting and grounded hardened aluminum substrate (McMaster Carr - .001 in diameter) as a collector material;

(4) a 0-30kV voltage supply fabricated by the author (power supplied by purchased Ultravolt A Series +30kVdc, 4W) that uses a spring clip to supply voltage to the needle.

One challenge was the design and fabrication of a high voltage supply capable of supplying at least 15-30 kV. To maintain economic viability, a high voltage supply was fabricated on the bench top instead of purchasing an expensive unit. The circuit and component parts were first designed, then assembled, and finally tested for reliability. The high voltage supply proved to be reliable and was successfully used to carry out this research.

In this arrangement of the apparatus, when high voltage is applied to the system, the drop of polysol at the tip of the needle will become electrically charged and the charge will spread across the surface of the drop. As a result, the polymer molecules will experience two types of electrostatic forces: the electrostatic repulsion between the induced surface charges and the Coulombic force exerted by the applied **E** field. Due to these electrostatic forces the polysol drop will morph into the Taylor cone (Ramakrishna, 2005). Once the strength of the **E** field has increased beyond the threshold voltage (>6kV), that force will overcome the surface tension of the polymer solution, forcing the ejection of a polysol jet from the needle tip and depositing onto the substrate due to electrostatic attraction, resulting in the formation of macro, micro, and most importantly, nano sized fibers.

As mentioned earlier, one potential process application of this proposed research (for the ultimate goal of biomanufacturing tissues and organs) includes the 3-dimensional structural patterning of the substrate material in order to create the highly mesh-like structure of a scaffold through fiber deposition. But first, the deposition process and contributing processing parameters affecting fiber morphology and dimension had to be understood. To study this further, the following experiments were executed.

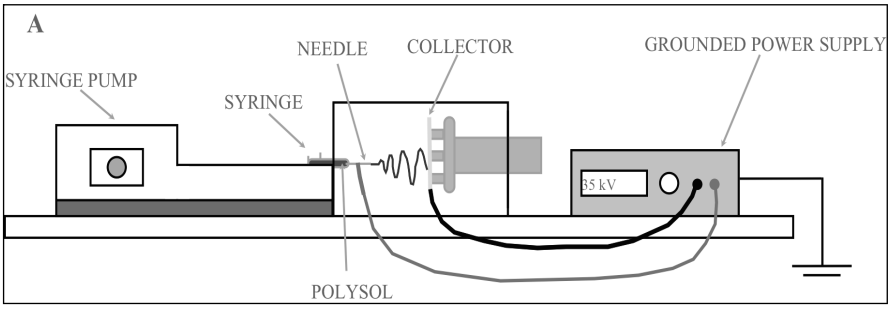

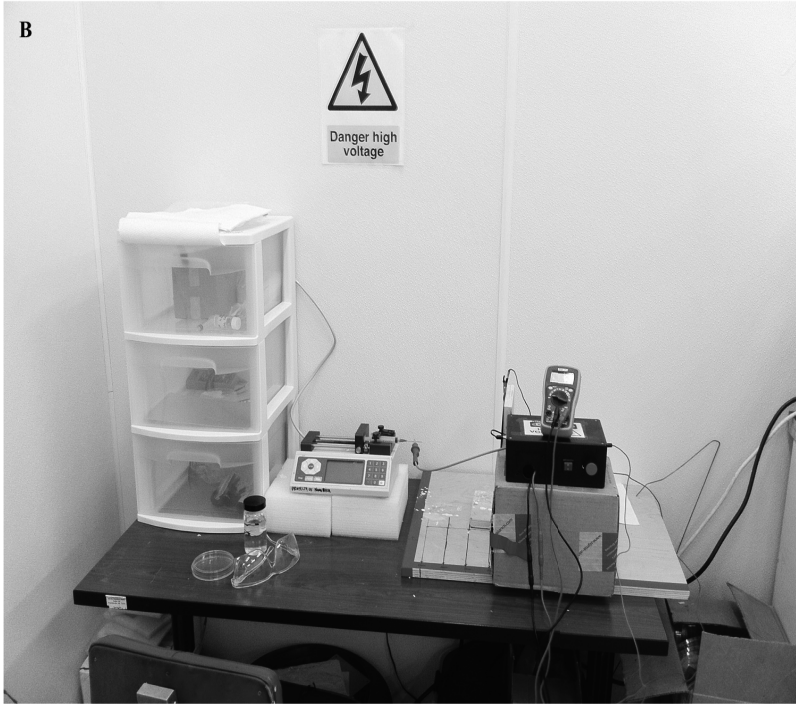

Figure 3. (A) Illustration depicting the design schematic of the electrospinning deposition system, pre-fabrication. (B) Photograph of the newly fabricated electrospinning deposition system at NanoMech, Inc..

2.3 Materials

Poly(methylmethacrylate) (PMMA) (Sigma-Aldrich, M_w = 120,000), was selected as the polymer for potential future biomedical research and applications (Wang, 2010). In order to inject the polymer as a solution, it first had to be solvated. N,N-dimethylformamide (DMF) (Sigma-Aldrich) was recommended by Ramakrishna (2005) as the solvent that was chemically able to solvate the PMMA polymer. Different concentrations of the PMMA/DMF polysol were created for this study. One significant challenge that the author overcame through the course of this experimentation was the correct preparation method for varying concentrations of polysol. Different concentrations of polysol were needed for the study. Both PMMA polymer and DMF solvent were not completely pure; therefore different stoichiometry calculations had to be computed. A polysol for a specific concentration, using the values for the stoichiometrically predetermined amounts of PMMA to DMF, was created by first adding the PMMA to the DMF. It is important to note that a homogeneous solution of polymer is required for electrospinning due to the ability of a solution to carry a uniform electric charge across its surface versus the inconsistent charge a mixture would carry (Ramakrishna, 2005). Through experimentation, it was discovered that the best polysol preparation method to insure the complete solvation of the PMMA in the mixture required the mixture to be stirred for fifteen minutes and then left for at least eight hours in a dark cool place.

2.4 Process Parameters

In order to fully understand the behavior of the newly fabricated apparatus and to examine the process control over fiber diameter that is necessary for biomedical applications, key processing parameters were varied. These parameters included: (1) distance between the polymer injection tip and the collection substrate (cm); (2) the applied voltage (kV); and (3) the concentration of PMMA in the PMMA/DMF solution (% (PMMA) by weight). Table 1 shows the process parameters (and their variation range) experimentally studied.

2.5 Characterization and Analytical Techniques

To explore the effect of these key parameters, the morphology, size and chemistry of the deposited polymeric material were studied. Optical analysis along with scanning electron microscopy (SEM; Nova NanoSEM, FEI) were used for morphological and micro/nano dimensional analysis. Fourier Transformed Infrared spectroscopy (FT-IR; NETZSCH) was applied to analyze polymer solution before deposition and deposited fiber web samples.

2.6 Challenges

The test apparatus was fabricated with an iterated approach in three 'generations' as previously described. However, the fabrication and assembly of the components was a major challenge, and it took six months for iterative optimization to realize an apparatus that was capable of being used for the necessary research. Key challenges were confronted due to the complexity of optimization involved in fabricating a apparatus that could conduct reproducible experiments and produce reliable data for the study. These challenges included: design of the electrospinning apparatus components, materials, fabrication of individual components, assembly of the apparatus and its optimization through three generations, reliability testing, experimental matrix design, and ultimately testing of the technique using the final system.

Table 1. Conditions and effects of various parameters on resulting morphologies.

Test	Collection Distance (cm)	Voltage (kV)	Polymer Concentration (wt%)	Morphology
1	10	10.68	5	Polymer beads
2	10	18.23	5	Smaller polymer beads
3	15	10.45	30	Macro to micron sized fibers
4	**15**	**15.03**	**20**	**Nanofibers**
5	15	20.22	30	Micron sized fibers
6	15	15.42	40	Macro sized fibers
7	20	15.35	30	Micron sized Fibers

3. Results

Voltage (V) supplied, distance (D) between the syringe tip and the grounded substrate, and the concentration (C) of PMMA polymer solution were each varied to identify the primary parameters required to deposit nanofibers during fabrication of the newly designed apparatus. It became apparent that this method of experimentation was unique in its ground-up methodological approach to fabrication of a "lab-top" electrospinning apparatus. In various experiments (see Table 1 for the most relevant cross-section of those experiments), V and D had a major effect on the morphology and dimension of the deposited polymer mesh, although C had a key secondary effect. This was most likely due to the viscosity of the injected PMMA polysol. A more thorough discussion of the results is presented later in this paper.

3.1 Morphological and Dimensional Analysis: SEM and visual observation

Figure 4(A) shows the image of the deposited web (Test 1 and 2 from Table 1). Smaller values of D and C, irrespective of V, yielded a thin polymer deposit or glob. Figure 5(A) shows the SEM micrographs of the deposits. At a higher magnification, it is observed that the deposits contained meso and micro scale beads of polymer without a mesh-like fiber matrix structure.

Figure 4(B) shows an image of the dense collection of fine PMMA fiber web deposited under the conditions of Test 4 (Table 1). Analysis of this mesh using SEM, seen in Figure 5(B), shows the presence of fibers with a diameter of 500 nm or less dispersed densely and uniformly in the fiber matrix. This fiber size is ideal for entrapping nanoparticles; i.e. drug-functionalized hydroxyapatite (HA), a natural ceramic that contributes to the strength and stability of human bones, which can improve the biocompatibility of scaffolds for biomedical implants such as advanced prosthetics (Balazsi 2009). Figure 4(C) shows the image of the web deposited under Test 7 (Table 1), where a uniform and dense mesh of fiber was observed. High magnification SEM, Figure 5(C), showed PMMA fibers of dimensions tens of microns in size. The comparison among this data demonstrates that there is a close dependency among the V, D and C parameters.

Figure 6 shows the SEM micrographs for the four conditions. To study this dependency further, D was held constant (at 15 cm) and the V and C parameters were varied (Tests 3 through 6 shown respectively in Figures 6(A) through 6(D)). Between Tests 3 and 5, D and C were held constant and V was varied. It was observed that a lower V yielded micro to macro sized PMMA fibers, whereas a higher V yielded only micro sized fibers. Between Tests 4 and 6, D and V were held constant and C was varied. It was observed that lower C yielded micro sized fibers, whereas a higher C yielded macro sized fibers. These experimental conditions were tested for repeatability and showed good reproducibility to deposit nano and micro sized PMMA fibers.

3.2 Chemical Analysis: FT-IR Spectroscopy

Chemical analysis and confirmation of the retention of the chemistry of PMMA polymer, before and after the electrospinning deposition process, is important to ensure that the electrostatic force interactions do not chemically dissociate the polymer chains or alter the polymer molecules. Assurance of the chemical structure is key for ensuring the retention of the biocompatibility property of PMMA polymer, which is the key for future biomedical applications (Mo, 2004; Wang, 2010).

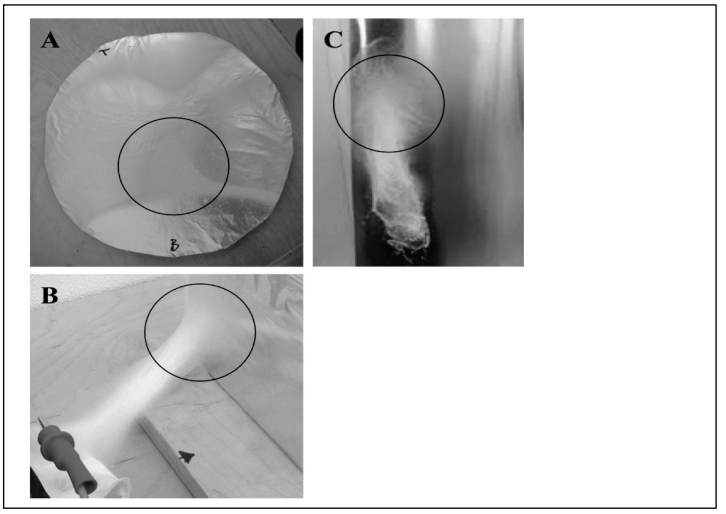

Figure 4. (A) Photograph of Test 1 and 2 from Table-1 (deposited polymer circled). (B) Photograph of Test 4 from Table-1 (depositd PMMA polymer nanofiber web matrix circled). (C) Photograph of Test 7 from Table-1 (deposited PMMA polymer micro fiber web matrix circled).

Figure 7(A) shows the FT-IR spectrum for the PMMA/DMF polysol before deposition, and Figure 7(B) for Test 4 during the nanofiber deposition. In order to prepare the samples for FT-IR analysis, they were first diluted in acetone before being added to the KBr disk for analysis. Both FT-IR spectral graphs match one-to-one, showing the retention of the PMMA polymer chemistry as a polysol before deposition and as a fiber mesh after deposition. Also, most of the molecular absorption peaks for the PMMA polysol and fiber FT-IR spectra match the standard data for PMMA (Kinusaga, 2011). The FT-IR spectra, for both the polysol and the deposited fiber, indicate the details of functional groups present in PMMA. A sharp intense peak at 1731 cm^{-1} is due to the presence of the ester carbonyl group stretching vibration. The broad peak, ranging from 1260-1000 cm^{-1}, can be explained by the C-O (ester bond) stretching vibration. The broad band from 950-650 cm^{-1} is due to the bending of the C-H bond. The broad peak ranging from 3100-2900 cm^{-1} is due to the presence of stretching vibration. The band at 3000 cm^{-1} is assigned to CH_3 stretch vibration. As stated above, these signature peaks for PMMA remained unaltered between the polysol sample and the fiber web (Test 4). Although initially unknown and discovered empirically through this research, the retention of PMMA chemistry does indeed occur after electrospinning.

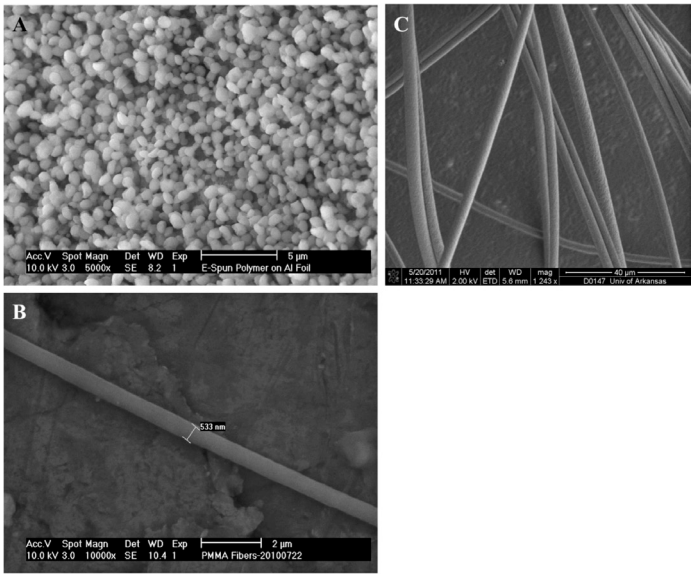

Figure 5. (A) SEM micrograph of Test 1 and 2 from Table-1. (B) SEM micrograph of Test 4 from Table-1 (with fiber diameter measured). (C) SEM micrograph of Test 7 from Table-1.

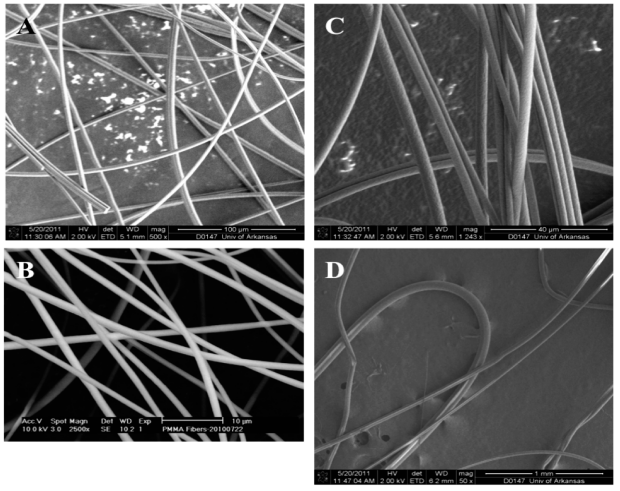

Figure 6. (A) SEM micrograph of Test 3 from Table-1. (B) SEM micrograph of Test 4 from Table 1. (C) SEM micrograph of Test 5 from Table-1. (D) SEM micrograph of Test 6 from Table-1.

4. Discussion

Two striking observations from this work are: a) the synthesis of 500 nm or smaller sized PMMA fibers under specific D, V and C conditions, and b) a close dependency of D and V on C in the outcome of the process. It is probable that the synthesis of nanofibers is due to whipping instability of the fluid jet under an applied electric bias of 15 kV (Li, 2004). The whipping instability is mainly caused by the electrostatic interactions between the external electrical field and the surface charges on the jet (Rutledge, 2001). It has also been occasionally observed that a single jet can "splay" into one or more jets, which others have shown yielded a web of PMMA nanofiber matrix (Li, 2004; Rutledge, 2001). Also related to the synthesis of 500 nm or smaller sized PMMA fibers are the effects of D, V and C on the polymer stretching process (region of "whipping" instability), as shown in Figure 2 during Stage (C). This includes elongation, evaporation, and deposition. During elongation, the polymer chains disentangle from macro to sub-micron sizes due to electrostatic attraction of individual molecules in the charged polysol (Ramakrishna, 2005). In the evaporation process, the solvent evaporates from the polymer, drying the fibers (Ramakrishna, 2005). Finally, the oppositely charged polymer fibers are attracted to the grounded collection substrate (evaporation also occurs after deposition) (Li, 2004). In this study, it appears that the effect of D, V, and C on the polymer stretching process occurred in Test 4, enabling the formation of nanoscale fibers. However in Tests 1-7, the effect of varying D, V, and C on the polymer stretching process allowed for the formation of PMMA beads and micro/macro sized fibers.

These observed effects of varying D, V, and C on the polymer stretching process may be explained as follows. First, varying D is known to directly influence both flight time of the jet and the **E** field strength (Ramakrishna, 2005). The flight time of the jet affects the dryness of the deposited fibers and the **E** field strength affects the resultant fiber diameter. If D is reduced, the flight time of the jet is reduced. The jet will travel a shorter distance, **E** field strength will increase, and jet acceleration will increase (Ramakrishna, 2005). This results in the deposition of polymer beads and increasingly wet deposits.

Secondly, varying V is known to affect the drawing acceleration of the polysol from the needle tip and subsequently, as described above, the size of the deposited fiber (Li, 2004). At a higher V, the polysol is pulled faster from the needle tip, leading to a bigger stretching effect with a consequent reduction in fiber size (Ramakrishna, 2005). A higher V will also encourage faster evaporation, yielding drier fibers upon deposition, although higher with a low C will increase the tendency for beads to form and be deposited. A lower V will decrease jet acceleration, increasing the

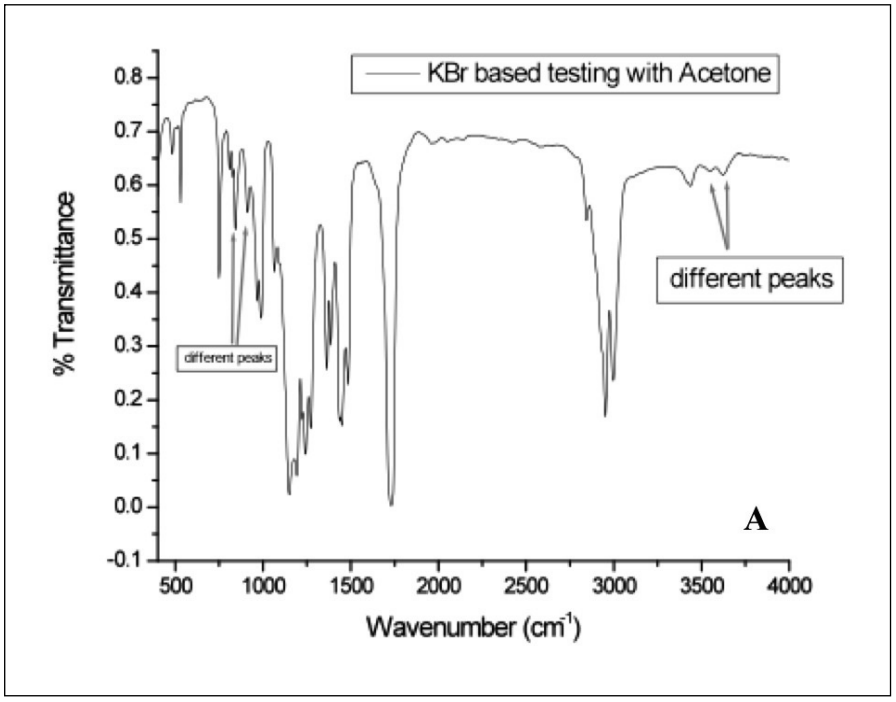

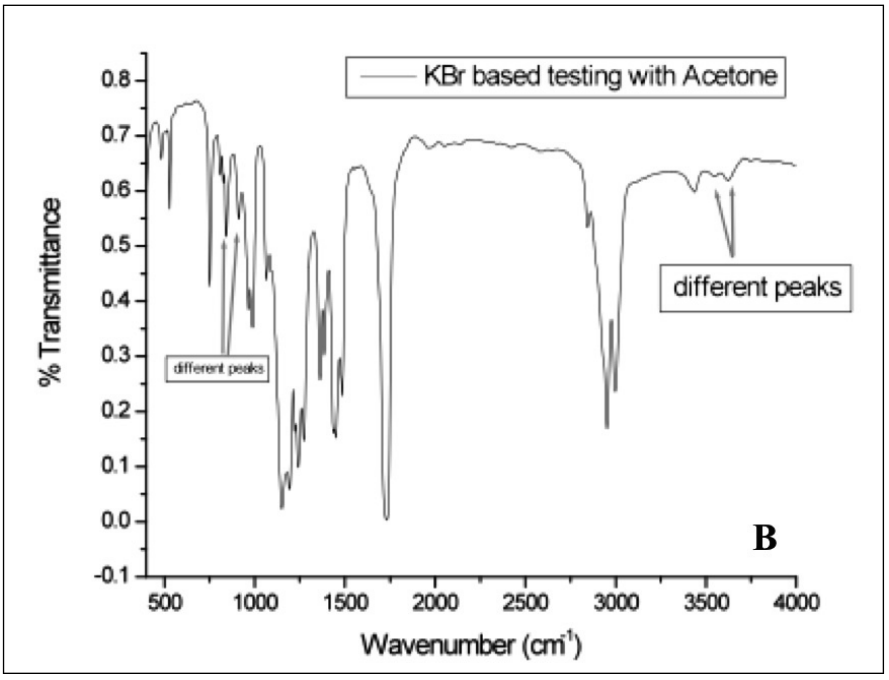

Figure 7. (A) FTIR spectrum for PMMA/DMF polymer solution sample. (B) FTIR spectrum for deposited PMMA fiber sample (both from Test 4 from Table-1).

jet flight time and may produce finer fibers (Ramakrishna, 2005).

Finally, the viscosity of a polysol depends directly on C, therefore varying C of the polysol directly changes the viscosity of the polysol and the effect viscosity has on fiber dimension (Li, 2004). When the viscosity of the polysol is too low, polymer beads form instead of fibers. However, when the viscosity is too high, polymer fibers form beads within their structures (Ramakrishna, 2004). Also, the retention of the PMMA polymer chemistry, determined by the FT-IR analysis, speaks to the potential of using PMMA fiber as a biocompatible scaffold-building material for biologically functionalized nanoparticle delivery and biocompatible prosthetic implants.

5. Conclusions and Future Work

In summary, the success of this research is apparent in two outcomes: fabrication and demonstration of an electrospinning system, and use of this system to deposit PMMA polymer in various form factors such as nanofibers, micro fibers and micro beads. The role of key process parameters and their interparametric dependency in the feasibility phase were also studied. The parameters included the distance between the polymer injection tip and the collection substrate, the voltage supplied, and the concentration of PMMA in the PMMA/DMF solution. This research on deposition of nanofibers was motivated by their potential use as carrier scaffolds for nanostructures such as drug molecules, HA nanoparticles, quantum dots, extracellular matrix mimicking scaffolds for tissue engineering advanced biocompatible implants and prosthetics. Future research will involve the analytical study of the process as well as applications of the established system to deposit chemically functionalized nanofibers on a 3D patterned scaffold mold used for printing, and ultimately for bio-printing applications.

References

1. Balazsi, C., et al. “Biopolymer-Hydroxyapatite Scaffolds for Advanced Prosthetics.” Composite Interfaces. 16. (2009): 191-200.

2. D. Li, Y. Xia. “Electrospinning of Nanofibers: Reinventing the Wheel?” Wiley-VCH Verlag GmbH & Co. KGaA, Weinheim. (2004)

3. Electrospinning: Map. Web. 22 May 2011. <http://maps.thefullwiki.org/Electrospinning>.

4. Wang, H., et al. “Electrospun poly(methyl methacrylate) nanofibers and microparticles.” Journal of Material Science (2010). 45: 1032-1038.

5. Kinugasa S, Tanabe K, and T Tamura. “Spectral Database for Organic Compounds SDBS.” National Institute of Advance Industrial Science and Technology (AIST), Japan. Web. April 2011. < http://riodb01.ibase.aist.go.jp/sdbs/cgi-bin/direct_frame_top.cgi>.

6. “Manufacturing at the Nanoscale.” National Nanotechnology Initiative, n.d. Web. 16 February 2011. <http://nano.gov/about-nni/what>.

7. Ramakrishna, Fujihara, Teo, Lim, & Ma, National University of Singapore. An Introduction to Electrospinning and Nanofibers. World Scientific Publishing Co. Pte. Ltd. (2005)

8. Rutledge, G.C. et al. “Electrospinning: A whipping fluid jet generate submicron polymer fibers.” American Institute of Physics. Applied Physics Letters, Vol. 78, num. 8. (2001)

9. Taylor, Geoffrey Sir. "Disintegration of water drops in an electric field." Proceedings of the Royal Society of London Series A, Mathematical and Physical, Vol. 280 No. 1382, pp. 383-397. The Royal Society Publishing Co. (1964).
10. Schiffman, Jessica D, and Caroline L Schauer. "A Review: Electrospinning of Biopolymer Nanofibers and their Applications." Polymer Reviews. 48. (2008): 317-352.
11. X.M. Mo, C. Y. Xu, M. Kotaki, S. Ramakrishna, Biomaterials. 2004, 25, 1883.

Mentor Comments: Professor Ajay Malshe and industry mentor Dr. Wenping Jiang served as joint advisors for Harsha Malshe's research, in part because the work involved initiatives of the company NanoMech, where Dr. Jiang serves as Chief Engineer, and in part because Dr. Malshe is Harsha's father (and every effort was made to avoid conflict of interest). Together they write:

Nano-bio materials and manufacturing is one of the fastest growing subjects to address the needs of growing and aging populations of the US and the world. Reduction of the cost of health care and providing better health care through innovations in materials and processes is at the heart of the progress. Harsha's project is at the intersection of these needs where NanoMech is interested in establishing an efficient and low cost manufacturing fiber coating process for producing basic nano building blocks, like nanofibers, and using them for drug and other chemical delivery.

More than a year ago, Harsha approached Dr. Wenping at NanoMech due to his interest in the biomedical field for a materials related project. The discussion between him and the co-advisors derived the direction to undertake this research. He contributed partly in conceiving this original project. His key contributions are in hands-on design, development and fabrication of electrospinning apparatus, and planning and execution of experiments interdependently working with advisors. This is a mainstream project for the company and he reported directly to the co-advisors. He also spent significant time in a detailed literature review, developing a fundamental understanding in physics and chemistry of process and materials, respectively. He performed analysis of the measurements and developed understanding of the process mechanisms in discussion with co-advisors. Last but not least, this is his first manuscript, and his enthusiasm, dedication, and writing impressed us. The work that he has presented is of good scientific importance and has laid the path for future advanced research, which we anticipate he will continue. Harsha's work is part of research and development for future nano materials with advanced health care applications.

UNIVERSITY OF
ARKANSAS